HOST IMMUNE RESPONSE TO MOUSE ADENOVIRUS TYPE 1

by

MARTIN L. MOORE

(Under the direction of Mary Bedell)

ABSTRACT

Mouse adenovirus type 1 (MAV-1) provides a model of adenovirus pathogenesis. MAV-1 induces dose-dependent encephalomyelitis. To characterize the role of specific mechanisms of immunity in MAV-1-induced disease, immunodeficient mouse models were utilized. T cells, major histocompatibility complex class I, and perforin contributed to MAV-1-induced acute disease. Mice lacking α/β T cells succumbed to MAV-1 infection 9 to 16 weeks post-infection. α/β T cells were required for clearance of infectious MAV-1 and for long-term survival. Mice lacking $CD8^+$ T cells and mice lacking $CD4^+$ T cells cleared MAV-1 like controls. These data are consistent with a model in which $CD8^+$ T cells induce acute immunopathology and either $CD8^+$ T cells or $CD4^+$ T cells are required for long-term control of MAV-1 replication.

B cell-deficient mice were highly susceptible to acute MAV-1 infection and succumbed with high viral loads, disseminated infection, and hepatitis. It was hypothesized that a T cell-independent (TI) B cell response is the critical protective mechanism. Bruton's tyrosine kinase-deficient mice have reduced numbers of B cells and are unable to mount TI B cell responses to some antigens. Loss of Btk in mice results in the classic X-linked immunodeficiency (Xid) phenotype. Btk was required for survival of acute MAV-1 infection, demonstrating for the first

time that Btk plays a role in protection from virus-induced disease in mice. Survival of acute MAV-1 infection correlated with TI antiviral IgM production, and treatment of lethally infected Btk-deficient mice with early anti-MAV-1 antiserum was protective.

The role of interferon-α/β (IFN-α/β) signaling in MAV-1 infection was investigated using IFN-α/β receptor null mice (IFN-α/β$R^{-/-}$). Surprisingly, MAV-1 virulence and replication in the brain was not significantly altered in IFN-α/β$R^{-/-}$ mice relative to control mice. However, IFN-α/β$R^{-/-}$ mice exhibited a more disseminated MAV-1 infection than controls, indicating that IFN-α/β is a determinant of MAV-1 organ tropism. IFN-stimulated genes (ISGs) whose steady-state mRNA levels were increased by MAV-1 infection in vitro and in vivo were identified. Northern analyses of mRNAs in infected mice suggest that interferon regulatory factor 7 and major histocompatibility complex class I play a role in IFN-α/β signaling-dependent control of MAV-1 organ tropism.

INDEX WORDS: Mouse adenovirus, pathogenesis, encephalomyelitis, immunopathology, T cells, B cells, Bruton's tyrosine kinase, T cell-independent, interferon

HOST IMMUNE RESPONSE TO MOUSE ADENOVIRUS TYPE 1

by

MARTIN L. MOORE

B.S., The University of Georgia, 1995

A Dissertation Submitted to the Graduate Faculty of the University of Georgia in Partial Fulfillment of the Requirements for the Degree

DOCTOR OF PHILOSOPHY

ATHENS, GA

2003

HOST IMMUNE RESPONSE TO MOUSE ADENOVIRUS TYPE 1

by

MARTIN L. MOORE

Major Professor: Mary Bedell

Committee: Katherine Spindler
Corrie C. Brown
Rick Tarleton
Michael Bender
Robert Ivarie

Electronic Version Approved:

Maureen Grasso
Dean of the Graduate School
The University of Georgia
December 2003

ACKNOWLEDGMENTS

Kathy Spindler, Gwen Hirsch, Adriana Kajon, Caroline Ingle, Carla Sturkie, James Stanton, Lei Fang, Amanda Welton, Katie Kemke, Erin McKissic, Libby McKinney, Om Parkash, Muthugapatti Kandasamy, Mary Bedell, Bob Ivarie, Corrie Brown, Lyndon Goodly, Emily Smith, Sripriya Rajaraman, Aparna Mahakali-Zama, Ivan Mott, Jeff Rapp, Bijoy Mohanty, Anne Marie, and David Ornelles trained and helped me at the bench.

I am grateful to my committee members, Kathy Spindler, Mary Bedell, Bob Ivarie, Rick Tarleton, Michael Bender, and Corrie Brown for suggestions and encouragement. I am also grateful for the attention of my ad hoc committee members, Mike Imperiale and Gary Huffnagle. I am thankful that the Genetics Department is dedicated to the training of graduate students and is scientifically diverse. I am grateful for the efforts Animal Resources at the University of Georgia. I am very grateful for the Genetics Department office staff. I am thankful that Sidney Kushner inspired me to go to graduate school.

I am especially grateful to Kathy Spindler for being my mentor and advisor. Kathy worked very hard these five to make a scientist out of me. In doing so, she invested a tremendous amount of valuable time and heartfelt care, as well as trust. Thank you.

I would like to thank Nick, Anne Marie, Carla, Gwen, Gene and Rebecca, and Tom for their friendship. I would like to thank my parents for their patience and support. Finally, I would like to thank the DNA Tumor Virus Meeting for introducing me to my best friend and wife, Dr. Amy Moore. It is with her continual support and understanding that I was able to complete this work.

TABLE OF CONTENTS

CHAPTER 1

INTRODUCTION AND LITERATURE REVIEW

Adenoviruses (Ads), originally cultured from human adenoids by Rowe and colleagues in 1953 (61), are species-specific and infect vertebrates (5). Ads are icosahedral, nonenveloped viruses with a double-stranded linear DNA genome organized into early and late transcription regions. There are more than 50 human Ad (hAd) serotypes, and some are well-characterized in vitro (65). Clinically, hAds infect a wide range of cells and tissues, and serotypes associated with respiratory tract infections are estimated to account for approximately 5% of acute respiratory disease in children under the age of 5 (30).

Human Ad pathogenesis

Insights into hAd pathogenesis have come from natural infections and inoculation of rodents, nonhuman primates, and people. Natural hAd infections are associated with self-limiting respiratory, conjunctival, and gastrointestinal disease. In immunocompromised patients, hAd infection can result in pneumonia, hepatitis, encephalitis, pancreatitis, gastroenteritis, or disseminated disease involving multiple organs (8, 76). Disseminated hAd infection usually results in death, the incidence of disseminated hAd disease is increasing with the increased number of immunocompromised children, and pediatric bone marrow transplant recipients are most at risk (7, 17, 19, 26). hAds do not replicate in rodents, but high dose (10^8 to 10^{10} plaque forming units (PFU) per animal) intranasal (i.n.) infection of cotton rats and mice induces pulmonary disease (20, 22). Experiments with hAd early gene region mutants in these disease models have identified immunomodulating properties of hAd early genes (21, 67). There is considerable interest in adenovirus immunopathogenesis because the immune system is a major obstacle to safe and effective adenovirus-mediated gene therapy. Robust T cell and antibody (Ab) responses to hAd gene therapy vectors have been characterized in mice (45, 82), nonhuman primates (85), and humans (28).

MAV-1 pathogenesis

Mouse adenovirus type 1 (MAV-1), isolated by Hartley and Rowe in 1960, produces fatal, disseminated disease in suckling mice infected intraperitoneally (i.p.) (6, 27). The MAV-1 genome has been sequenced (51), and MAV-1 early gene mutants have been characterized in vitro and in vivo (4, 9, 66, 83). MAV-1 permits the study of a replicating Ad in vivo and provides a good model of Ad pathogenesis.

The outcome of infection of adult mice with MAV-1 depends on the dose and strain of virus, the inoculation route, and the mouse strain. MAV-1 induces dose-dependent acute encephalomyelitis in adult outbred (46), C57BL/6 (B6) (24), and SJL/J (68) mice. In contrast to wt MAV-1, a plaque type variant of MAV-1 (*pt*4) has a distinct pulmonary tropism in C3H/HeN mice (81). Outbred mice infected i.n. with MAV-1 exhibit less disease and have protracted infection kinetics compared to mice infected i.p. (38, 79), and intracerebral inoculation of outbred mice results in significant infection of the adrenal gland (50). In most strains mice infected by the i.p. route, MAV-1 infects cells of the monocyte/macrophage lineage and endothelial cells of the vasculature throughout the mouse; and highest levels of virus are found in the spleen and central nervous system (CNS) (11, 24, 38, 47). MAV-1 nucleic acid is also detected in the renal tubular epithelium of adult outbred mice infected i.p. or i.n. (38). Infectious MAV-1 has been isolated from urine up to 24 months p.i. (74). MAV-1-infected athymic *nu*/*nu* mice on a mixed NIH Swiss and C3H/HeN background succumb to a wasting disease with characteristic duodenal hemorrhage and intranuclear adenovirus particles in endothelial cells (80). Mice that are homozygous for the severe combined immunodeficiency (SCID) mutation on a CB.17 or BALB/c background succumb to MAV-1 infection with diffuse hepatic injury that resembles Reye syndrome pathology (11, 58). Since *nu*/*nu* mice are T cell-deficient and SCID

mice are T cell- and B cell-deficient, these studies suggest that adaptive (specific) immunity protects adult mice from MAV-1-induced disease.

Viral pathogenesis is defined as the mechanism(s) by which viruses perturb normal host cell function to produce signs of disease, but natural virus infection rarely causes significant disease (73). A central issue for viral pathogenesis is the balance between immune-mediated clearance of virus infection and immune-mediated pathology, or immunopathology. Immunopathology is the dominant cause of virus-induced disease. There are many small animal models of virus-induced disease, and these have led to the discovery of fundamental mechanisms of immunity (1). Importantly, animal models of virus-induced disease also reveal the many ways that known immune mechanisms can be modulated to contribute to or reduce disease. Modulation of immunity to prevent disease is a goal of vaccination, and modulation of immunity to treat disease is a goal of immunotherapy. The immunogenicity of Ads is being explored for vaccine and immunotherapy strategies (52, 53). Thus the relevance of Ad pathogenesis extends beyond acute hAd-induced disease.

Cell-mediated immunity

T lymphocytes are principle mediators of virus clearance and immunopathology. Cell-mediated immunity (CMI) describes effector functions of T cells, and these can be broadly classified as cytotoxicity and cytokine production. Via T cell receptors and CD8 co-receptors, naïve $CD8^+$ T cells can bind specific peptides displayed by major histocompatibility complex (MHC) class I molecules on the cell surface of antigen presenting cells (APCs) and differentiate into effector cytotoxic T cells (CTL) (1). CTL migrate to sites of inflammation and deliver cytotoxic granule proteins such as perforin and Fas ligand to target cells by an antigen-dependent process (37). $CD8^+$ T cells can also produce antiviral cytokines that have the potential to clear

viruses from infected cells (25). $CD4^+$ T cells interact with peptide-MHC class II molecules on the surface of APCs to become prolific cytokine producers, and $CD4^+$ effector T cells can have cytotoxic potential (1). Key points of T cell regulation include the kinetics and abundance of antigen presentation in secondary lymphoid tissue, the effects of costimulatory host molecules, and the cytokine and chemokine milieus regulated by innate immune mechanisms (3, 36, 84).

Humoral immunity

Secreted antibodies (Ab) produced by B cells mediate humoral immunity to protein and nonprotein antigens. The importance of antibodies for preventing virus infection and reinfection is unquestioned, and the mechanisms involved in T cell-dependent immunoglobulin (Ig) class-switching and Ab affinity maturation are well studied. Cell sorting technologies have led to several classifications of naïve B cell subpopulations, including B-2, B-1a (CD5+) and B-1b cells; transitional type 1 and 2 immature B cells; marginal zone and follicular B cells; and virgin, immature, and recirculating B cells (2, 29, 49, 57). The functional relevance of these subpopulations for viral infections is not understood.

B cell maturation differs between mice and humans, and this has functional consequences for Ab responses to virus infection. Mutations in Bruton's tyrosine kinase (Btk) result in X-linked agammaglobulinemia (XLA) in humans and X-linked immune deficiency (Xid) in mice (44). There is a complete absence of B cells in XLA, whereas Xid results in a reduction in conventional B cells and the absence of peritoneal B-1 cells (43, 64). XLA patients are unable to mount Ab responses but Xid mice are able to mount T cell-dependent Ab responses. However Xid mice are unable to mount T cell-independent (TI) Ab responses to some antigens (54). Antigens have been classified into two groups based on whether they induce TI Ab in Xid mice (TI-1) or not (TI-2). Several viruses express molecules that act as TI-2 antigens; that is, they

induce TI Abs in immunocompetent but not Xid mice (72). Polyoma virus (PyV) expresses a TI-2 antigen and elicits protective TI IgM and IgG in T cell-deficient mice, suggesting that TI Ab can play a role in viral pathogenesis (70, 71).

Type I interferon

The interferon-alpha/beta (IFN-α/β) system, also called type I IFN, is a hallmark of innate immunity to viruses; α and β IFNs are cytokines secreted by most cells in culture in response to virus infection (75). IFN-α/β cytokines exert their autocrine and paracrine activity via interaction with the IFN-α/β receptor (IFN-α/βR) and subsequent activation of JAK-STAT signal transduction pathways, leading to a regulated cascade of transcription of interferon-stimulated genes (ISGs) (63). ISGs establish an antiviral state by modulating cellular functions such as protein synthesis, transcription, antigen processing and presentation, the cell cycle, arachidonic acid metabolism, and nitric oxide synthesis. There are over 300 known human ISGs (13, 14). Many viruses that replicate in mammalian cells have been assessed for sensitivity or resistance to type I IFN in vitro, and many viral gene products, including MAV-1 early region 1A (E1A), have been shown to counter the effects of type I IFN in vitro (16, 39). Infection of type I IFN-deficient mice has repeatedly demonstrated the importance of this system for protection against virus infection in vivo, particularly in protecting against virus dissemination and systemic infection (15, 18, 23, 48, 55, 56, 62, 69). In addition to establishing an intracellular antiviral state, type I IFN plays an important role in promoting adaptive immunity by modulating antigen processing and increasing the expression of MHC class I and II molecules. Thus innate immunity primes adaptive immunity. Janeway stressed the contribution of innate immunity in activating adaptive responses and suggested that innate immunity makes the discrimination

between self and nonself by priming adaptive immune systems in the presence of a pathogen or not priming in the absence of a pathogen (35).

Immune response to MAV-1

The immune response to MAV-1 involves innate, cell-mediated, and humoral immunity. Charles and coworkers quantitated cytokine and chemokine mRNAs in mock-infected and MAV-1-infected B6 and BALB/c brains because BALB/c mice are more resistant to MAV-1-induced encephalomyelitis than B6 mice (24). MAV-1 increases the mRNA steady-state levels of the cytokines interferon-gamma (IFN-γ), tumor necrosis factor alpha (TNF-α), interleukin-1 (IL-1), IL-6, and lymphotoxin (LT) in B6 and BALB/c brains 4 days p.i. (11). MAV-1 also increases the mRNA steady-state levels of the chemokine receptors CCR1 to -5 in B6 and BALB/c brains 4 days p.i. (10). Steady-state mRNA levels of the chemokines interferon gamma-induced protein 10 (IP-10), monocyte chemoattractant protein 1 (MCP-1), and T cell activation gene 3 (TCA-3) are increased by MAV-1 infection in B6 but not BALB/c brains 4 days p.i. (10), suggesting that innate immune responses contribute to MAV-1-induced encephalomyelitis in B6 mice. Outbred mice infected i.p. with a sublethal dose develop MAV-1-specific cytotoxic T cell (CTL) that are detectable 4 days p.i., peak at 10 days p.i., then rapidly decline (31-34). These kinetics are typical of acute virus infection in mice. Outbred mice infected i.p. with a sublethal dose of MAV-1 develop high neutralizing antibody (nAb) titers two weeks p.i., and nAb titers increase for one year then decline (74). MAV-1 infection of CBA/Ht mice with 10^7 50% infectious doses (ID_{50}) results in significant splenic B cell proliferation at 10 days p.i. (12).

MAV-1 genes involved in virulence

The identification and analysis of MAV-1 virulence genes aids the study of MAV-1 pathogenesis. The MAV-1 E1A and early region 3 (E3) genes are not required for replication in vitro (9, 83). E1A null mutants are five orders of magnitude less virulent than wt MAV-1 in outbred mice, as measured by 50% lethal dose (LD_{50}) assay (66). E1A null mutants are able to establish infection in the same cell types and organs as wt MAV-1, albeit at lower levels, and E1A null mutants are able to persist like wt MAV-1. An E3 null mutant (*pm*E314) is six orders of magnitude less virulent than wt MAV-1 in outbred mice (9). Like E1A mutants, *pm*E314 is not altered in cell or organ tropism relative to wt virus, and *pm*E314 replicates in mice to levels comparable to wt virus. Interestingly, the brains of *pm*E314-infected mice had dramatically reduced inflammation compared to wt virus-infected mice. Thus adenovirus genetics, a powerful tool for studying molecular biology, is also useful for investigating viral pathogenesis.

Host genetics and MAV-1 disease

Another powerful tool for studying viral pathogenesis is mouse genetics. Genetic mapping has identified susceptibility loci for important pathogens in mice (59). Mouse strains that are susceptible and resistant to MAV-1 infection have been identified. Kring and colleagues found that Swiss outbred mice from two commercial suppliers differ in susceptibility to MAV-1-induced disease by three orders of magnitude (46). As mentioned above, BALB/c mice are more resistant than B6 mice to MAV-1-induced encephalomyelitis; BALB/c mice are approximately two orders of magnitude more resistant to MAV-1-induced disease than B6 mice (24). A more thorough screen of inbred mouse strains for susceptibility to MAV-1 infection revealed that SJL/J mice are five orders of magnitude more susceptible to MAV-1-induced disease than B6 or BALB/c, and sublethal irradiation of resistant mice renders them susceptible to MAV-1 infection

(68). (BALBxSJL)F_1 mice have an intermediate susceptibility, and mapping susceptibility to MAV-1 infection in backcross mice is in progress (A. Welton and K. Spindler, unpublished data). In addition to mapping studies, differences in immune function between inbred mouse strains have been determined empirically, and these differences can provide clues about viral pathogenesis. For example, SJL/J mice have a "low NK cell" phenotype (40, 41). SJL/J mice also have a defect in CD5+ B cells (77). 129 Sv/Ev mice have a defect in inflammatory cell recruitment (78). B6 and BALB/c mice differ significantly in cytokine and chemokine responses to virus infection, including MAV-1 (10, 42, 60). Genetic differences between inbred mouse strains have a significant impact on disease outcomes to virus infection, emphasizing the importance of host factors in virus-induced disease.

Evaluation of the roles of T cells, B cells, and type I IFN in MAV-1 pathogenesis

Although innate, cell-mediated, and humoral immunity are involved in MAV-1 infection, the role of these processes in MAV-1 pathogenesis remained largely unexplored. Mice with targeted mutations in immune-related genes provide another powerful tool for investigating viral pathogenesis. In this work, the roles of T cells, B cells, and type I IFN in MAV-1 pathogenesis were investigated utilizing immunodeficient mouse strains. Each of these systems of immunity was shown to play a distinct role in protecting against MAV-1 infection. T cells induced acute immunopathology but were required for long-term survival. B cells played a critical role in protecting against acute MAV-1 infection, and survival correlated with early T cell-independent antiviral IgM. Type I IFN was important for preventing systemic MAV-1 infection but was not important for protection against MAV-1-induced encephalomyelitis.

REFERENCES

1. **Abbas, A. K., A. H. Lichtman, and J. S. Pober.** 2000. Cellular and molecular immunology, 4th ed. W.B. Saunders Co., Philadelphia.

2. **Amano, M., N. Baumgarth, M. D. Dick, L. Brossay, M. Kronenberg, L. A. Herzenberg, and S. Strober.** 1998. CD1 expression defines subsets of follicular and marginal zone B cells in the spleen: beta 2-microglobulin-dependent and independent forms. J. Immunol. **161:**1710-7.

3. **Baggiolini, M.** 1998. Chemokines and leukocyte traffic. Nature **392:**565-8.

4. **Beard, C. W., and K. R. Spindler.** 1996. Analysis of early region 3 mutants of mouse adenovirus type 1. J. Virol. **70:**5867-5874.

5. **Benko, M., and B. Harrach.** 2003. Molecular evolution of adenoviruses. Curr. Top. Microbiol. Immunol. **272:**3-35.

6. **Blailock, Z. R., E. R. Rabin, and J. L. Melnick.** 1967. Adenovirus endocarditis in mice. Science **157:**69-70.

7. **Blanke, C., C. Clark, E. R. Broun, G. Tricot, I. Cunningham, K. Cornetta, A. Hedderman, and R. Hromas.** 1995. Evolving pathogens in allogeneic bone marrow transplantation: increased fatal adenoviral infections. Am. J. Med. **99:**326-328.

8. **Carrigan, D. R.** 1997. Adenovirus infections in immunocompromised patients. Am. J. Med. **102:**71-74.

9. **Cauthen, A. N., C. C. Brown, and K. R. Spindler.** 1999. In vitro and in vivo characterization of a mouse adenovirus type 1 early region 3 mutant. J. Virol. **73:**8640-8646.

10. **Charles, P. C., X. Chen, M. S. Horwitz, and C. F. Brosnan.** 1999. Differential chemokine induction by the mouse adenovirus type-1 in the central nervous system of susceptible and resistant strains of mice. J. Neurovirol. **5:**55-64.

11. **Charles, P. C., J. D. Guida, C. F. Brosnan, and M. S. Horwitz.** 1998. Mouse adenovirus type-1 replication is restricted to vascular endothelium in the CNS of susceptible strains of mice. Virology **245:**216-228.

12. **Coutelier, J.-P., P. G. Coulie, P. Wauters, H. Heremans, and J. T. M. van der Logt.** 1990. In vivo polyclonal B-lymphocyte activation elicited by murine viruses. J. Virol. **64:**5383-8388.

13. **de Veer, M. J., M. Holko, M. Frevel, E. Walker, S. Der, J. M. Paranjape, R. H. Silverman, and B. R. Williams.** 2001. Functional classification of interferon-stimulated genes identified using microarrays. J. Leukoc. Biol. **69:**912-20.

14. **Der, S. D., A. Zhou, B. R. Williams, and R. H. Silverman.** 1998. Identification of genes differentially regulated by interferon alpha, beta, or gamma using oligonucleotide arrays. Proc. Natl. Acad. Sci. U S A. **95:**15623-15628.

15. **Fiette, L., C. Aubert, U. Muller, S. Huang, M. Aguet, M. Brahic, and J. F. Bureau.** 1995. Theiler's virus infection of 129Sv mice that lack the interferon alpha/beta or interferon gamma receptors. J. Exp. Med. **181:**2069-76.

16. **Flint, S. J., L. W. Enquist, R. M. Krug, V. R. Racaniello, and A. M. Skalka.** 2000. Principles of virology: Molecular biology, pathogenesis, and control. American Society for Microbiology, Washington, DC.

17. **Flomenberg, P., J. Babbitt, W. R. Drobyski, R. C. Ash, D. R. Carigan, G. V. Sedmak, T. McAuliffe, B. Camitta, M. M. Horowitz, N. Bunin, and J. T. Casper.** 1994. Increasing incidence of adenovirus disease in bone marrow transplant recipients. J. Inf. Dis. **169:**775-781.

18. **Garcia-Sastre, A., R. K. Durbin, H. Zheng, P. Palese, R. Gertner, D. E. Levy, and J. E. Durbin.** 1998. The role of interferon in influenza virus tissue tropism. J. Virol. **72:**8550-8558.

19. **Gavin, P. J., and B. Z. Katz.** 2002. Intravenous ribavirin treatment for severe adenovirus disease in immunocompromised children. Pediatrics **110:**1-8.

20. **Ginsberg, H. S., R. L. Horswood, R. M. Chanock, and G. A. Prince.** 1990. Role of early genes in pathogenesis of adenovirus pneumonia. Proc. Natl. Acad. Sci. USA **87:**6191-6195.

21. **Ginsberg, H. S., L. L. Moldawer, and G. A. Prince.** 1999. Role of the type 5 adenovirus gene encoding the early region 1B 55-kDa protein in pulmonary pathogenesis. Proc. Natl. Acad. Sci. USA **96:**10409-10411.

22. **Ginsberg, H. S., L. L. Moldawer, P. B. Sehgal, M. Redington, P. L. Kilian, R. M. Chanock, and G. A. Prince.** 1991. A mouse model for investigating the molecular pathogenesis of adenovirus pneumonia. Proc. Natl. Acad. Sci. USA **88:**1651-1655.

23. **Grieder, F. B., and S. N. Vogel.** 1999. Role of interferon and interferon regulatory factors in early protection against Venezuelan equine encephalitis virus infection. Virol. **257:**106-118.

24. **Guida, J. D., G. Fejer, L.-A. Pirofski, C. F. Brosnan, and M. S. Horwitz.** 1995. Mouse adenovirus type 1 causes a fatal hemorrhagic encephalomyelitis in adult C57BL/6 but not BALB/c mice. J. Virol. **69:**7674-7681.

25. **Guidotti, L. G., R. Rochford, J. Chung, M. Shapiro, R. Purcell, and F. V. Chisari.** 1999. Viral clearance without destruction of infected cells during acute HBV infection. Science **284:**825-829.

26. **Hale, G. A., H. E. Heslop, R. A. Krance, M. A. Brenner, D. Jayawardene, D. K. Srivastava, and C. C. Patrick.** 1999. Adenovirus infection after pediatric bone marrow transplantation. Bone Marrow Transplant **23:**277-282.

27. **Hartley, J. W., and W. P. Rowe.** 1960. A new mouse virus apparently related to the adenovirus group. Virology **11:**645-647.

28. **Harvey, B. G., N. R. Hackett, T. El-Sawy, T. K. Rosengart, E. A. Hirschowitz, M. D. Lieberman, M. L. Lesser, and R. G. Crystal.** 1999. Variability of human systemic humoral immune responses to adenovirus gene transfer vectors administered to different organs. J. Virol. **73:**6729-42.

29. **Herzenberg, L. A., and A. B. Kantor.** 1993. B-cell lineages exist in the mouse. Immunol. Today. **14:**79-83; discussion 88-90.

30. **Horwitz, M. S.** 2001. Adenoviruses, p. 2301-2326. *In* D. M. Knipe and P. M. Howley (ed.), Fields Virology, 4th ed, vol. 2. Lippincott Williams & Wilkins, Philadelphia.

31. **Inada, T., and H. Uetake.** 1978. Cell-mediated immunity assayed by ^{51}Cr release test in mice infected with mouse adenovirus. Infect. Immun. **20:**1-5.

32. **Inada, T., and H. Uetake.** 1980. Cell-mediated immunity to mouse adenovirus infection: Blocking of macrophage migration inhibition and T cell-mediated cytolysis of infected cells by anti-S antigen or anti-alloantigen serum. Microbiol. Immunol. **24:**525-535.

33. **Inada, T., and H. Uetake.** 1978. Cell-mediated immunity to mouse adenovirus infection: Macrophage migration inhibition test. Microbiol. Immunol. **22:**391-401.

34. **Inada, T., and H. Uetake.** 1978. Nature and specificity of effector cells in cell-mediated cytolysis of mouse adenovirus-infected cells. Infect. Immun. **22:**119-124.

35. **Janeway, C. A., Jr.** 2001. How the immune system works to protect the host from infection: a personal view. Proc. Natl. Acad. Sci. U S A **98:**7461-8.

36. **Kaech, S. M., E. J. Wherry, and R. Ahmed.** 2002. Effector and memory T-cell differentiation: Implications for vaccine development. Nat. Rev. Immunol. **2:**251-262.

37. **Kagi, D., B. Ledermann, K. Burki, P. Seiler, B. Odermatt, K. J. Olsen, E. R. Podack, R. M. Zinkernagel, and H. Hengartner.** 1994. Cytotoxicity mediated by T cells and natural killer cells is greatly impaired in perforin-deficient mice. Nature **369:**31-37.

38. **Kajon, A. E., C. C. Brown, and K. R. Spindler.** 1998. Distribution of mouse adenovirus type 1 in intraperitoneally and intranasally infected adult outbred mice. J. Virol. **72:**1219-1223.

39. **Kajon, A. E., and K. R. Spindler.** 2000. Mouse adenovirus type 1 replication *in vitro* is resistant to interferon. Virology **274:**213-219.

40. **Kaminsky, S. G., I. Nakamura, and G. Cudkowicz.** 1985. Genetic control of the natural killer cell activity in SJL and other strains of mice. J. Immunol. **135:**665-671.

41. **Kaminsky, S. G., I. Nakamura, and G. Cudkowicz.** 1983. Selective defect of natural killer and killer cell activity against lymphomas in SJL mice: low responsiveness to interferon inducers. J. Immunol. **130:**1980-1984.

42. **Karupiah, G.** 1998. Type 1 and type 2 cytokines in antiviral defense. Vet. Immunol. Immunopathol. **63:**105-9.

43. **Khan, W. N., F. W. Alt, R. M. Gerstein, B. A. Malynn, I. Larsson, G. Rathbun, L. Davidson, S. Muller, A. B. Kantor, L. A. Herzenberg, F. S. Rosen, and P. Sideras.** 1995. Defective B cell development and function in Btk-deficient mice. Immunity **3:**283-299.

44. **Khan, W. N., P. Sideras, F. S. Rosen, and F. W. Alt.** 1995. The role of Bruton's tyrosine kinase in B-cell development and function in mice and man. Ann. N.Y. Acad. Sci. **764:**27-38.

45. **Kim, M., and K. Kim.** 2002. Diversity and complexity of CD8+ T cell responses against a single epitope of adenovirus E1B. Virology **295:**238-49.

46. **Kring, S. C., C. S. King, and K. R. Spindler.** 1995. Susceptibility and signs associated with mouse adenovirus type 1 infection of adult outbred Swiss mice. J. Virol. **69:**8084-8088.

47. **Kring, S. C., and K. R. Spindler.** 1990. Sequence of mouse adenovirus type 1 DNA encoding the amino terminus of protein IVa2. Nucleic Acids Res. **18:**4003.

48. **Luker, G. D., J. L. Prior, J. Song, C. M. Pica, and D. A. Leib.** 2003. Bioluminescence imaging reveals systemic dissemination of herpes simplex virus type 1 in the absence of interferon receptors. J. Virol. **77:**11082-10093.

49. **MacLennan, I. C.** 1998. B-cell receptor regulation of peripheral B cells. Curr. Opin. Immunol. **10:**220-5.

50. **Margolis, G., L. Kilham, and E. M. Hoenig.** 1974. Experimental adenovirus infection of the mouse adrenal gland. I. Light microscopic observations. Am. J. Pathol. **75:**363-372.

51. **Meissner, J. D., G. N. Hirsch, E. A. LaRue, R. A. Fulcher, and K. R. Spindler.** 1997. Completion of the DNA sequence of mouse adenovirus type 1: Sequence of E2B, L1, and L2 (18-51 map units). Virus Res. **51:**53-64.

52. **Miller, G., S. Lahrs, V. G. Pillarisetty, A. B. Shah, and R. P. DeMatteo.** 2002. Adenovirus infection enhances dendritic cell immunostimulatory properties and induces natural killer and T-cell-mediated tumor protection. Cancer Res. **62:**5260-5266.

53. **Molinier-Frenkel, V., R. Lengagne, F. Gaden, S. S. Hong, J. Choppin, H. Gahery-Segard, P. Boulanger, and J. G. Guillet.** 2002. Adenovirus hexon protein is a potent adjuvant for activation of a cellular immune response. J. Virol. **76:**127-35.

54. **Mond, J. J., I. Scher, D. E. Mosier, M. Baese, and W. E. Paul.** 1978. T-independent responses in B cell-defective CBA/N mice to Brucella abortus and to trinitrophenyl (TNP) conjugates of Brucella abortus. Eur. J. Immunol. **8:**459-463.

55. **Mrkic, B., J. Pavlovic, T. Rülicke, P. Volpe, C. J. Buchholz, D. Hourcade, J. P. Atkinson, A. Aguzzi, and R. Cattaneo.** 1998. Measles virus spread and pathogenesis in genetically modified mice. J. Virol. **72:**7420-7427.

56. **Muller, U., U. Steinhoff, L. F. L. Reis, S. Hemmi, J. Pavlovic, R. M. Zinkernagel, and M. Aguet.** 1994. Functional role of type I and type II interferons in antiviral defense. Science **264:**1918-1921.

57. **Petro, J. B., R. M. Gerstein, J. Lowe, R. S. Carter, N. Shinners, and W. N. Khan.** 2002. Transitional type 1 and 2 B lymphocyte subsets are differentially responsive to antigen receptor signaling. J. Biol. Chem. **277:**48009-19.

58. **Pirofski, L., M. S. Horwitz, M. D. Scharff, and S. M. Factor.** 1991. Murine adenovirus infection of SCID mice induces hepatic lesions that resemble human Reye syndrome. Proc. Natl. Acad. Sci. USA **88:**4358-4362.

59. **Qureshi, S. T., E. Skamene, and E. Malo.** 1999. Comparative genomics and host resistance against infectious diseases. Emerg. Infect. Dis. **5:**36-43.

60. **Raj, N. B., S. C. Cheung, I. Rosztoczy, and P. M. Pitha.** 1992. Mouse genotype affects inducible expression of cytokine genes. J. Immunol. **148:**1934-40.

61. **Rowe, W. P., R. J. Huebner, L. K. Gilmore, R. H. Parrot, and T. G. Ward.** 1953. Isolation of a cytopathic agent from human adenoids undergoing spontaneous degeneration in tissue culture. Proc. Soc. Exp. Biol. Med. **84:**570-573.

62. **Ryman, K. D., W. B. Klimstra, K. B. Nguyen, C. A. Biron, and R. E. Johnston.** 2000. Alpha/beta interferon protects adult mice from fatal Sindbis virus infection and is an important determinant of cell and tissue tropism. J. Virol. **74:**3366-3378.

63. **Samuel, C. E.** 2001. Antiviral actions of interferons. Clin. Microbiol. Rev. **14:**778-809.

64. **Sanna, P. P., and D. R. Burton.** 2000. Role of antibodies in controlling viral disease: Lessons from experiments of nature and gene knockouts. J. Virol. **74:**9813-9817.

65. **Shenk, T. E.** 2001. Adenoviridae: the viruses and their replication, p. 2265-2300. *In* D. M. Knipe and P. M. Howley (ed.), Fields Virology, 4th ed, vol. 2. Lippincott Williams & Wilkins, Philadelphia.

66. **Smith, K., C. C. Brown, and K. R. Spindler.** 1998. The role of mouse adenovirus type 1 early region 1A in acute and persistent infections in mice. J. Virol. **72:**5699-5706.

67. **Sparer, T. E., R. A. Tripp, D. L. Dillehay, T. W. Hermiston, W. S. Wold, and L. R. Gooding.** 1996. The role of human adenovirus early region 3 proteins (gp19K, 10.4K, 14.5K, and 14.7K) in a murine pneumonia model. J. Virol. **70:**2431-2439.

68. **Spindler, K. R., L. Fang, M. L. Moore, C. C. Brown, G. N. Hirsch, and A. K. Kajon.** 2001. SJL/J mice are highly susceptible to infection by mouse adenovirus type 1. J. Virol. **75:**12039-12046.

69. **Steinhoff, U., U. Muller, A. Schertler, H. Hengartner, M. Aguet, and R. M. Zinkernagel.** 1995. Antiviral protection by vesicular stomatitis virus-specific antibodies in alpha/beta interferon receptor-deficient mice. J. Virol. **69:**2153-2158.

70. **Szomolanyi-Tsuda, E., J. D. Brien, J. E. Dorgan, R. L. Garcea, R. T. Woodland, and R. M. Welsh.** 2001. Antiviral T-cell-independent type 2 antibody responses induced *in vivo* in the absence of T and NK cells. Virology **280:**160-168.

71. **Szomolanyi-Tsuda, E., and R. M. Welsh.** 1996. T cell-independent antibody-mediated clearance of polyomavirus in T cell-deficient mice. J. Exp. Med. **280:**160-168.

72. **Szomolanyi-Tsuda, E., and R. M. Welsh.** 1998. T-cell-independent antiviral antibody responses. Curr. Op. Immunol. **10:**431-435.

73. **Tyler, K. L., and B. N. Fields.** 1996. Pathogenesis of viral infections, p. 173-218. *In* B. N. Fields, D. M. Knipe, and P. M. Howley (ed.), Fields Virology, Third ed. Lippincott-Raven, Philadelphia.

74. **van der Veen, J., and A. Mes.** 1973. Experimental infection with mouse adenovirus in adult mice. Arch. Gesamte Virusforsch. **42:**235-241.

75. **Vilcek, J., and G. C. Sen.** 1996. Interferons and other cytokines, p. 375-399. *In* B. N. Fields, D. M. Knipe, and P. M. Howley (ed.), Fields Virology, Third ed. Lippincott-Raven, Philadelphia.

76. **Walls, T., A. G. Shankar, and D. Shingadia.** 2003. Adenovirus: an increasingly important pathogen in paediatric bone marrow transplant patients. Lancet Infect. Dis. **3:**79-86.

77. **Wang, B.** 1993. Characteristics of intrathymic B cells in normal and chimera mice. Hokkaido Igaku Zasshi **68:**496-506.

78. **White, P., S. A. Liebhaber, and N. E. Cooke.** 2002. 129X1/SvJ mouse strain has a novel defect in inflammatory cell recruitment. J. Immunol. **168:**869-874.

79. **Wigand, R.** 1980. Age and susceptibility of Swiss mice for mouse adenovirus, strain FL. Arch. Virol. **64:**349-358.

80. **Winters, A. L., and H. K. Brown.** 1980. Duodenal lesions associated with adenovirus infection in athymic "nude" mice. Proc. Soc. Exp. Bio. Med. **164:**280-286.

81. **Winters, A. L., H. K. Brown, and J. K. Carlson.** 1981. Interstitial pneumonia induced by a plaque-type variant of mouse adenovirus. Proc. Soc. Exp. Biol. Med. **167:**359-364.

82. **Yang, Y., F. A. Nunes, K. Berencsi, E. E. Furth, E. Gönczöl, and J. M. Wilson.** 1995. Cellular immunity to viral antigens limits E1-deleted adenoviruses for gene therapy. Proc. Natl. Acad. Sci. USA **91:**4407-4411.

83. **Ying, B., K. Smith, and K. R. Spindler.** 1998. Mouse adenovirus type 1 early region 1A is dispensable for growth in cultured fibroblasts. J. Virol. **72:**6325-6331.

84. **Zinkernagel, R. M., and H. Hengartner.** 2001. Regulation of the immune response by antigen. Science **293:**251-253.

85. **Zotlick, P. W., N. Chirmule, M. A. Schnell, G.-P. Gao, J. V. Hughes, and J. M. Wilson.** 2001. Biology of E1-deleted adenovirus vectors in nonhuman primate muscle. J. Virol. **75:**5222-5229.

CHAPTER 2

T CELLS CAUSE ACUTE IMMUNOPATHOLOGY AND ARE REQUIRED FOR LONG TERM SURVIVAL IN MOUSE ADENOVIRUS TYPE 1-INDUCED ENCEPHALOMYELITIS[1]

[1] Moore, M.L., Brown, C.C., and K. R. Spindler. 2003. J. Virol. 77: 10060-10070.

ABSTRACT

Infection of adult C57BL/6 (B6) mice with mouse adenovirus type 1 (MAV-1) results in dose-dependent encephalomyelitis. Utilizing immunodeficient mice, we analyzed the roles of T cells, T cell subsets, and T cell-related functions in MAV-1-induced encephalomyelitis. T cells, major histocompatibility complex (MHC) class I, and perforin contributed to acute disease signs at 8 days post-infection (p.i.). Acute MAV-1-induced encephalomyelitis was absent in mice lacking T cells and mice lacking perforin. Mice lacking α/β T cells had higher levels of infectious MAV-1 at 8 days, 21 days, and 12 weeks p.i, and these mice succumbed to MAV-1-induced encephalomyelitis at 9 to 16 weeks p.i. Thus α/β T cells were required for clearance of MAV-1. MAV-1 was cleared in mice lacking perforin, MHC class I or II, $CD4^+$ T cells, or $CD8^+$ T cells. Our results are consistent with a model in which either $CD8^+$ or $CD4^+$ T cells are sufficient for clearance of MAV-1. Furthermore, perforin contributed to MAV-1 disease but not viral clearance. We have established two critical roles for T cells in MAV-1-induced encephalomyelitis. T cells caused acute immunopathology and were required for long term host survival of MAV-1-infection.

INTRODUCTION

Most insights into adenovirus pathogenesis have come from natural infections because adenoviruses are species specific. A better understanding of how adenoviruses interact with the host immune system would be beneficial because adenoviruses are important human pathogens (30) and because the immune system limits the efficacy of adenovirus-mediated gene therapy (80). In fact a greater appreciation of the immunogenicity of adenoviruses has led to the use of adenovirus vectors in immunotherapy/therapeutic vaccine strategies (51). Determining how

adenoviruses and T cells interact will improve strategies for adenovirus-mediated immunotherapy. Mouse adenovirus type 1 (MAV-1) provides an ideal model system for the investigation of adenovirus-host interactions at the level of immunity.

Study of MAV-1 permits the examination of a replicating adenovirus in vivo. The double-stranded, linear DNA genome of MAV-1 is similar to those of human adenoviruses (hAds) in overall organization (50). The virus causes acute and persistent infections in mice (reviewed in 64). Doses as low as 1-100 PFU cause fatal disease in newborn and adult mice, and disease outcomes depend on the dose and strain of virus and the strain of mice infected (24, 45, 56, 66). Inoculation of adult immunocompetent mice with wild-type MAV-1 results in a systemic infection of cells of the mononuclear phagocyte system and endothelial cells of the microvasculature (11, 39). In adult C57BL/6 (B6) mice, this leads to dose-dependent encephalomyelitis (24). Brains of infected mice exhibit perivascular edema, and moribund infected mice also exhibit endothelial cell reactivity, vasculitis, vascular wall degeneration, and viral inclusion bodies (11, 24, 39, 45, 66). Although MAV-1 can be detected in organs throughout the mouse, the highest levels of virus are found in the spleen and central nervous system (45, 63). In situ hybridization and immunohistochemistry have shown that the virus is excluded from B cells and T cells in the spleen (39). The endothelial tropism of MAV-1 is striking: the virus has not been observed in the brain parenchyma and is restricted to the vascular endothelium (11, 24, 39).

The immune response to acute MAV-1 infection involves innate (10), cellular (32, 34), and humoral (14) immunity. By 96 hours post-infection (p.i.), brains of B6 mice infected with MAV-1 have increased levels of mRNAs of the cytokines interleukin-1, tumor necrosis factor alpha, lymphotoxin, and interleukin-6; the chemokines IP-10, MCP-1, MIP-1α, MIP-1β, and

RANTES; and the chemokine receptors CCR1 to -5 (10, 11). Neutralizing and complement-fixing antibodies are detected 2-3 weeks p.i. in adult mice infected with MAV-1, and antibody titers decline after 24 months (68). Sublethally infected adult mice develop MAV-1-specific cytotoxic T cells (CTL) that are detectable at 4 days p.i, peak at 10 days p.i, then rapidly decline (31-34). Inbred mouse strains have been identified that are resistant and susceptible to MAV-1, and sublethal irradiation of resistant C3H/HeJ mice renders them susceptible (66). Taken together, these studies suggest that immune responses are determinants of MAV-1 pathogenesis. However the role of these processes in MAV-1 disease is largely unexplored.

T cells can limit pathology due to viral infection and/or cause collateral pathologic damage in the context of acute (13, 40) and persistent (28, 54) viral infections. The balance between an effective antiviral T-cell response and T-cell-mediated immunopathogy is critical for host survival. The parameters that govern this balance vary among virus-host systems (26, 53). However the kinetics and abundance of viral antigen presentation in secondary lymphoid tissue and the effects of costimulatory host molecules are key determinants of T-cell activation (reviewed in 36, 79). Cell-mediated immunity (CMI) describes the effector functions of T cells, and these can be broadly classified into two types: cytotoxicity and cytokine production. αβ $CD8^+$ T cells can undergo differentiation into effector CTL by a major histocompatibility complex (MHC) class I-dependent process, and they deliver cytotoxic granule proteins such as perforin to target cells (reviewed in 38). $CD8^+$ T cells can also produce antiviral cytokines (reviewed in 25). αβ $CD4^+$ T cells interact with peptide-MHC class II molecules on the surface of antigen presenting cells (APCs) to become potent cytokine producers, and $CD4^+$ effector T cells can have cytotoxic potential (2). γδ T cells are largely double negative for CD4 and CD8, are abundant in epithelial tissues, are excluded from the lymphoid parenchyma, can recognize

antigens in the absence of MHC, and can secrete cytokines or mediate cytotoxic cell killing (reviewed in 29).

Using available immunodeficient mice, we evaluated the roles of T cells, T-cell subsets, MHC class I, MHC class II, and perforin in protection from and contribution to MAV-1 disease. Mice lacking α/β or α/β and γ/δ T cells were resistant to acute disease, exhibited less acute histopathology than control mice, failed to limit MAV-1 replication, and succumbed at 9 to 16 weeks p.i. Mice lacking MHC class I function were resistant to acute disease signs although they had higher viral loads than control mice in the acute phase. Mice lacking MHC class I function eventually cleared MAV-1. Mice lacking perforin showed fewer acute disease signs than controls but cleared MAV-1 similarly. No difference between control and MHC class II-deficient mice was detected. Our observations establish two critical roles for T cells in MAV-1-induced encephalomyelitis. T cells contributed to acute immunopathology and were required for long-term host survival in MAV-1-infected mice.

MATERIALS AND METHODS

Virus and mice. Wild-type MAV-1, originally obtained from S. Larsen (5), was grown and passaged in NIH 3T6 fibroblasts, and titers of viral stocks were determined by plaque assay on 3T6 cells as previously described (9). All animal work complied with all relevant federal and institutional policies. C57BL/6J (B6), B6.129S-*Tcra*^{tm1Mom} (T-cell receptor alpha-negative [TCRα$^{-/-}$]), B6.129P-*Tcrb*^{tm1Mom}*Tcrd*^{tm1Mom} (TCRβxδ$^{-/-}$), B6.129P2-*Tcrd*^{tm1Mom} (TCRδ$^{-/-}$), C57BL/6-*Pfp*^{tm1Sdz} (perforin-negative [Pfp$^{-/-}$]), B6.129S6-*Cd4*^{tm1Knw} (CD4$^{-/-}$), and B6.129S2-*Cd8a*^{tm1Mak} (CD8$^{-/-}$) mice were purchased from the Jackson Laboratory. B6.129-Abb^{tm1}N5 (MHC class II-deficient) and B6.129P2-*B2m*^{tm1}N5 (MHC class I-deficient)

mice were purchased from Taconic. C57BL/6NCr (B6) mice were purchased from the National Cancer Institute. In all assays we have done to date on infected B6/J or B6/NCr mice, the two strains have behaved indistinguishably (this work and data not shown). These include survival experiments, viral growth, histopathology, and in situ hybridization. Mice were infected with the indicated doses by the intraperitoneal (i.p.) route in a volume of 0.1 ml of phosphate-buffered saline. Mice were housed in microisolator cages, age and sex matched, and infected between 4-6 weeks of age. Infected mice were scored twice daily for the presence or absence of any disease signs, i.e., hunched posture, ataxia, ruffled fur, and also, in moribund mice, abdominal breathing, hindlimb paralysis, seizure, tremor. Moribund mice were euthanized by CO_2 asphyxiation.

Quantitation of virus from organs. Organs were harvested aseptically from euthanized mice, and homogenates were prepared as described previously (66). Virus was titrated by plaque assay on 3T6 cells as previously described (9). Briefly, 20 to 200 mg of tissue was homogenized in phosphate-buffered saline in a microcentrifuge tube by using a plastic pestle and sterile sand. Organ homogenates (5 to 10% wt/vol) were serially diluted and assayed. The means of the log titers were compared by a two-tailed *t* test, assuming equal variance. Counts of fewer than 20 plaques per 60 mm diameter plate were considered unreliable. Therefore, 2×10^3 PFU/g of tissue was calculated as the detection limit. Values below the detection limit were excluded from statistical analyses (calculations of means and t test statistics).

Histology. The following organs were harvested and fixed in 10% formalin: spleen, kidney, liver, small and large intestine, Peyer's patches, mandibular lymph nodes, thymus, lung, heart, and brain. Tissues were formalin fixed and paraffin embedded as previously described (39). Hematoxylin and eosin (H-E)-stained sections were viewed by light microscopy.

ISH. In situ hybridization (ISH) was performed as previously described (39). Briefly, sections were deparaffinized, rehydrated, digested with proteinase K, and probed with an antisense digoxigenin riboprobe transcribed from a segment of the E3 region inserted into pBluescript SK(-) vector. Following hybridization, slides were incubated with antidigoxigenin-alkaline phosphatase (Boehringer Mannheim), and the substrate nitroblue tetrazolium and 5-bromo-4-chloro-3-indolylphosphate (Boehringer Mannheim) was added. Slides were lightly counterstained with hematoxylin and coverslipped with Permount.

PCR and reverse transcription-PCR (RT-PCR). For DNA isolation, approximately 50 mg of tissue was incubated overnight at 55^{O} C in 700 μl of 50 mM Tris pH 8.0-100 mM EDTA-100 mM NaCl-1% sodium docecyl sulfate-0.5 mg of proteinase K per ml. Samples were mixed with an equal volume of phenol and then centrifuged 18,400 X g for 5 min at room temperature. The aqueous layer was mixed with an equal volume of chloroform-isoamyl alcohol (24:1). The aqueous layer was precipitated with 95% ethanol and washed once with 70% ethanol. The pellets were air dried and resuspended in 100 μl 0.1X SSC (1X SSC is 0.15M NaCl plus 0.015M sodium citrate) at 65^{O} C. For RNA isolation, approximately 50 mg of harvested tissue stored in RNAlater (Ambion) was homogenized in 900 μl of TRI Reagent (Molecular Research Center, Inc.) at room temperature in a microcentrifuge tube using sterile sand and a plastic pestle. Sand and tissue debris were removed by centrifugation (5 min, 700 X *g*), and RNA was isolated according to the manufacturer's instructions. Positive control RNA was prepared as previously described (8) from 3T6 fibroblasts infected with MAV-1 at a multiplicity of infection of 5.

For PCR analysis, 1 μg of DNA obtained from spleen or brain was used as template in a 55-cycle reaction. Reaction conditions and the MAV-1 E3-specific primers MAVR24718 and MAVR25148 were as described previously (66). For RT-PCR analysis, spleen and brain RNA

were reverse-transcribed with avian myeloblastosis virus reverse transcriptase as previously described (6) and PCR amplified in a 35-cycle reaction. MAVR24718 and MAVR25148 span an E3 intron and therefore can be used to distinguish cDNA from any contaminating genomic DNA. PCR and RT-PCR products were visualized on 7% polyacrylamide gels.

RESULTS

Virulence of acute MAV-1 infection in B6 and mutant mouse strains. Since in various virus-host systems T cells can be important for viral clearance and can cause immunopathology, we wanted to determine whether the clinical outcome of MAV-1 infection was altered in T-cell-deficient mice. Mice were infected intraperitoneally at various doses and monitored for disease signs and mortality at 8 days p.i. This time point corresponds to the acute phase of infection. The dose-dependent mortality of control mice listed in Table 2.1 agrees with published MAV-1 50% lethal doses for B6 mice (24, 66). TCR$\alpha^{-/-}$ mice lack α/β T cells, and TCRβx$\delta^{-/-}$ mice lack both α/β and γ/δ T cells (52). Unlike MAV-1-infected control mice, MAV-1-infected TCR$\alpha^{-/-}$ and TCRβx$\delta^{-/-}$ mice exhibited no clinical disease signs up to 8 days p.i. at all doses tested (Table 2.1). Also, TCRβx$\delta^{-/-}$ mice infected with 10^4 PFU of MAV-1 exhibited 100% survival at 8 days p.i, in contrast to control mice (Table 2.1). To dissect what α/β T cell-function could be contributing to MAV-1 disease, we infected mice deficient for certain T-cell subsets and CMI functions. α/β T-cell development depends on the surface expression of MHC molecules (23, 44, 59). Mice with targeted mutation of the MHC class II A_β^b gene have a deficiency in $CD4^+$ T cells and MHC class II-dependent CMI (23). Mice with a targeted disruption of the β_2-microglobulin (β_2m) gene are deficient in $CD8^+$ T cells and MHC class I-dependent CMI (44). $\beta_2m^{-/-}$ mice are also deficient for CD1 expression and lack NKT cells (7, 12). ($A_\beta^{b\ -/-}$ and $\beta_2m^{-/-}$

mice will hereafter be referred to according to their primary deficiencies, i.e., MHC class II and I, respectively, although these mice have deficiencies in specific T cell subsets. We acknowledge that immunodeficient mice used in these studies may also have other, uncharacterized phenotypes that could alter MAV-1 pathogenesis.) There was no difference in the proportion of survival between control and MHC class II-deficient mice, and they had similar disease signs (Table 2.1). In contrast, MHC class I-deficient mice showed no disease signs up to 8 days p.i. (Table 2.1). We tested the role of perforin, a cytolytic pore-forming protein known to be secreted by effector $CD8^+$ T cells (20), $CD4^+$ T cells (2, 72), and NK cells (62). Mice lacking perforin ($Pfp^{-/-}$) were resistant to acute MAV-1 disease, showing no disease signs or mortality at 8 days p.i. (Table 2.1). Together, the observations with mice lacking perforin, MHC class I function, and T cells indicate that acute MAV-1 disease is dependent on MHC class I and lymphocyte-mediated cytotoxicity.

Quantitation of infectious virus from organs of acutely infected B6 and mutant mouse strains. We tested whether the altered virulence of MAV-1 in immunodeficient mice compared to B6 controls correlated with the level of virus replication in tissues of MAV-1-infected mice. MAV-1 replicates to highest levels in the spleen and central nervous system (39, 45). We harvested spleens and brains of infected mice and titrated infectious virus by plaque assay. There was no difference in viral titers in spleens and brains between B6 mice and mice lacking α/β T cells 6 days p.i. (Figure 2.1A) or in mice lacking α/β and γ/δ T cells 7 days p.i (Figure 2.1B). Figure 2.1C shows that at 8 days p.i. viral titers in spleens and brains of mice lacking α/β T cells were higher than in B6 mice. Similar to the T-cell-deficient mice assayed 8 days p.i. in Table 2.1, the T-cell-deficient mice in Figure 2.1 exhibited no disease signs 6 to 8 days p.i., whereas control mice exhibited typical dose-dependent MAV-1 disease signs (Table 2.1 and data

not shown). We tested the role of MHC class I in limiting MAV-1 replication. Figure 2.1D shows that at 8 days p.i. levels of infectious virus were the same in spleens of MHC class I-deficient and B6 mice, but there was more virus in the brains of MHC class I-deficient mice (P = 0.03).

We tested the role of perforin in limiting MAV-1 replication. Figure 2.1E shows that perforin did not play a role in control of MAV-1 replication at 8 days p.i., because levels of virus were the same in spleens and brains of control and $Pfp^{-/-}$ mice. We tested whether MHC class II has a role in limiting MAV-1 replication. At 9 days p.i., there was no detectable infectious virus in MHC class II-deficient or B6 spleens and brains (data not shown), suggesting that control of MAV-1 in the acute phase does not depend on MHC class II. Together the data indicate that control of acute MAV-1 replication was T cell-dependent, but perforin and MHC class II independent.

Histopathology and ISH analysis of acutely infected T-cell-deficient, perforin-deficient, and control mice. Since T-cell- and perforin-deficient mice had altered MAV-1 disease phenotypes compared to B6 controls (Table 2.1), we assessed the histological evidence of MAV-1 disease in these mice. Figure 2.2A to D show representative histopathology and ISH of brain sections of B6 and TCRβxδ$^{-/-}$ mice infected with 700 PFU and harvested 7 days p.i. (same mice as Fig. 2.1B). In infected B6 mice there was perivascular edema, vascular wall degeneration, and small numbers of inflammatory cells in the brain (Figure 2.2A). In contrast, the microvasculature of infected TCRβxδ$^{-/-}$ brains appeared normal (Fig. 2.2C). This strongly suggests that T cells mediate acute immunopathology in the brain. H-E staining of mock-infected B6 brain is shown in Fig. 2.2E. Mock-infected brains of all strains in Fig. 2.2 had a similar appearance (data not shown). We assessed the cell tropism of MAV-1 in the presence and absence of T cells by an ISH assay. Figures 2.2B and D show that there was similar ISH-staining of viral nucleic acid in

brain microvascular endothelial cells of both control and TCRβxδ$^{-/-}$ mice. Similarly, in other tissues no difference in cell tropism between control and TCRβxδ$^{-/-}$ mice was observed (data not shown). Figures 2.2E to L show histopathology and ISH of brains sections from B6 and Pfp$^{-/-}$ mice mock infected or infected with 10^4 PFU of MAV-1 and harvested 8 days p.i. (same mice as Fig. 2.1E). In infected Pfp$^{-/-}$ brains, there was minimal inflammation (Fig. 2.2G). In contrast, the microvasculature of infected B6 brains exhibited large numbers of inflammatory cells, perivascular edema, and vascular wall degeneration (Fig. 2.2I, K, and L). Brain endothelial cell staining for MAV-1 nucleic acid was not different between control and Pfp$^{-/-}$ mice at 8 days p.i, indicating that there was no difference in the cell tropism of MAV-1 between these mice (Fig. 2.2H and J). Taken together, the data show that acute MAV-1 encephalomyelitis correlated with the presence of T cells and perforin and not the level of infectious virus (Fig. 2.1B and E and 2.2A to L).

Long-term infection of T-cell-deficient mice. Mice lacking α/β or α/β and γ/δ T cells succumbed to MAV-1 infection at 9 to 16 weeks p.i. (Figure 2.3). Moribund T-cell-deficient mice exhibited typical signs of MAV-1 encephalomyelitis, such as ataxia, ruffled fur, hindlimb paralysis, and tremor. Interestingly, all MHC class II-deficient, MHC class I-deficient, and Pfp$^{-/-}$ mice that survived the acute phase of MAV-1 infection survived past 12 weeks p.i. and showed no disease signs (data not shown). To directly assess the contribution of CD4$^+$ and CD8$^+$ T cells to protection from MAV-1 we infected CD4$^{-/-}$ mice and CD8$^{-/-}$ mice. These mice did not succumb to MAV-1 infection; they survived to 12 weeks p.i. (Fig 2.3C). Fig. 2.3D shows that mice lacking α/β T cells succumbed to MAV-1 infection 9 to 15 weeks p.i. whereas mice lacking γ/δ T cells survived. Thus, α/β T cells were required for long term survival of MAV-1

infection, but γ/δ T cells, perforin, MHC class I function, MHC class II function, $CD8^+$ T cells, and $CD4^+$ T cells were not.

Replication of MAV-1 in long-term-infected T-cell-deficient mice and persistence of MAV-1 in B6 mice. We determined the level of infectious virus in long-term-infected T-cell-deficient mice. High levels of virus were detected in spleen and brain 3 weeks p.i. in $TCR\alpha^{-/-}$ mice, relative to undetectable infectious virus in organs of B6 mice (Fig. 2.4A). Figure 4B shows titration of infectious virus from the $TCR\beta x\delta^{-/-}$ mice shown in Figure 2.3A that were euthanized when moribund at 9 to 12 weeks p.i. Attempts to isolate infectious virus from organs of long-term-infected B6, MHC class II-deficient, and MHC class I-deficient mice yielded no plaques even when organ homogenates were blind passaged sequentially 2 to 3 times on 3T6 cells (data not shown). Figure 2.4C shows quantitation of infectious virus from spleens and brains of mice surviving to 12 weeks p.i. and shown in Figure 2.3C. No infectious virus was recovered from B6, $CD8^{-/-}$, and $CD4^{-/-}$ mice, whereas high titers were recovered from the two surviving $TCR\beta x\delta^{-/-}$ mice. Although infectious MAV-1 was undetectable in B6 mice 12 weeks p.i, we used PCR to assay B6 brains and spleens for MAV-1 DNA and mRNA at 12 weeks p.i. Figure 2.5 shows the presence of MAV-1 DNA and early region 3 (E3) MAV-1 mRNA in B6 mice at 12 weeks p.i. Thus, in spleens and brains of B6 mice, MAV-1 DNA persists, but if infectious virus is produced it is not lethal. In contrast, virus replicates to high levels and is lethal in mice lacking α/β T cells (both $TCR\alpha^{-/-}$ and $TCR\beta x\delta^{-/-}$).

Histopathology and ISH analysis of long-term-MAV-1-infeced T-cell-deficient and control mice. Fig. 2.2M to T show histopathology and ISH of brain and liver sections from B6 and $TCR\beta x\delta^{-/-}$ mice infected with 700 PFU of MAV-1 and euthanized at 12 weeks p.i. (same mice as for Fig. 2.3C and 2,4C). There was no histological evidence of disease or MAV-1 nucleic acid

as detected by ISH in B6 brains (Fig. 2.2M and 2.2N) and livers (Fig. 2.2O and 2.2P). There was also no histological evidence of disease or positive ISH staining in $CD4^{-/-}$ mice and $CD8^{-/-}$ mice at 12 weeks p.i. (data not shown). In contrast, there was evidence of typical MAV-1 encephalomyelitis in the brains of $TCR\beta x\delta^{-/-}$ mice (Fig. 2.2Q), and viral nucleic acid was observed in brain endothelial cells by ISH (Fig. 2.2R). The livers of B6 and $TCR\beta x\delta^{-/-}$ mice appeared histologically normal (Fig. 2.2O and 2.2S). However, MAV-1 nucleic acid was detectable in liver endothelial cells of $TCR\beta x\delta^{-/-}$ mice 12 weeks p.i, indicating disseminated MAV-1 replication in the absence of T cells (Fig. 2.2T).

DISCUSSION

This study was undertaken to determine the roles of T cells in MAV-1-induced encephalomyelitis. We have analyzed the pathogenesis of MAV-1 in mice deficient for T cells, T cell subsets, and T cell-related functions. Our results demonstrate that α/β T cells and perforin contribute to acute MAV-1 encephalomyelitis and that α/β T cells are required for control of MAV-1 replication and long term survival of infection. Our data suggest that mechanisms contributing to T-cell-mediated disease and T-cell-mediated clearance of MAV-1 are different.

CTL were implicated in contributing to disease severity in the acute phase of MAV-1 infection. Since α/β T-cell-deficient, α/β and γ/δ T-cell-deficient, MHC class I-deficient, and perforin-deficient mice were resistant to acute MAV-1 disease, whereas MHC class II-deficient mice were not resistant to MAV-1 disease (Table 2.1), we reason that $CD8^+$ CTL contributed to acute disease. Experiments to directly test this hypothesis and to assess the role of NK cells in perforin-mediated acute MAV-1 disease are in progress.

Mice with T cells had immunopathology in acute MAV-1 infection that was manifested as encephalomyelitis, and this was not seen in T-cell-deficient mice. Histological evidence of disease in MAV-1-infected B6 mice and the absence of such evidence in MAV-1-infected T-cell-deficient mice correlated with disease signs and not with viral titers (Fig. 2.1B, 2.2A, and 2.2C). Furthermore, at 7 days p.i. endothelial cell staining of viral nucleic acid in the brain was similar for control and TCRβxδ$^{-/-}$ animals (Figs 2.2B and D). Thus at 7 days p.i. mice without T cells had no acute disease but had levels of infectious MAV-1 and endothelial infection similar to mice with a normal T-cell compartment.

Perforin clearly contributed to immunopathology and disease but did not play a role in limiting MAV-1 replication. Pfp$^{-/-}$ mice exhibited less MAV-1-induced encephalomyelitis and showed fewer disease signs than control mice at 8 days p.i. (Table 2.1; Fig. 2.2G and I). Perforin-deficient mice, like TCRβxδ$^{-/-}$ and control mice, had brain endothelial staining for viral nucleic acid (Fig 2.2H and 2.2J). Levels of infectious MAV-1 were the same in spleens and brains of Pfp$^{-/-}$ and control mice at 8 days p.i. (Fig. 2.1E), and no infectious virus was recovered from Pfp$^{-/-}$ and control spleens and brains at 24 weeks p.i. (data not shown). The role of perforin in MAV-1-induced encephalomyelitis may be similar to the role of perforin in coxsackievirus B3 (CVB3)-induced myocarditis. Perforin-deficient mice are resistant to acute CVB3 disease and exhibit less myocarditis and inflammatory cell infiltration than controls, but perforin plays no role in clearance of CVB3 (21). This similarity in pathogenesis of CVB3 and MAV-1 is intriguing because both viruses infect endothelial cells. That Pfp$^{-/-}$ mice exhibit reduced cellular inflammation in response to MAV-1 (Fig. 2.2G and 2.2I) and CVB3 (21) compared to controls suggests that perforin may mediate inflammatory cell recruitment. Perforin may be less important for control of lytic viruses than for control of nonlytic viruses (38). Our results with

MAV-1 support this hypothesis. Although MAV-1 is cytopathic in vitro (27), it can replicate to high titers in vivo in the absence of T cells without extensive cellular damage (this report).

MHC class I-deficient mice had statistically higher levels of infectious MAV-1 than control mice in brains but not spleens at 8 days p.i. (Fig. 2.1D). However the effect of MHC class I deficiency on viral load was transient, because MHC class I-deficient mice cleared the virus by 12 weeks p.i. (data not shown). Resistance to acute disease and delayed but effective viral clearance from the brain have also been observed in MHC class I-deficient mice infected with neuroadapted Sindbis virus (43). Our data suggest that mechanisms limiting MAV-1 replication in the brain and spleen may differ. MAV-1 infects cells of the monocyte/macrophage lineage and endothelial cells of the microvasculature (24, 39). In spleens, MAV-1-infected cells identified by ISH or immunohistochemistry are more often macrophages than endothelial cells, whereas in brains, the MAV-1-infected cells are always endothelial (M. L. Moore, C. C. Brown, and K. R. Spindler, unpublished data). Further experiments are needed to clarify the role of MHC class I in limiting acute MAV-1 replication.

MHC class II was not required for control of viral load in MAV-1-infected mice. Like control mice, MHC class II-deficient mice cleared infectious MAV-1 by 9 days p.i. (data not shown). We know that MHC class II expression is required for antiviral immunoglobulin G detected at 12 weeks p.i. (Chapter 3, M.L. Moore and K.R. Spindler, unpublished data.) However, MHC class II-deficient and $CD4^{-/-}$ mice did not differ from controls in disease severity or levels of infectious virus in acute or long-term infection (Table 2.1 and data not shown). Taken together, the data on T cells, perforin, and MHC class I and II strongly suggest that $CD8^{+}$ CTL contribute to immunopathology by a perforin-dependent mechanism in acute MAV-1 encephalomyelitis.

Chemokine expression may mediate CTL responses and immunopathology in MAV-1-induced disease. Guida et al. showed that MAV-1 causes encephalomyelitis in B6 mice but not in BALB/c mice (24). Charles et al. then showed that brains and spleens of MAV-1-infected B6 mice have higher levels of chemokine and mRNA expression than brains and spleens of MAV-1-infected BALB/c mice (10). In that report, at 3 and 4 days p.i. the chemokine RANTES was highly expressed in MAV-1-infected B6 brains but was expressed at lower levels in MAV-1-infected BALB/c brains. We have also detected upregulated RANTES expression in B6 brains but not BALB/c brains at 9 days p.i. (M. L. Moore and K. R. Spindler, unpublished data). The chemokine RANTES attracts T cells and monocytes to sites of inflammation and is required for T-cell function (48). RANTES has been shown to contribute to immunopathology in mouse hepatitis virus-infected mice (46). We hypothesize that the differential chemokine responses between B6 and BALB/c mice result in an immunopathological T-cell response in B6 mice that does not occur in BALB/c mice.

α/β T cells were required for long-term survival of MAV-1 infection. Although α/β T cells contributed to early pathology through a perforin-dependent mechanism, α/β T-cell deficiency resulted in uncontrolled viral replication and eventual death. Thus, a regulated T-cell response is crucial for control of MAV-1 without pathology. TCRβxδ$^{-/-}$ and TCRα$^{-/-}$ mice, both lacking α/β T cells, succumbed to MAV-1 encephalomyelitis 9 to 16 weeks p.i. (Fig. 2.2Q and 2.3). MAV-1 was present at high levels in mice lacking α/β T cells (Fig. 2.1C and 2.4). In contrast, MHC class I-deficient, MHC class II-deficient, Pfp$^{-/-}$, CD8$^{-/-}$, CD4$^{-/-}$, and TCRδ$^{-/-}$ mice survived past twelve weeks (Fig 2.3C and 2.3D and data not shown), and infectious MAV-1 was undetectable from these strains of mice at 12 weeks p.i., even when organ homogenates were serially passaged on 3T6 cells (Fig 2.4C and data not shown). It is likely that either CD8^{+} T cells

or $CD4^+$ T cells alone are sufficient for clearance of MAV-1. $CD4^+$ T cell-independent activation of $CD8^+$ T cells has been experimentally demonstrated (70). An alternative hypothesis is that control of MAV-1 replication requires α/β T cells that express neither CD8 nor CD4. It has been suggested that double negative (CD8- CD4-) α/β T cells contribute to immunity to influenza virus in CD4-deficient mice (60).

One interpretation of the role of T cells in MAV-1 pathogenesis is that in the absence of α/β T cells, acute MAV-1 replication is not limited during the acute phase, and MAV-1 continues to replicate productively without causing morbidity and mortality until 9 to 16 weeks p.i. It is also possible that T cells are important for suppressing replication of persistent MAV-1. These two roles for T cells are not mutually exclusive. T cells have been shown to be important for protection against persistent viral infections (35, 54). For example, humans with specific T-cell deficiencies (e.g. DiGeorge syndrome and X-linked lymphoproliferative syndrome) are susceptible to productive infections of viruses that are normally persistent (4, 15, 16, 22). MAV-1 establishes persistent infections in outbred mice (reviewed in 64). In B6 mice, persistent MAV-1 DNA and mRNA were detected at 12 weeks p.i. (Fig. 2.5). It is not known whether the E3 mRNA detected in B6 spleens and brains at this time represents low-level chronic replication or whether MAV-1 can establish a latent phase in which E3 is transcribed. Sublethal irradiation of outbred mice persistently infected with MAV-1 results in increased levels of MAV-1 DNA (63). This suggests that replication of persistent MAV-1 is controlled by an immune mechanism.

Different T-cell subsets and effector functions can mediate immunopathology and viral clearance in various virus-host systems (19). However the signals and events leading to differential T-cell responses to viruses remain poorly understood. Since the immune system evolved to counter a variety of pathogens, comparative viral pathogenesis aids our understanding

of innate and adaptive immunity. Both $CD4^+$ and $CD8^+$ T cells have been shown to contribute to pathology in Sindbis virus (58), lymphocyte choriomeningitis virus (77), Borna disease virus (57), and mouse hepatitis virus (74) infections in mice, although the relative contributions of $CD4^+$ and $CD8^+$ T cells to pathology varies among these systems. Perforin-deficient mice have been shown to be resistant to acute disease induced by lymphocyte choriomeningitis virus (37), Murray Valley encephalitis virus (47), coxsackievirus B (21), cowpox virus (53), and MAV-1 (this report), but are susceptible to acute ectromelia virus infection (53). It is likely that factors such as the cell type(s) infected and mode of virus replication determine T cell responses to viruses (76). Like MAV-1, Hantaan virus targets macrophage/monocyte cells and endothelial cells (78), and its pathogenesis bears similarity to that of MAV-1. Both viruses establish persistent infections in mice, their natural host (18, 64), and both viruses cause acute encephalitis in adult B6 mice that is characterized by perivascular edema (compare Fig. 2 in this report to ref. 71). Infection of athymic nude mice with Hantaan virus resulted in prolonged virus replication compared to rapid clearance in BALB/c controls (3). These observations parallel results reported here. Macrophages and endothelial cells are both APCs known to express MHC class I and MHC class II molecules (1). Many viruses infect APCs; this strategy enables modulation of the host immune response, systemic dissemination, and viral persistence (19). Adenoviruses infect endothelial cells of many animal species, including cattle, moose, dog, cat, deer, chicken, pig, and 12 species of reptiles (41, 42, 55, 61, 65, 67, 69, 73). Our understanding of host immune responses will benefit from comparison of pathogenesis phenotypes induced by different viruses with similar target cell types.

We are pursuing identification of T-cell-dependent functions required for clearance of replicating MAV-1 and for survival of MAV-1 infection, such as the role of Fas ligand in T cell-

dependent clearance of MAV-1. Preliminary evidence indicates that the cytokine interferon gamma contributes to early protection but is dispensable for MAV-1 clearance and long-term host survival (M. L. Moore and K R. Spindler, unpublished data).

T cells are known to be involved in immune responses to natural and experimental hAd infections (reviewed in 30). In acute pediatric upper respiratory disease caused by hAds, a significant increase in T cells and NK cells was observed, leading Matsubara et al. (49) to suggest that increased T-cell activation may be a useful parameter for determining the severity of adenovirus infection. It is likely that T cells contribute to disease severity in acute hAd infections. CMI causes disease in the context of many acute viral infections in animal models (13, 46, 47, 58), and T cells are implicated in acute immunopathology in human viral disease (17). Also, in murine and primate models of hAd-mediated gene therapy, T cells are a primary cause of inflammation and cellular damage (75, 80). These observations suggest that T-cell immunopathology may be a general component of both human and mouse adenovirus-induced disease.

ACKNOWLEDGMENTS

We thank Gwen Hirsch, Adriana Kajon, Carla Pretto, James Stanton, Brian Waters, and Amanda Welton for technical assistance. We thank Keith Bishop, Lei Fang, Gary Huffnagle, Michael Imperiale, Steve Kunkel, and Rick Tarleton for critical review of the manuscript. This work was supported by NIH grant R01 AI023762 to K.R.S. and by an NIH predoctoral traineeship (GM 07103) and an ARCS Foundation Scholarship to M.L.M.

REFERENCES

1. **Abbas, A. K., A. H. Lichtman, and J. S. Pober.** 2000. Cellular and molecular immunology, 4th ed. W.B. Saunders Co., Philadelphia.

2. **Appay, V., J. J. Zaunders, L. Papagno, J. Sutton, A. Jaramillo, A. Waters, P. Easterbrook, P. Grey, D. Smith, A. J. McMichael, D. A. Cooper, S. L. Rowland-Jones, and A. D. Kelleher.** 2002. Characterization of CD4(+) CTLs ex vivo. J. Immunol. **168:**5954-5958.

3. **Asada, H., M. Tamura, K. Kondo, Y. Okuno, Y. Takahashi, Y. Dohi, T. Nagai, T. Kurata, and K. Yamanishi.** 1987. Role of T lymphocyte subsets in protection and recovery from Hantaan virus infection in mice. J. Gen. Virol. **68:**1961-1969.

4. **Asamoto, H., and M. Furuta.** 1977. Di George syndrome associated with glioma and two kinds of viral infection. N. Engl. J. Med. **296:**1235.

5. **Ball, A. O., C. W. Beard, P. Villegas, and K. R. Spindler.** 1991. Early region 4 sequence and biological comparison of two isolates of mouse adenovirus type 1. Virology **180:**257-265.

6. **Beard, C. W., and K. R. Spindler.** 1996. Analysis of early region 3 mutants of mouse adenovirus type 1. J. Virol. **70:**5867-5874.

7. **Bendelac, A., D. Killeen, D. R. Littman, and R. H. Schwartz.** 1994. A subset of CD4+ thymocytes selected by MHC class I molecules. Science **263:**1774-1778.

8. **Berk, A. J., F. Lee, T. Harrison, J. Williams, and P. A. Sharp.** 1979. Pre-early adenovirus 5 gene product regulates synthesis of early viral messenger RNAs. Cell **17:**935-944.

9. **Cauthen, A. N., and K. R. Spindler.** 1999. Construction of mouse adenovirus type 1 mutants, p. 85-103. *In* W. S. M. Wold (ed.), Adenovirus methods and protocols. Humana Press, Totowa, NJ.

10. **Charles, P. C., X. Chen, M. S. Horwitz, and C. F. Brosnan.** 1999. Differential chemokine induction by the mouse adenovirus type-1 in the central nervous system of susceptible and resistant strains of mice. J. Neurovirol. **5:**55-64.

11. **Charles, P. C., J. D. Guida, C. F. Brosnan, and M. S. Horwitz.** 1998. Mouse adenovirus type-1 replication is restricted to vascular endothelium in the CNS of susceptible strains of mice. Virology **245:**216-228.

12. **Chen, Y. H., N. M. Chiu, M. Mandal, N. Wang, and C. R. Wang.** 1997. Impaired NK1+ T cell development and early IL-4 production in CD1-deficient mice. Immunity **6:**459-467.

13. **Cole, G. A., N. Nathanson, and R. A. Prendergast.** 1972. Requirement for theta-bearing cells in lymphocytic choriomeningitis virus-induced central nervous system disease. Nature **238:**335-337.

14. **Coutelier, J.-P., P. G. Coulie, P. Wauters, H. Heremans, and J. T. M. van der Logt.** 1990. In vivo polyclonal B-lymphocyte activation elicited by murine viruses. J. Virol. **64:**5383-8388.

15. **Deerojanawong, J., A. B. Chang, P. A. Eng, C. F. Robertson, and A. S. Kemp.** 1997. Pulmonary diseases in children with severe combined immune deficiency and DiGeorge syndrome. Pediatr. Pulmonol. **24:**324-330.

16. **Dutz, J. P., L. Benoit, X. Wang, D. J. Demetrick, A. Junker, D. de Sa, and R. Tan.** 2001. Lymphocytic vasculitis in X-linked lymphoproliferative disease. Blood **97:**95-100.

17. **Ennis, F. A., J. Cruz, C. F. Spiropoulou, D. Waite, C. J. Peters, S. T. Nichol, H. Kariwa, and F. T. Koster.** Hantavirus pulmonary syndrome: CD8+ and CD4+ cytotoxic T lymphocytes to epitopes on Sin Nombre virus nucleocapsid protein isolated during acute illness. Virology **238:**380-390.

18. **Feuer, R., J. D. Boone, D. Netski, S. P. Morzunov, and S. C. St Jeor.** 1999. Temporal and spatial analysis of Sin Nombre virus quasispecies in naturally infected rodents. J. Virol. **73:**9544-9554.

19. **Flint, S. J., L. W. Enquist, R. M. Krug, V. R. Racaniello, and A. M. Skalka.** 2000. Principles of virology: Molecular biology, pathogenesis, and control. American Society for Microbiology, Washington, DC.

20. **Garcia-Sanz, J. A., G. Plaetinck, F. Velotti, D. Masson, J. Tschopp, H. R. MacDonald, and M. Nabholz.** 1987. Perforin is present only in normal activated Lyt2+ T lymphocytes and not in L3T4+ cells, but the serine protease granzyme A is made by both subsets. EMBO J. **6:**933-938.

21. **Gebhard, J. R., C. M. Perry, S. Harkins, T. Lane, I. Mena, V. C. Asensio, I. L. Campbell, and J. L. Whitton.** 1998. Coxsackievirus B3-induced myocarditis: perforin

exacerbates disease, but plays no detectable role in virus clearance. Am. J. Pathol. **153:**417-428.

22. **Gilger, M. A., D. O. Matson, M. E. Conner, H. M. Rosenblatt, M. J. Finegold, and M. K. Estes.** 1992. Extraintestinal rotavirus infections in children with immunodeficiency. J. Pediatrics **120:**912-917.

23. **Grusby, M. J., R. S. Johnson, V. E. Papaioannou, and L. H. Glimcher.** 1991. Depletion of $CD4^+$ T cells in major histocompatibility complex class II-deficient mice. Science **253:**1417-1420.

24. **Guida, J. D., G. Fejer, L.-A. Pirofski, C. F. Brosnan, and M. S. Horwitz.** 1995. Mouse adenovirus type 1 causes a fatal hemorrhagic encephalomyelitis in adult C57BL/6 but not BALB/c mice. J. Virol. **69:**7674-7681.

25. **Guidotti, L. G., and F. V. Chisari.** 2000. Cytokine-mediated control of viral infections. Virology **273:**221-227.

26. **Guidotti, L. G., R. Rochford, J. Chung, M. Shapiro, R. Purcell, and F. V. Chisari.** 1999. Viral clearance without destruction of infected cells during acute HBV infection. Science **284:**825-829.

27. **Hartley, J. W., and W. P. Rowe.** 1960. A new mouse virus apparently related to the adenovirus group. Virology **11:**645-647.

28. **Hausmann, J., W. Hallensleben, J. C. De La Torre, A. Pagenstechier, C. Zimmermann, H. Pircher, and P. Staeheli.** 1999. T cell ignorance in mice to Borna

disease virus can be overcome by peripheral expression of the viral nucleoprotein. Proc. Natl. Acad. Sci. USA **96:**9769-9774.

29. **Hayday, A. C.** 2000. γ/δ cells: a right time and a right place for a conserved third way of protection. Annu. Rev. Immunol. **18:**975-1026.

30. **Horwitz, M. S.** 2001. Adenoviruses, p. 2301-2326. *In* D. M. Knipe and P. M. Howley (ed.), Fields Virology, 4th ed, vol. 2. Lippincott Williams & Wilkins, Philadelphia.

31. **Inada, T., and H. Uetake.** 1978. Cell-mediated immunity assayed by ^{51}Cr release test in mice infected with mouse adenovirus. Infect. Immun. **20:**1-5.

32. **Inada, T., and H. Uetake.** 1980. Cell-mediated immunity to mouse adenovirus infection: Blocking of macrophage migration inhibition and T cell-mediated cytolysis of infected cells by anti-S antigen or anti-alloantigen serum. Microbiol. Immunol. **24:**525-535.

33. **Inada, T., and H. Uetake.** 1978. Cell-mediated immunity to mouse adenovirus infection: Macrophage migration inhibition test. Microbiol. Immunol. **22:**391-401.

34. **Inada, T., and H. Uetake.** 1978. Nature and specificity of effector cells in cell-mediated cytolysis of mouse adenovirus-infected cells. Infect. Immun. **22:**119-124.

35. **Iwashiro, M., K. Peterson, R. J. Messer, I. M. Stromnes, and K. J. Hasenkrug.** 2001. CD4(+) T cells and gamma interferon in the long-term control of persistent Friend retrovirus infection. J. Virol **75:**52-60.

36. **Kaech, S. M., E. J. Wherry, and R. Ahmed.** 2002. Effector and memory T-cell differentiation: Implications for vaccine development. Nat. Rev. Immunol. **2:**251-262.

37. **Kagi, D., B. Ledermann, K. Burki, P. Seiler, B. Odermatt, K. J. Olsen, E. R. Podack, R. M. Zinkernagel, and H. Hengartner.** 1994. Cytotoxicity mediated by T cells and natural killer cells is greatly impaired in perforin-deficient mice. Nature **369:**31-37.

38. **Kagi, D., B. Ledermann, K. Burki, R. M. Zinkernagel, and H. Hengartner.** 1996. Molecular mechanisms of lymphocyte-mediated cytotoxicity and their role in immunological protection and pathogenesis in vivo. Annu. Rev. Immunol. **14:**207-232.

39. **Kajon, A. E., C. C. Brown, and K. R. Spindler.** 1998. Distribution of mouse adenovirus type 1 in intraperitoneally and intranasally infected adult outbred mice. J. Virol. **72:**1219-1223.

40. **Kaplan, M. M., T. J. Wiktor, and H. Koprowski.** 1975. Pathogenesis of rabies in immunodeficient mice. J. Immunol. **114:**1761-1765.

41. **Kelly, W. R.** 1993. The liver and biliary system, p. 239-312. *In* K. V. F. Jubb, P. C. Kennedy, and N. Palmer (ed.), Pathology of domestic animals, 4th ed. Academic Press, San Diego, Calif.

42. **Kennedy, F. A., and T. P. Mullaney.** 1993. Disseminated adenovirus infection in a cat. J. Vet. Diagn. Invest. **5:**273-276.

43. **Kimura, T., and D. E. Griffin.** 2000. The role of CD8+ T cells and major histocompatibility complex class I expression in the central nervous system of mice infected with neuroadapted Sindbis virus. J. Virol. **74:**6117-6125.

44. **Koller, B. H., P. Marrack, J. W. Kappler, and O. Smithies.** 1990. Normal development of mice deficient in β2M, MHC class I proteins, and $CD8^+$ T cells. Science **248:**1227-1230.

45. **Kring, S. C., C. S. King, and K. R. Spindler.** 1995. Susceptibility and signs associated with mouse adenovirus type 1 infection of adult outbred Swiss mice. J. Virol. **69:**8084-8088.

46. **Lane, T. E., M. T. Liu, B. P. Chen, V. C. Asensio, R. M. Samawi, A. D. Paoleti, I. L. Campbell, S. L. Kunkell, H. S. Fox, and M. J. Buchmeier.** 2000. A central role for CD4+ T cells and RANTES in virus-induced central nervous system inflammation and demyelination. J. Virol. **74:**1415-1424.

47. **Licon Luna, R. M., E. Lee, A. Mullbacher, R. V. Blanden, R. Langman, and M. Lobigs.** 2002. Lack of both Fas ligand and perforin protects from flavivirus-mediated encephalitis in mice. J. Virol. **76:**3202-3211.

48. **Makino, Y., D. N. Cook, O. Smithies, O. Y. Hwang, E. G. Neilson, L. A. Turka, H. Sato, A. D. Wells, and T. M. Danoff.** 2002. Impaired T cell function in RANTES-deficient mice. Clin. Immunol. **102:**302-309.

49. **Matsubara, T., T. Inoue, N. Tashiro, K. Katayama, T. Matsuoka, and S. Furukawa.** 2000. Activation of peripheral blood CD8+ T cells in adenovirus infection. Pediatr. Infect. Dis. **19:**166-768.

50. **Meissner, J. D., G. N. Hirsch, E. A. LaRue, R. A. Fulcher, and K. R. Spindler.** 1997. Completion of the DNA sequence of mouse adenovirus type 1: Sequence of E2B, L1, and L2 (18-51 map units). Virus Res. **51:**53-64.

51. **Miller, G., S. Lahrs, V. G. Pillarisetty, A. B. Shah, and R. P. DeMatteo.** 2002. Adenovirus infection enhances dendritic cell immunostimulatory properties and induces natural killer and T-cell-mediated tumor protection. Cancer Res. **62:**5260-5266.

52. **Mombaerts, P., A. R. Clarke, M. A. Rudnicki, J. Iacomini, S. Itohara, J. J. Lafaille, L. Wang, Y. Ichikawa, R. Jaenisch, M. L. Hooper, and S. Tonegawa.** 1992. Mutations in T-cell antigen receptor genes α and β block thymocyte development at different stages. Nature **360:**225-231.

53. **Mullbacher, A., R. T. Hla, C. Museteanu, and M. Simon.** 1999. Perforin is essential for control of ectromelia virus but not related poxviruses in mice. J. Virol. **73:**1665-1667.

54. **Murray, P. D., K. D. Pavelko, J. Leibowitz, X. Lin, and M. Rodriguez.** 1998. CD4+ and CD8+ T cells make discrete contributions to demyelination and neurologic disease in a viral model of multiple sclerosis. J. Virol. **72:**7320-7329.

55. **Perkins, L. E., R. P. Campagnoli, B. G. Harmon, C. R. Gregory, W. L. Steffens, K. Latimer, S. Clubb, and M. Crane.** 2001. Detection and confirmation of reptilian adenovirus infection by in situ hybridization. J. Vet. Diagn. Invest. **13:**365-368.

56. **Pirofski, L., M. S. Horwitz, M. D. Scharff, and S. M. Factor.** 1991. Murine adenovirus infection of SCID mice induces hepatic lesions that resemble human Reye syndrome. Proc. Natl. Acad. Sci. USA **88:**4358-4362.

57. **Planz, O., T. Bilzer, and L. Stitz.** 1995. Immunopathogenic role of T-cell subsets in Borna disease virus-induced progressive encephalitis. J. Virol. **69:**896-903.

58. **Rowell, J. F., and D. E. Griffin.** 2002. Contribution of T cells to mortality in neurovirulent Sindbis virus encephalomyelitis. J. Neuroimmmunol. **127:**106-114.

59. **Scott, B., H. Bluthmann, H. S. Teh, and H. von Boehmer.** 1989. The generation of mature T cells requires interaction of the alpha beta T-cell receptor with major histocompatibility antigens. Nature **338:**591-593.

60. **Sha, Z., and R. W. Compans.** 2000. Induction of CD4(+) T-cell-independent immunoglobulin responses by inactivated influenza virus. J. Virol. **74:**4999-5005.

61. **Shilton, C. M., D. A. Smith, L. W. Woods, G. J. Crawshaw, and H. D. Lehmkuhl.** 2002. Adenoviral infection in captive moose (Alces alces) in Canada. J. Zoo. Wildl. Med. **33:**73-79.

62. **Shinkai, Y., K. Takio, and K. Okumura.** 1988. Homology of perforin to the ninth component of complement (C9). Nature **334:**525-527.

63. **Smith, K., C. C. Brown, and K. R. Spindler.** 1998. The role of mouse adenovirus type 1 early region 1A in acute and persistent infections in mice. J. Virol. **72:**5699-5706.

64. **Smith, K., and K. R. Spindler.** 1999. Murine adenovirus, p. 477-484. *In* R. Ahmed and I. Chen (ed.), Persistent viral infections. John Wiley & Sons, New York.

65. **Smyth, J. A., D. A. Moffett, E. van Garderen, and J. P. Orr.** 1999. Examination of adenovirus-types in intestinal vascular endothelial inclusions in fatal cases of enteric disease in cattle, by in situ hybridisation. Vet. Microbiol. **70:**1-6.

66. **Spindler, K. R., L. Fang, M. L. Moore, C. C. Brown, G. N. Hirsch, and A. K. Kajon.** 2001. SJL/J mice are highly susceptible to infection by mouse adenovirus type 1. J. Virol. **75:**12039-12046.

67. **Tang, K. N., C. A. Baldwin, J. L. Mansell, and E. L. Styer.** 1995. Disseminated adenovirus infection associated with cutaneous and visceral hemorrhages in a nursing piglet. Vet. Pathol. **32:**433-437.

68. **van der Veen, J., and A. Mes.** 1973. Experimental infection with mouse adenovirus in adult mice. Arch. Gesamte Virusforsch. **42:**235-241.

69. **Veit, H. P., C. H. Domermuth, and W. B. Gross.** 1981. Histopathology of avian adenovirus group II splenomegaly of chickens. Avian Dis. **25:**866-73.

70. **Wang, B., C. C. Norbury, R. Greenwood, J. R. Bennink, J. W. Yewdell, and J. A. Frelinger.** 2001. Multiple paths for activation of naive CD8+ T cells: CD4-independent help. J. Immunol. **167:**1283-1289.

71. **Wichmann, D., H.-J. Grone, M. Frese, J. Pavlovic, B. Anheier, O. Haller, H.-D. Klenk, and H. Feldman.** 2002. Hantaan virus infection causes acute neurological disease that is fatal in adult laboratory mice. J. Virol. **76:**8890-8899.

72. **Williams, N. S., and V. H. Engelhard.** 1996. Identification of a population of CD4+ CTL that utilizes a perforin- rather than a Fas ligand-dependent cytotoxic mechanism. J. Immunol. **156:**153-159.

73. **Woods, L. W., R. S. Hanley, P. H. Chiu, M. Burd, R. W. Nordhausen, M. H. Stillian, and P. K. Swift.** 1997. Experimental adenovirus hemorrhagic disease in yearling black-tailed deer. J. Wildl. Dis. **33:**801-811.

74. **Wu, G. F., A. A. Dandekar, L. Pewe, and S. Perlman.** 2000. CD4 and CD8 T cells have redundant but not identical roles in virus-induced demyelination. J. Immunol. **165:**2278-2286.

75. **Yang, Y., Q. Li, H. C. J. Ertl, and J. M. Wilson.** 1995. Cellular and humoral immune responses to viral antigens create barriers to lung-directed gene therapy with recombinant adenoviruses. J. Virol. **69:**2004-2015.

76. **Zajac, A. J., J. M. Dye, and D. G. Quinn.** 2003. Control of lymphocytic choriomeningitis virus infection in granzyme B deficient mice. J. Virol. **305:**1-9.

77. **Zajac, A. J., D. G. Quinn, P. L. Cohen, and J. A. Frelinger.** 1996. Fas-dependent CD4+ cytotoxic T-cell-mediated pathogenesis during virus infection. Proc. Natl. Acad. Sci. U.S.A **93:**14730-14735.

78. **Zaki, S. R., P. W. Greer, L. M. Coffield, C. S. Goldsmith, K. B. Nolte, K. Foucar, R. M. Feddersen, R. E. Zumwalt, G. L. Miller, and A. S. Khan.** 1995. Hantavirus pulmonary syndrome. Pathogenesis of an emerging infectious disease. Am. J. Pathol. **146:**552-579.

79. **Zinkernagel, R. M., and H. Hengartner.** 2001. Regulation of the immune response by antigen. Science **293:**251-253.

80. **Zotlick, P. W., N. Chirmule, M. A. Schnell, G.-P. Gao, J. V. Hughes, and J. M. Wilson.** 2001. Biology of E1-deleted adenovirus vectors in nonhuman primate muscle. J. Virol. **75:**5222-5229.

Table 2.1. Virulence of MAV-1 at 8 days p.i.

Mouse Strain (abbreviation)	Deficiency	Intraperitoneal dose (PFU)	No. of mice with signs of disease[a] at 8 days p.i.[b]	Survival at 8 days p.i.[b]
C57BL/6J (B6), C57BL/6NCr (B6)	None	100	1/12[b]	12/12
		700	46/54	49/54
		10^4	5/5	2/5
B6.129S-Tcra^{tm1Mom} (TCR$\alpha^{-/-}$)	T cells (TCRα)	100	0/6	6/6
		700	0/3	ND[c]
B6.129P-Tcrb^{tm1Mom}Tcrd^{tm1Mom} (TCRβx$\delta^{-/-}$)	T cells (TCRβ,δ)	700	0/16	16/16
		10^4	0/5	5/5
B6.129-Abb^{tm1}N5 (MHC class II deficient)	MHC Class II, CD4$^+$ T cells	700	7/9	8/9
B6.129P2-B2m^{tm1Unc} (MHC class I deficient)	MHC Class I, CD8$^+$ T cells	700	0/6	6/6
C57BL/6-Pfp^{tm1Sdz} (Pfp$^{-/-}$)	Perforin	10^4	0/8	8/8

[a] Hunched posture, ataxia, ruffled fur; also, in moribund mice, abdominal breathing, hindlimb paralysis, seizure, tremor

[b] The cumulative disease signs and survival for multiple B6 control infections are indicated. The number of B6 mice used as proximate controls for each of the mutant mouse strains was as follows: TCR$\alpha^{-/-}$, 100 PFU, n=3; TCR$\alpha^{-/-}$, 700 PFU, n=3; TCRβx$\delta^{-/-}$, 700 PFU, n=18; TCRβx$\delta^{-/-}$, 10^4 PFU, n=5; MHC class II-deficient, n=9; MHC class I-deficient, n=6; Pfp$^{-/-}$, n=8.

[c] ND, not determined

FIG. 2.1. Quantitation of virus from organs of acutely infected immunodeficient and control mice. Organs were homogenized, and virus was titrated by plaque assay. Each symbol represents an individual mouse. The short horizontal lines represent the means of the log-transformed titers. The dotted line at 2 x 10^3 represents the lower limit of detection of the assay. (A) Spleens and brains obtained 6 days p.i from B6 (■) and TCR$\alpha^{-/-}$ (△) mice infected with 10^4 PFU of MAV-1; (B) spleens and brains obtained 7 days p.i. from B6 (■) and TCRβx$\delta^{-/-}$ (□) mice infected with 700 PFU of MAV-1; (C) spleens and brains obtained 8 days p.i. from B6 (■) and TCR$\alpha^{-/-}$ (△) infected with 700 PFU of MAV-1; (D) spleens and brains obtained 8 days p.i. from B6 (■) and MHC class I-deficient (◇) mice infected with 700 PFU of MAV-1; and (E) spleens and brains obtained 8 days p.i. from B6 (■) and Pfp$^{-/-}$ (○) mice infected with 10^4 PFU of MAV-1. Data points below the limit of detection were excluded when calculating mean titers and t statistics. *, $P = 0.03$ compared to titers in B6 brain.

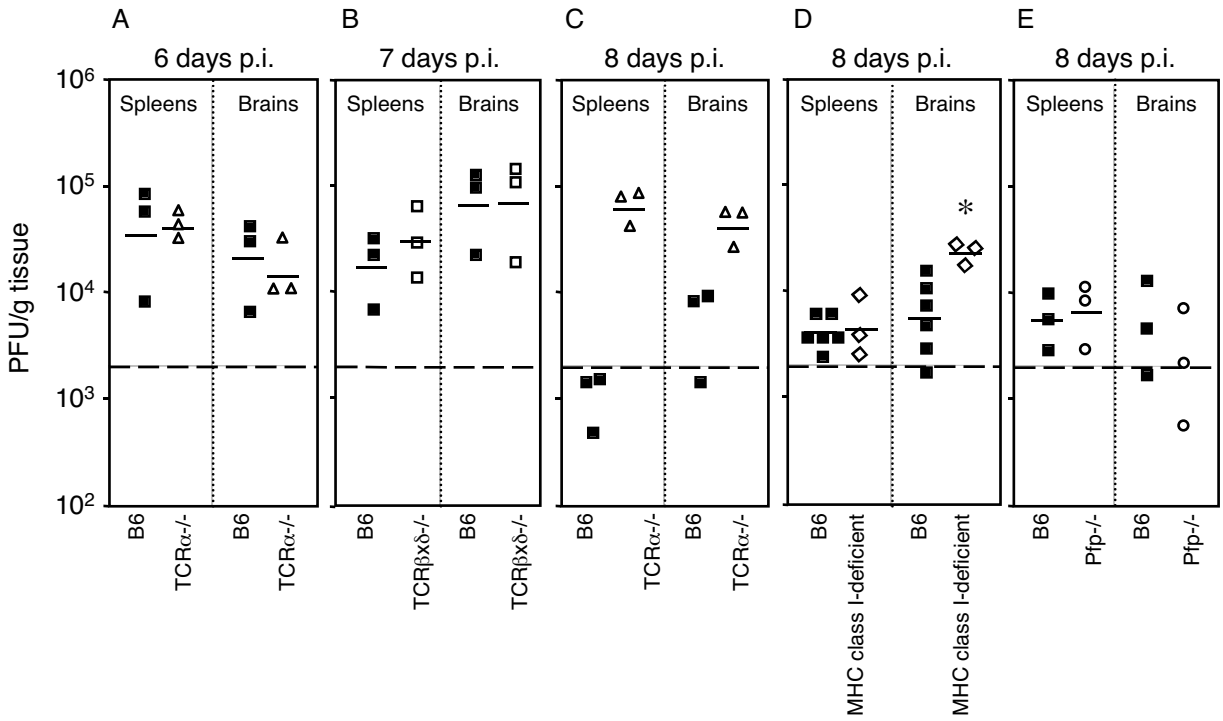
A
6 days p.i.
B
7 days p.i.
C
8 days p.i.
D
8 days p.i.
E
8 days p.i.
PFU/g tissue
10^6
10^5
10^4
10^3
10^2
Spleens
Brains
B6
TCRα-/-
TCRβxδ-/-
MHC class I-deficient
Pfp-/-
*

FIG. 2.2. Histopathology and ISH of infected mice. Sequential sections from paraffin-embedded tissues were stained with H-E or processed for ISH. (A to D) Brains were harvested 7 days p.i. from B6 and TCRβxδ$^{-/-}$ mice infected with 700 PFU of MAV-1. Shown are sequential H-E- and ISH-stained sections, respectively of B6 (A and B) and TCRβxδ$^{-/-}$ (C and D) mice. Note the perivascular fibrin deposition and edema in B6 (A) but not TCRβxδ$^{-/-}$ (C) brain (arrows). ISH of B6 (B) and TCRβxδ$^{-/-}$ (D) mice showed equivalent positive brown staining of viral nucleic acid in vascular endothelial cells with a MAV-1 probe (arrowheads). (E to L) Brains were harvested 8 days p.i. from B6 and Pfp$^{-/-}$ mice mock infected or infected with 10^4 PFU of MAV-1. Shown are sequential H-E- and ISH-stained sections, respectively, from mock-infected B6 (E and F), MAV-1-infected Pfp$^{-/-}$ (G and H), and MAV-1-infected B6 (I and J) mice. Note the presence of inflammatory cells in infected B6 (I) but not Pfp$^{-/-}$ (G) brain (arrows). Note equivalent ISH (positive brown staining) of vascular endothelial cells stained with a MAV-1 probe in B6 (J) and Pfp$^{-/-}$ (H) mice (arrowheads). (K and L) Additional H-E-stained B6 brain sections showing severe inflammation and vascular pathology. (M-T) Brains and livers were harvested 12 weeks p.i. from B6 and TCRβxδ$^{-/-}$ mice infected with 700 PFU of MAV-1. Shown are sequential H-E- and ISH-stained sections, respectively, from B6 brain (M and N), B6 liver (O and P), TCRβxδ$^{-/-}$ brain (Q and R), and TCRβxδ$^{-/-}$ liver (S and T). MAV-1-induced encephalomyelitis is apparent in the TCRβxδ$^{-/-}$ but not the B6 brain (arrows). Note positive MAV-1 ISH of vascular endothelial cells present in TCRβxδ$^{-/-}$ (R and T) but not B6 (N and P) mice (arrowheads). Bar, 50 μm.

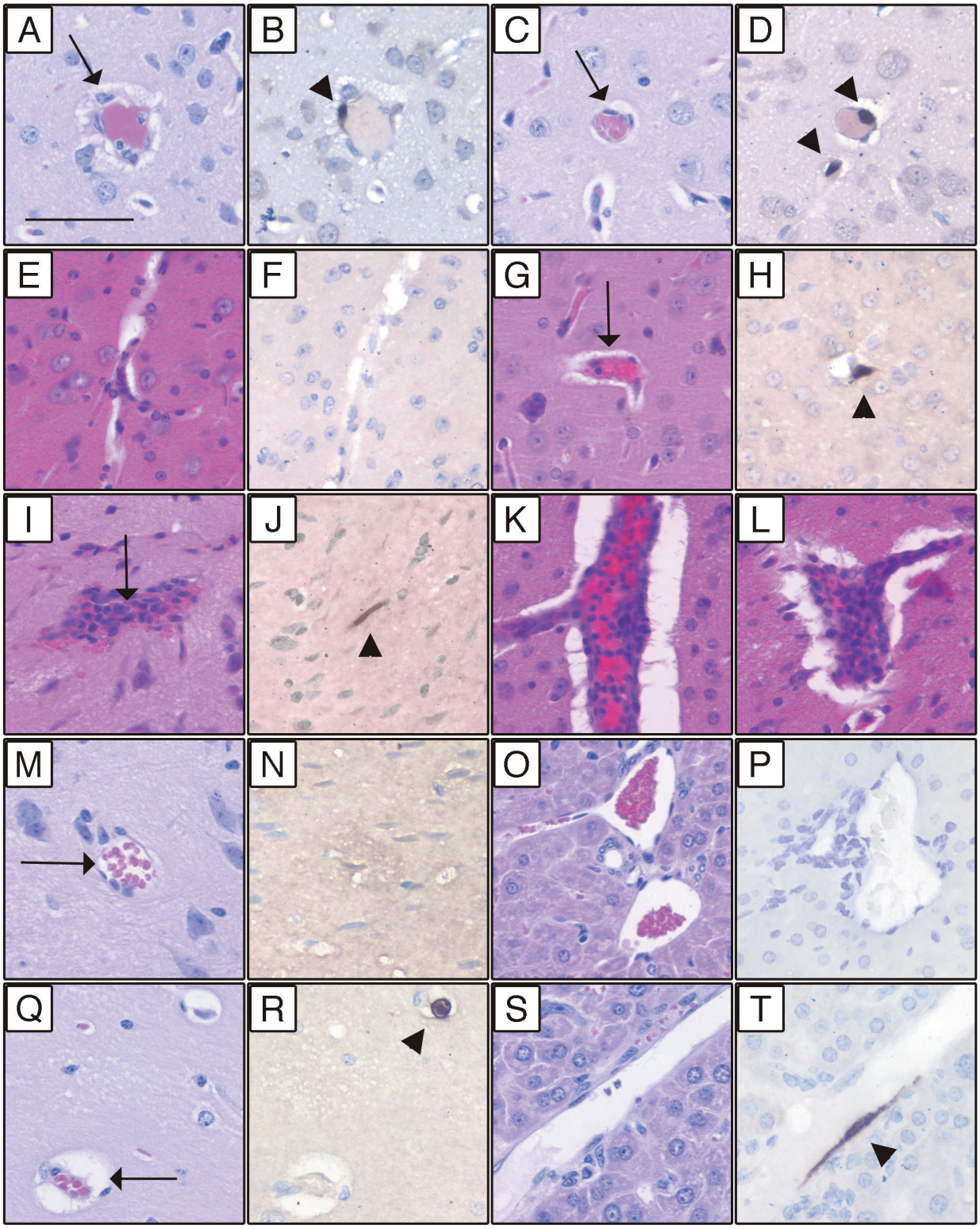
A
B
C
D
E
F
G
H
I
J
K
L
M
N
O
P
Q
R
S
T

FIG. 2.3. Susceptibility of B6, TCRβxδ$^{-/-}$, CD8$^{-/-}$, and CD4$^{-/-}$, TCRα$^{-/-}$, and TCRδ$^{-/-}$ mice to MAV-1. (A) B6 (n=6) and TCRβxδ$^{-/-}$ (n=4) mice were infected with 700 PFU of MAV-1, and survivors were euthanized at 12 weeks p.i. (B) B6 (n=5) and TCRβxδ$^{-/-}$ (n=5) mice were infected with 10^4 PFU of MAV-1, and survivors were euthanized at 16 weeks p.i. (C) B6 (n=5), CD8$^{-/-}$ (n=5), CD4$^{-/-}$ (n=4), and TCRβxδ$^{-/-}$ (n=5) mice were infected with 700 PFU of MAV-1, and survivors were euthanized at 12 weeks p.i. (D) TCRβxδ$^{-/-}$ (n=4), TCRα$^{-/-}$ (n=4), and TCRδ$^{-/-}$ (n=4) mice were infected with 100 PFU of MAV-1 and survivors euthanized 15 weeks p.i.

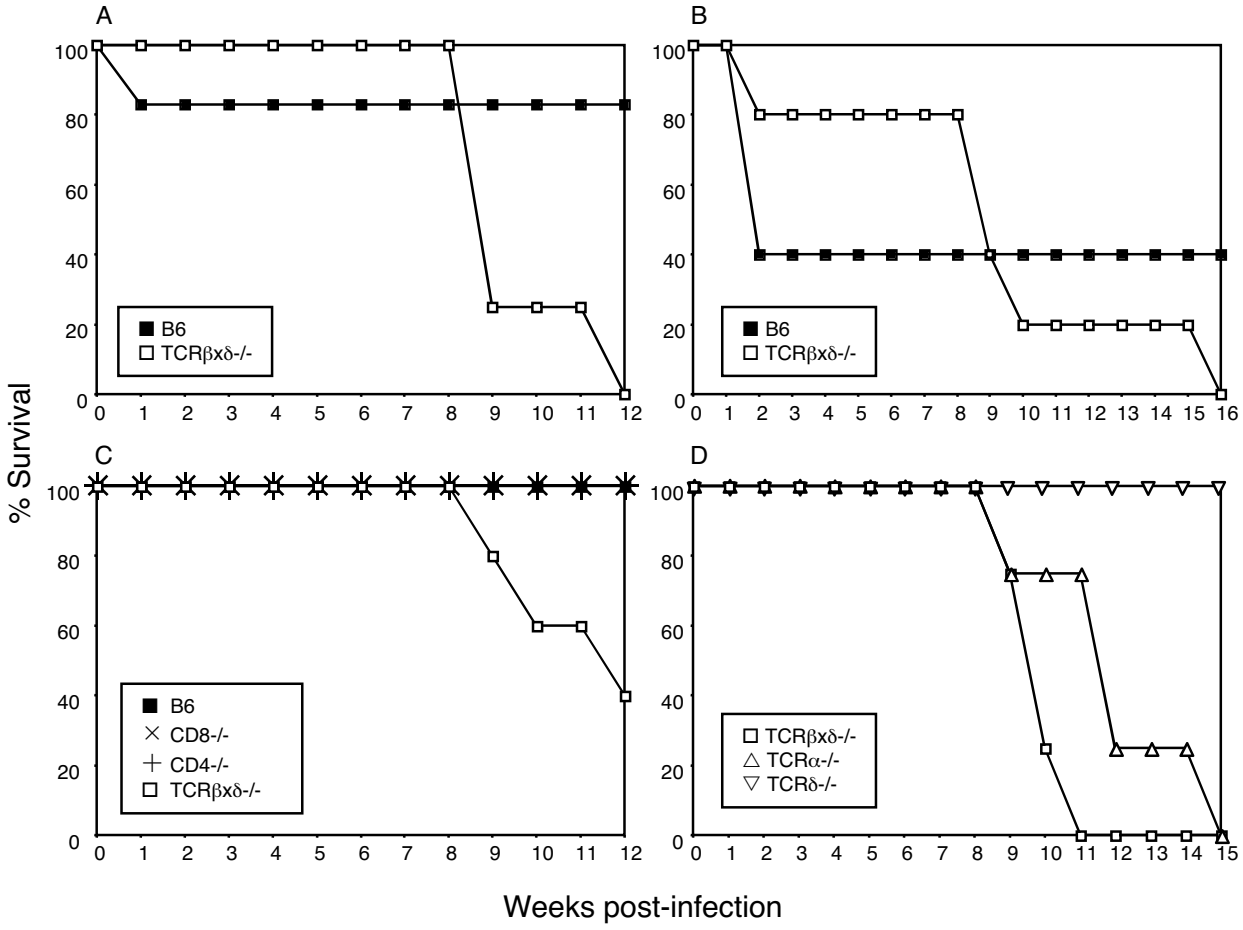
A
B
C
D
% Survival
Weeks post-infection
B6
TCRβxδ-/-
CD8-/-
CD4-/-
TCRα-/-
TCRδ-/-

FIG. 2.4. Replication of MAV-1 in T cell-deficient mice. (A) Quantitation of virus from spleens and brains obtained at 21 days p.i. from B6 (■) and TCR$\alpha^{-/-}$ (△) mice infected with 100 PFU of MAV-1. (B) Quantitation of virus from spleens and brains obtained 9 to 12 weeks p.i. from moribund TCRβx$\delta^{-/-}$ mice infected with 700 PFU of MAV-1. (C) Quantitation of virus from spleens and brains obtained 12 weeks p.i. from B6 (■), TCRβx$\delta^{-/-}$ (□), CD8$^{-/-}$ (×), and CD4$^{-/-}$ (+) mice infected with 700 PFU of MAV-1. Virus levels were determined and are depicted as described in the legend to Fig. 1. Data points below the limit of detection were excluded in calculating mean titers and t statistics.

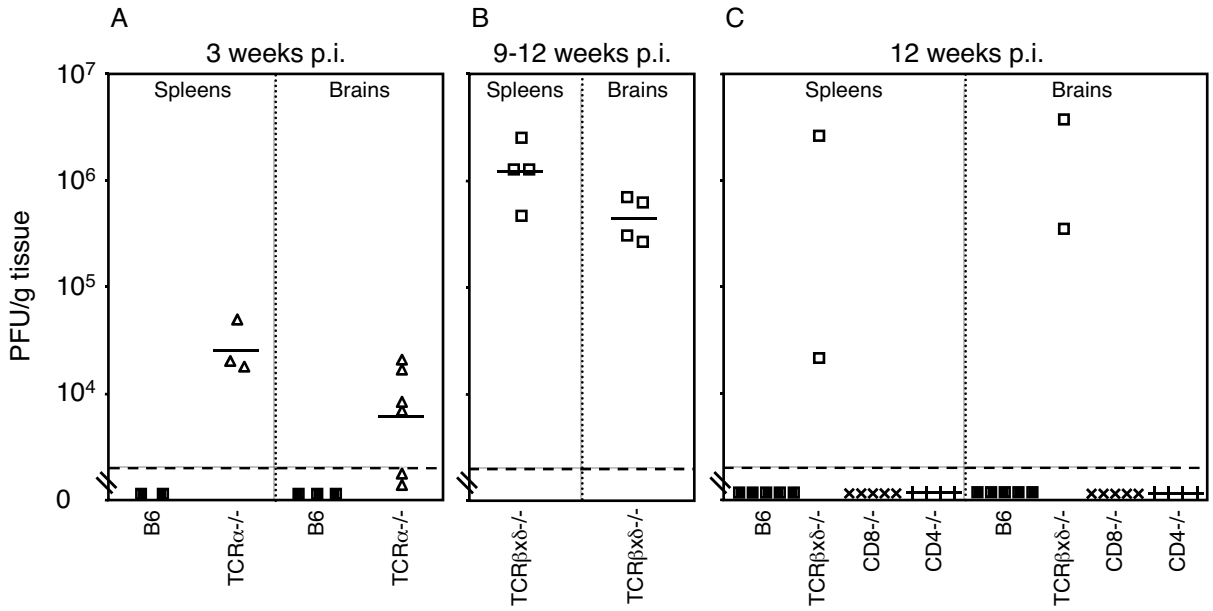
A
3 weeks p.i.
B
9-12 weeks p.i.
C
12 weeks p.i.
Spleens
Brains
PFU/g tissue
10^7
10^6
10^5
10^4
0
B6
TCRα-/-
TCRβxδ-/-
CD8-/-
CD4-/-

FIG. 2.5. Presence of MAV-1 nucleic acid in B6 mice at 12 weeks p.i. (A) DNA was isolated from spleens (odd-numbered lanes) and brains (even-numbered lanes) of B6 mice mock infected or infected with 100 PFU of MAV-1 and was analyzed by PCR with MAV-1 E3-specific primers MAVR24718 and MAVR25148 for 55 cycles. The positive DNA control template (+DNA) was 1 μg of DNA isolated from an acutely infected mouse brain known to be positive for infectious virus, and the negative control was water (w). The arrow indicates the 426-bp PCR product from viral DNA. (B) RNA was isolated from spleens (odd numbered lanes) and brains (even numbered lanes) of B6 mice mock infected or infected with 700 PFU of MAV-1 and analyzed by RT-PCR with MAV-1 E3-specific primers MAVR24718 and MAVR25148 for 35 cycles. The positive cDNA control template (+cDNA) was from RNA isolated at 20 h p.i. from mouse 3T6 fibroblasts infected with MAV-1 at a multiplicity of infection of 5, and the negative control was water (w). The arrow indicates the 269-bp PCR product from viral cDNA. Each spleen and brain pair (lanes 1 and 2, 3 and 4, etc.) corresponds to a single animal.

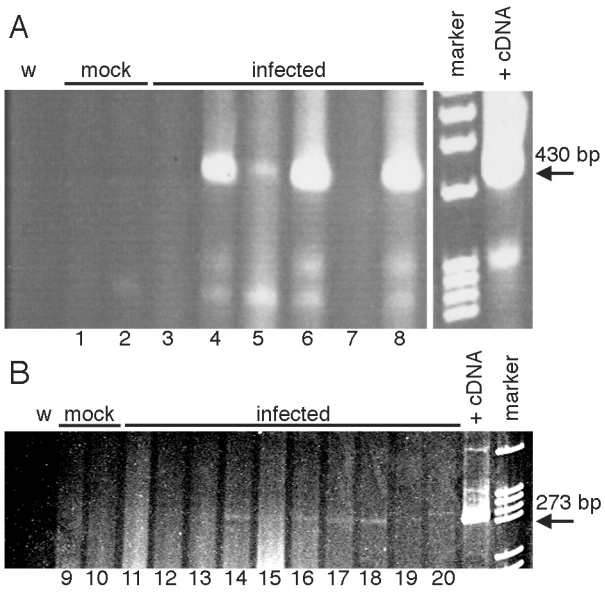
A
w
mock
infected
marker
+ cDNA
430 bp
1 2 3 4 5 6 7 8
B
w mock
infected
+ cDNA
marker
273 bp
9 10 11 12 13 14 15 16 17 18 19 20

CHAPTER 3

FATAL DISSEMINATED MOUSE ADENOVIRUS TYPE 1 INFECTION IN MICE LACKING B CELLS OR BRUTON'S TYROSINE KINASE[1]

[1]Moore, M.L., McKissic, E.L., Brown, C.C., Wilkinson, J.E., and K.R. Spindler. Submitted to Journal of Virology, 10/7/03

ABSTRACT

Mouse adenovirus type 1 (MAV-1) infection of B cell-deficient and Bruton's tyrosine kinase (Btk)-deficient mice resulted in fatal disseminated disease resembling human adenovirus infections in immunocompromised patients. Mice lacking B cells or Btk were highly susceptible to acute MAV-1 infection, in contrast to controls or mice lacking T cells. To our knowledge this is the first demonstration that mice with an X-linked immunodeficiency (Xid) phenotype (Btk-deficient) are susceptible to virus-induced disease. Mice lacking B cells or Btk on a C57BL/6 background succumbed with encephalomyelitis, hepatitis, and lymphoid necrosis. Mice lacking B cells on a BALB/c background succumbed with enteritis and hepatitis. Survival of acute MAV-1 infection correlated with early T cell-independent (TI) neutralizing Ab (nAb) and TI antiviral IgM. Treatment of MAV-1-infected $Btk^{-/-}$ mice 4 to 9 days post-infection (d.p.i) with antiserum harvested 6 to 9 d.p.i. from MAV-1-infected $Btk^{+/+}$ mice was therapeutic. Our findings implicate a critical role for B cell function in preventing disseminated MAV-1 infection, particularly production of early TI antiviral IgM.

INTRODUCTION

Human adenoviruses (hAds) are associated with self-limiting respiratory, conjunctival, and gastrointestinal disease. In immunocompromised people, hAd infection can result in pneumonia, hepatitis, encephalitis, pancreatitis, gastroenteritis, or disseminated disease involving multiple organs (8, 44). Disseminated hAd infection usually results in death, the incidence of disseminated hAd disease is increasing with the increased number of immunocompromised children, and pediatric bone marrow transplant recipients are most at risk (5, 13, 14, 17).

hAd species-specificity limits the study of hAd pathogenesis in animal models. Study of the closely related mouse adenovirus type 1 (MAV-1) permits the analysis of a replicating adenovirus in its natural host. The outcome of MAV-1 infection depends on the virus dose and mouse strain (16, 26, 33 and Chapter 2, 41). In outbred and C57BL/6 (B6) inbred mouse strains, MAV-1 infects cells of the monocyte/macrophage lineage and endothelial cells (EC) (11, 21, 33 and Chapter 2). The highest levels of virus are found in the spleen and brain (21, 26, 40). MAV-1-specific cytotoxic T cells peak at 10 days post-infection (d.p.i.) then decline (19). T cells cause acute immunopathology and are required for survival 9 to 16 weeks p.i. in MAV-1-induced encephalomyelitis (33 and Chapter 2). There are inbred mouse strains susceptible or resistant to MAV-1, and sublethal irradiation of resistant mice renders them susceptible (41). Mice with a severe combined immunodeficiency (SCID) mutation are susceptible to MAV-1 (11, 35).

Here we report findings that survival of acute MAV-1 infection is B cell-dependent and T cell-independent (TI). We postulated that Bruton's tyrosine kinase (Btk) plays a role in protection from MAV-1. Loss of Btk in mice results in the X-linked immunodeficiency (Xid) phenotype (23). $Btk^{-/-}$ mice have reductions in serum immunoglobulin (natural Ab), conventional B cells, and peritoneal B-1 cells relative to control mice (23). Here we demonstrate that Btk is required for survival of MAV-1 infection. We present data indicating that early TI antiviral IgM plays a pivotal role in protection against disseminated MAV-1 infection.

MATERIALS AND METHODS

Virus and mice. WT MAV-1 was propagated and titrated in 3T6 cells (9). Mice used are indicated in Table 3.1 (12, 15, 24, 25, 29-31). $A^{b}{}_{\beta}{}^{-/-}$ and Jh mice were purchased from Taconic.

C57BL/6NCr and BALB/CAnNCr mice were purchased from the National Cancer Institute. All other mice were purchased from Jackson Laboratory. The LD_{50} was determined as described (37). Sera were heat-inactivated at 57° for 45 min before passive transfer.

Quantitation of virus. Organ homogenates were prepared as described (41), or in phosphate-buffered saline (PBS) with 1 mm glass beads (BioSpec Products, Bartlesville, OK) in 2 ml/well 96-well plates (Axygen, Union City, CA) using a Mini Beadbeater (BioSpec) and the manufacturer's protocol. Virus was titrated by plaque assay as described previously (9). Means of the log titers were compared by a two-tailed *t* test. Counts of fewer than 10 plaques/60 mm plate were considered unreliable; thus 2 x 10^3 PFU/g was the detection limit. Values below detection limit were excluded from statistical analyses.

Histology and ISH. The following organs were formalin-fixed: spleen, kidney, liver, small and large intestine, Peyer's patches, thymus, lung, heart, and brain. Tissue sections were stained or processed for in situ hybridization (ISH) as previously described (21) with an antisense digoxigenin MAV-1 early region 3 riboprobe.

Neutralizing Ab (nAb) Assay. Heat-inactivated mouse sera were diluted two-fold in a solution containing 4 x 10^6 PFU/mL MAV-1 and incubated 1 hour at 37° C. Dulbecco's modified Eagle's medium (DMEM)/5% heat-inactivated calf serum was removed from wells of a 96 well plate containing confluent 3T6 cells, 25 µl of the virus/serum mixtures (corresponding to a multiplicity of infection of 10) were added to wells in duplicate, and the virus was allowed to adsorb for 1 hour at 37° C. DMEM/1% heat-inactivated calf serum was added, and wells were monitored 4 to 6 days for cytopathic effect (CPE), given scores of 0 (no CPE), 1/2 (some CPE), or + (complete CPE). The nAb titer was the last dilution exhibiting less than complete CPE.

ELISA. A MAV-1 stock was precipitated with polyethylene glycol (9). The virus pellet was resuspended in 1X DMEM in 0.01 of the original stock volume. Immulon 2 HB ELISA plates (Fisher Scientific) were coated overnight with polyethylene glycol-precipitated MAV-1 diluted 1:100 in PBS or media diluted 1:20 in PBS. The wells were coated with the same concentration of protein, as determined by a Bradford assay. Plates were washed, blocked with 1% bovine serum albumin, and serial dilutions of sera in PBS were added. Mouse anti-MAV-1 antisera were detected with secondary peroxidase-conjugated goat anti-mouse IgG serum (Amersham) or anti-mouse IgM (BioSource International) using 1-Step Turbo-TMB (Pierce) as the substrate.

Northern Analysis. Liver samples were homogenized in 900 μL TRI Reagent, and RNA was isolated by the manufacturer's protocol (Molecular Research Center, Inc.). PolyA+ RNA was isolated using the PolyATract System (Promega). 1 μg of each polyA+ RNA was electrophoresed on a 1% agarose/3% formaldehyde/40 mM MOPS pH 7.0/10 mM NaOAc/1 mM EDTA gel and then transferred to a nylon membrane (Boehringer Mannheim). For probes, oligonucleotides (β-actin 3' primer, (39); Fas ligand (FasL) probe, (46); regulated upon activation, normal T cell expressed and secreted (RANTES) 3' primer (27)) were end-labeled with γ-^{32}P using polynucleotide kinase. Membranes were hybridized, stripped, and re-probed as described (22). mRNA levels were quantitated with a phosphorimager using ImageQuant software (Molecular Dynamics) and compared by a two-tailed *t* test.

RESULTS

B cell- and Btk-deficient mice are highly susceptible to MAV-1 infection. MAV-1 induces dose-dependent encephalomyelitis in B6 mice (16). We first assessed the role of T and B cells in MAV-1 disease using immunodeficient mice on a B6 background. RAG-1$^{-/-}$ mice, which lack T

and B cells, were more susceptible to MAV-1 infection than B6 controls (Fig. 3.1A). These data are consistent with published results for CB.17/SCID (35) and BALB/SCID mice (11), which also lack T and B cells. To determine the relative contribution of T and B cells to protection from MAV-1, we infected mice lacking T cells (TCRβxδ$^{-/-}$) and mice lacking B cells (μMT). μMT mice were highly susceptible to MAV-1 infection, whereas TCRβxδ$^{-/-}$ mice survived like controls (Fig. 3.1B). T cell-deficient mice exhibit fewer acute MAV-1 disease signs than controls, and T cell-mediated acute immunopathology in MAV-1 disease is perforin- and MHC class I-dependent (33 and Chapter 2). Thus B cells but not T cells were required for survival of acute MAV-1 infection in B6 mice.

MAV-1 does not cause encephalomyelitis in BALB/c mice, which are more resistant to MAV-1 infection than B6 mice (16). To test whether the B cell requirement for survival in μMT mice is specific to the B6 background, we infected B cell-deficient mice (Jh) on a BALB/c background. Jh mice were highly susceptible to MAV-1 infection (Fig. 3.1C).

Since survival of acute MAV-1 infection was B cell-dependent and TI (Fig. 3.1B), we hypothesized that Btk plays a role in protection from MAV-1-induced disease. Btk$^{-/-}$ mice were highly susceptible to MAV-1 infection (Fig. 3.1C and D). The LD_{50} of Btk$^{-/-}$ mice was 0.1 PFU. This corresponds to 100 virus particles because the MAV-1 particle/PFU ratio is ~1000 in 3T6 cells (data not shown). Although Btk$^{-/-}$ mice are on a mixed B6 and 129 genetic background, the LD_{50}s for B6 and 129 mice are the same (>$10^{4.4}$ PFU) (41). Thus Btk is required for survival of MAV-1 infection. To our knowledge, this is the first demonstration that Btk plays a role in protection from virus-induced disease in mice.

B cell and Btk deficiency result in systemically high viral loads. We determined virus loads in organs of MAV-1-infected B cell-deficient, Btk-deficient, and control mice by plaque assay.

MAV-1 titers were higher in brain, spleen, liver, and kidney of μMT mice than controls, and μMT mice had a more disseminated infection (Fig 3.2A to C). MAV-1-infected BALB/c mice had no detectable virus 9 d.p.i, whereas Jh mice had virus in brain, spleen, and liver (Fig. 3.2D). Viral loads in organs of mice infected i.p. or i.v. with 10^4 PFU were significantly higher in $Btk^{-/-}$ mice than B6 mice (Fig. 3.2E). Infection of B cell- and Btk-deficient mice i.v. or i.n. with MAV-1 resulted in lethality and high viral loads (Fig. 3.2C, 3.2E, and data not shown). At 12 d.p.i. with 1 PFU, viral loads were higher in moribund $Btk^{-/-}$ mice than in B6 or $Btk^{-/-}$ mice not showing disease signs (Fig. 3.2F). Taken together, the results were that mice deficient for B cells or Btk had elevated MAV-1 titers and disseminated infection, and this correlated with death.

MAV-1 induces hepatitis, encephalomyelitis, and lymphoid necrosis in μMT and $Btk^{-/-}$ mice and induces hepatitis and enteritis in Jh mice. We examined the histological consequences of fatal MAV-1 disease in mice lacking B cells or Btk at 7 d.p.i. There was perivascular edema in brains of infected control B6 mice (inset, Fig. 3.3A), but spleen, liver, and small intestine appeared unaffected (Fig. 3.3B to D). In comparison, μMT and $Btk^{-/-}$ mice had perivascular edema and also vascular degeneration in brains, evident by perivascular fibrin deposition (Fig. 3.3E and I), and there was significant hepatic necrosis (Fig. 3.3G and K). In moribund B6 mice given high doses of MAV-1, vascular degeneration in the brain has been observed, but not liver pathology (16; data not shown). Spleens of μMT and $Btk^{-/-}$ mice showed lymphoid necrosis (Fig. 3.3F and J) that was not seen in B6 controls. ISH positive staining of EC is shown for each organ in which it was observed (insets, Fig. 3.3A to L). Overall, the B cell- and Btk-deficient mice had more disseminated disease than B6 controls.

Analysis of tissues 9 d.p.i. from control BALB/c and moribund Jh mice infected with 700 PFU (same mice as Fig. 3.2D) revealed that Jh mice succumbed with hemorrhagic enteritis and

hepatic necrosis (Fig. 3.3M to T). Enteritis has been observed in MAV-1-infected outbred and BALB/SCID mice (11, 26). Typical MAV-1 inclusion bodies were seen in hematoxylin and eosin (H&E)-stained small intestine (Fig. 3.3T). Interestingly, like μMT mice, Jh mice had elevated viral titers in brain (Fig. 3.2D), but unlike μMT mice, Jh mice had no brain pathology (Fig. 3.3Q), suggesting that host factors contributing to MAV-1 pathogenesis in B cell-deficient mice are strain-specific. Peyer's patches and spleen lymphoid follicles of infected control BALB/c mice were activated; they had defined germinal centers (Fig. 3.3N and P). In contrast, spleens of infected Jh mice appeared disorganized but had no necrosis (Fig. 3.3R). B cell-deficient mice on the BALB/c background thus showed more disease than BALB/c controls.

Analysis of tissues 12 d.p.i. from B6 and $Btk^{-/-}$ mice mock-infected or infected with the low dose of 1 PFU (same mice as Fig. 3.2F) revealed cellular inflammation in infected mice of both mouse strains, though it was more extensive in $Btk^{-/-}$ mice (Fig. 3.4). Infected B6 mice had vasculitis in brain (Fig. 3.4D) and defined germinal centers in spleen (Fig. 3.4E). Moribund $Btk^{-/-}$ mice had vasculitis, meningeal vascular necrosis, and vascular degeneration in brain (Fig. 3.4J and data not shown); their spleens had excessive lymphoid necrosis (Fig 3.4K), and livers had significant lymphoplasmacytic hepatitis (Fig. 3.4L).

FasL and RANTES mRNA levels are altered in MAV-1-infected Jh mice. BALB/SCID and CB.17/SCID mice are susceptible to MAV-1 infection, and MAV-1 targets the liver in these mice (11, 35). However, hepatic disease induced by MAV-1 in CB.17/SCID mice resembled Reye syndrome; there was no significant hepatic necrosis or inflammation (35). In contrast, MAV-1-infected Jh mice exhibited significant hepatic necrosis (Fig. 3.3S) resembling acute hAd hepatitis in immunosuppressed patients (45). Since T cells are present in Jh mice but not BALB/SCID mice, we hypothesized that T cells contribute to acute hepatitis in MAV-1-infected

Jh mice. To address this hypothesis, we analyzed liver mRNA levels of genes associated with T cell function. The Fas/FasL pathway is an important mechanism of T cell-mediated cytotoxicity (20). We found that FasL liver mRNA levels were elevated in infected Jh mice but not control BALB/c mice (Fig. 3.5). These results are consistent with T cells contributing to hepatitis in Jh mice.

RANTES is a chemokine that attracts T cells and monocytes and is required for normal T cell function in mice (28). We found that liver mRNA levels of the chemokine RANTES were reduced in infected Jh mice 9 d.p.i. compared to BALB/c controls (Fig. 3.5). This was surprising because RANTES mRNA levels were elevated in BALB/c spleen, B6 spleen, and B6 brain 96 hr p.i. with MAV-1 (10), and we have observed an increase in RANTES mRNA levels upon MAV-1 infection in brains of B6 mice 9 d.p.i (data not shown). Thus, RANTES mRNA levels are elevated or reduced upon MAV-1 infection depending on the mouse strain and/or the organ infected, and RANTES may play a role in MAV-1-induced hepatitis.

Early TI Ab correlates with survival of acute MAV-1 infection. We analyzed the humoral immune response to MAV-1. There was an increase in nAb titer and antiviral IgM 6 d.p.i. in sera of B6 and T cell-deficient mice but not $Btk^{-/-}$ mice after infection with 10^4 PFU (Fig. 3.6A and 3.7A, same mice as Fig. 3.2E). Similarly, TI antiviral IgM was detected 6 d.p.i. in B6 and T cell-deficient mice infected with a lower dose, 700 PFU (Fig. 3.7B). Antiviral IgG levels were low or undetectable in sera shown in Fig. 3.7A and 3.7B (data not shown). Sera of B6 but not $Btk^{-/-}$ mice infected with 700 PFU (same mice as Fig. 3.1C) had nAb titers 7 d.p.i. (Fig. 3.6B). nAb was induced in MHC class II-deficient ($A_\beta^{b-/-}$) and control mice (Fig. 3.6C). B6 mice infected with 1 PFU produced nAb antiviral IgM and IgG 12 d.p.i, whereas $Btk^{-/-}$ mice did not (Fig. 3.6D and 3.7C, same mice as Fig. 3.2F). At 12 weeks p.i, MHC class II was required for anti-MAV-1 IgG

whereas CD4 was dispensable (Fig. 3.7D). Interestingly, $A_{\beta}^{b-/-}$ and $CD4^{-/-}$ mice survive to 12 weeks p.i. like controls (33 and Chapter 2); thus antiviral IgG is not required for survival of MAV-1 infection. Taken together, the results show that TI antiviral IgM and TI nAb correlated with survival of acute MAV-1 infection whereas the absence of antiviral IgG had no effect on survival.

Passive transfer of immune antisera protects RAG-$1^{-/-}$ and $Btk^{-/-}$ mice from MAV-1 infection. We first tested whether nAb or natural Ab could protect RAG-$1^{-/-}$ mice from MAV-1 infection. Treatment of $RAG^{-/-}$ mice with naïve B6 serum (natural Ab) on 0 to 7 d.p.i. had no effect on virus loads, whereas treatment with MAV-1-immune serum reduced them significantly (Fig. 3.8A). We then tested whether early nAb could protect MAV-1-infected $Btk^{-/-}$ mice. Treatment 4 to 9 d.p.i. with serum from 6 to 9 day-infected mice that had both antiviral IgM and IgG (Fig. 3.8B) protected 3 of 4 $Btk^{-/-}$ mice (Fig. 3.8C).

DISCUSSION

We demonstrate a crucial role for B cells and Btk in preventing fatal disseminated MAV-1 disease. B cell- and Btk-deficient mice were highly susceptible to MAV-1 and succumbed with high viral loads and disseminated infection (Figs. 3.1 and 3.2). This parallels the observation that Btk-deficient people exhibit increased susceptibility to hAds (38), suggesting that Btk may be an integral component of the immune response to Ads.

Infection of B cell- or Btk-deficient mice with MAV-1 resulted in hepatitis (Fig. 3.3G, K, and S) histologically similar to hAd hepatitis in immunocompromised patients (6, 7, 45). μMT and $Btk^{-/-}$ mice infected with 700 PFU succumbed with hepatic necrosis with mild cellular inflammation (Fig. 3.3G and K). MAV-1 EC tropism (insets, Fig. 3.3G and K) is consistent with

previous findings for mice with a B6 or 129 background (11; data not shown, 16). $Btk^{-/-}$ mice infected with as low as 1 PFU also succumbed with hepatic necrosis but had significant cellular inflammation (Fig. 3.4L). Thus pathology of MAV-1 hepatitis in $Btk^{-/-}$ mice depended on virus dose and presumably kinetics of inflammation. In contrast, Jh mice (B cell-deficient on a BALB/c background) infected with 700 PFU succumbed with confluent, glassy hepatic necrosis without inflammation (Fig. 3.3S). MAV-1 inclusion bodies were seen in hepatocytes of Jh but not μMT mice (data not shown) and have been observed in hepatocytes of infected BALB/SCID and CB.17/SCID mice (11, 35). It is likely that the host genetic background contributes to differences in cell and organ tropism and pathology observed in MAV-1-infected μMT and Jh mice. Residual B cells in μMT mice (34) may also contribute to the phenotypic differences.

We hypothesize that T cells play a key role in MAV-1 hepatitis because the virus induces hepatitis in B cell-deficient but not SCID (T cell- and B cell-deficient) mice (11, 35; Fig. 2G and S). Furthermore, mice lacking T cells succumb to MAV-1 infection 9 to 16 weeks p.i. with encephalomyelitis and MAV-1 dissemination to the liver but no liver pathology (33 and Chapter 2). T cell function may be defective in MAV-1-infected B cell-deficient mice, as is the case for LCMV-infected μMT mice (18). FasL mRNA levels were induced in MAV-1-infected Jh livers (Fig. 3.5), suggesting that the Fas/FasL cytolytic pathway plays a role in MAV-1-induced hepatitis. FasL contributes to LCMV-induced hepatitis (1). Furthermore, Northern analyses revealed that mRNA levels of the chemokine RANTES were reduced in MAV-1-infected Jh livers (Fig. 5), suggesting that the inflammatory response to MAV-1 is aberrant in Jh mice. Our data are consistent with a model in which early TI antiviral IgM plays a pivotal role in protection against MAV-1 infection. In the absence of such IgM (in B cell- or Btk-deficient mice), a disseminated infection ensues in which T cells induce immunopathology. Experiments

testing the role of T cells, FasL, and RANTES in MAV-1 hepatitis may reveal an immunoregulatory role for early TI Ab.

Early TI nAb and TI antiviral IgM correlated with survival of acute MAV-1 infection (Figs. 3.6 and 3.7). In contrast, the absence of anti-MAV-1 IgG had no effect on survival (33 and Chapter 2; Fig. 5Bd). Antigens (Ag) that activate B cells in the absence of T cells have been classified into two groups based on whether they induce Ab in Xid mice (TI-1) or not (TI-2) (32). Polyoma virus (PyV) is a TI-2 Ag and elicits protective TI IgM and IgG in T cell-deficient mice (42, 43). Our results showed that MAV-1 expresses a TI-2 Ag (Figs. 3.6 and 3.7). Natural and early virus-induced IgM contribute to protection against influenza virus (3). However, in contrast to MAV-1 infection, μMT and Btk-deficient mice are not susceptible to PyV- or influenza-induced disease (4, 36). Baumgarth has proposed that TI IgM regulates B cell activation (2). MAV-1 may be useful for testing this model.

MAV-1 infection of B cell- and Btk-deficient mice resulted in high viral loads, disseminated infection, hepatitis resembling hAd-induced hepatitis in immunocompromised people, and lethality. Our data indicate that early TI nAb and TI IgM play a crucial role in protection from disseminated MAV-1 infection. Treatment of MAV-1-infected $Btk^{-/-}$ mice with early antiviral antiserum had a significant effect on mortality (Fig. 3.8B and C). Though modestly neutralizing in vitro (Fig. 3.8B), early Ab (e.g. IgM) may have potent antiviral and/or immunostimulatory potential in vivo.

ACKNOWLEDGMENTS

We thank James Stanton, Adriana Kajon, Carla Sturkie, Lei Fang, Katie Kempke, and Amanda Welton for technical assistance. We thank Mike Imperiale, Gary Huffnagle, and

Rosemary Rochford for critical review of the manuscript. This work was supported by NIH grant R01 AI023762 to K.R.S. and by an NIH predoctoral traineeship (GM 07103) and an ARCS Foundation Scholarship to M.L.M.

REFERENCES

1. **Balkow, S., A. Kersten, T. T. Tran, T. Stehle, P. Grosse, C. Museteanu, O. Utermohlen, H. Pircher, F. von Weizsacker, R. Wallich, A. Mullbacher, and M. M. Simon.** 2001. Concerted action of the FasL/Fas and perforin/granzyme A and B pathways is mandatory for the development of early viral hepatitis but not for recovery from viral infection. J. Virol. **75:**8781-8791.

2. **Baumgarth, N.** 2000. A two-phase model of B-cell activation. Immunol. Rev. **176:**171-180.

3. **Baumgarth, N., O. C. Herman, G. C. Jager, L. E. Brown, L. A. Herzenberg, and J. Chen.** 2000. B-1 and B-2 cell-derived immunoglobulin M antibodies are nonredundant components of the protective response to influenza virus infection. J. Exp. Med. **192:**271-280.

4. **Berke, Z., H. Mellin, S. Heidari, T. Wen, A. Berglof, G. Klein, and T. Dalianis.** 1998. Adult X-linked immunodeficiency (XID) mice, IGM-/- single knockout and IGM-/-CD8-/- double knockout mice do not clear polyomavirus infection. In Vivo **12:**143-148.

5. **Blanke, C., C. Clark, E. R. Broun, G. Tricot, I. Cunningham, K. Cornetta, A. Hedderman, and R. Hromas.** 1995. Evolving pathogens in allogeneic bone marrow transplantation: increased fatal adenoviral infections. Am. J. Med. **99:**326-328.

6. **Cames, B., J. Rahier, G. Burtomboy, J. de Ville de Goyet, R. Reding, M. Lamy, J. B. Otte, and E. M. Sokal.** 1992. Acute adenovirus hepatitis in liver transplant recipients. J. Pediatr. **120:**33-37.

7. **Carmichael, G. P., J. M. Zahvadnik, and G. H. Moyer.** 1979. Adenovirus hepatitis in an immunosuppressed adult patient. Am. J. Clin. Pathol. **71:**352-355.

8. **Carrigan, D. R.** 1997. Adenovirus infections in immunocompromised patients. Am. J. Med. **102:**71-74.

9. **Cauthen, A. N., and K. R. Spindler.** 1999. Construction of mouse adenovirus type 1 mutants, p. 85-103. *In* W. S. M. Wold (ed.), Adenovirus methods and protocols. Humana Press, Totowa, NJ.

10. **Charles, P. C., X. Chen, M. S. Horwitz, and C. F. Brosnan.** 1999. Differential chemokine induction by the mouse adenovirus type-1 in the central nervous system of susceptible and resistant strains of mice. J. Neurovirol. **5:**55-64.

11. **Charles, P. C., J. D. Guida, C. F. Brosnan, and M. S. Horwitz.** 1998. Mouse adenovirus type-1 replication is restricted to vascular endothelium in the CNS of susceptible strains of mice. Virology **245:**216-228.

12. **Chen, J., M. Trounstine, F. W. Alt, F. Young, C. Kurahara, J. F. Loring, and D. Huszar.** 1993. Immunoglobulin gene rearrangement in B cell deficient mice generated by targeted deletion of the JH locus. Int. Immunol. **5:**647-656.

13. **Flomenberg, P., J. Babbitt, W. R. Drobyski, R. C. Ash, D. R. Carigan, G. V. Sedmak, T. McAuliffe, B. Camitta, M. M. Horowitz, N. Bunin, and J. T. Casper.** 1994. Increasing incidence of adenovirus disease in bone marrow transplant recipients. J. Inf. Dis. **169:**775-781.

14. **Gavin, P. J., and B. Z. Katz.** 2002. Intravenous ribavirin treatment for severe adenovirus disease in immunocompromised children. Pediatrics **110:**1-8.

15. **Grusby, M. J., H. J. Auchincloss, R. Lee, R. S. Johnson, J. P. Spencer, M. Zulstra, R. Jaenisch, V. E. Papaionnou, and L. H. Glimcher.** 1993. Mice lacking major histocompatibility complex class I and class II molecules. Proc. Natl. Acad. Sci. USA **90:**3913-3917.

16. **Guida, J. D., G. Fejer, L.-A. Pirofski, C. F. Brosnan, and M. S. Horwitz.** 1995. Mouse adenovirus type 1 causes a fatal hemorrhagic encephalomyelitis in adult C57BL/6 but not BALB/c mice. J. Virol. **69:**7674-7681.

17. **Hale, G. A., H. E. Heslop, R. A. Krance, M. A. Brenner, D. Jayawardene, D. K. Srivastava, and C. C. Patrick.** 1999. Adenovirus infection after pediatric bone marrow transplantation. Bone Marrow Transplant **23:**277-282.

18. **Homann, D., A. Tishon, D. P. Berger, W. O. Weigle, M. G. von Herrath, and M. B. Oldstone.** 1998. Evidence for an underlying CD4 helper and CD8 T-cell defect in B-cell-deficient mice: failure to clear persistent virus infection after adoptive immunotherapy with virus-specific memory cells from muMT/muMT mice. J. Virol. **72:**9208-9216.

19. **Inada, T., and H. Uetake.** 1980. Cell-mediated immunity to mouse adenovirus infection: Blocking of macrophage migration inhibition and T cell-mediated cytolysis of infected cells by anti-S antigen or anti-alloantigen serum. Microbiol. Immunol. **24:**525-535.

20. **Kagi, D., F. Vignaux, B. Ledermann, K. Burki, V. Depraetere, S. Nagata, H. Hengartner, and P. Golstein.** 1994. Fas and perforin pathways as major mechanisms of T cell-mediated cytotoxicity. Science **265:**528-530.

21. **Kajon, A. E., C. C. Brown, and K. R. Spindler.** 1998. Distribution of mouse adenovirus type 1 in intraperitoneally and intranasally infected adult outbred mice. J. Virol. **72:**1219-1223.

22. **Kajon, A. E., and K. R. Spindler.** 2000. Mouse adenovirus type 1 replication *in vitro* is resistant to interferon. Virology **274:**213-219.

23. **Khan, W. N., F. W. Alt, R. M. Gerstein, B. A. Malynn, I. Larsson, G. Rathbun, L. Davidson, S. Muller, A. B. Kantor, L. A. Herzenberg, F. S. Rosen, and P. Sideras.** 1995. Defective B cell development and function in Btk-deficient mice. Immunity **3:**283-299.

24. **Khan, W. N., P. Sideras, F. S. Rosen, and F. W. Alt.** 1995. The role of Bruton's tyrosine kinase in B-cell development and function in mice and man. Ann. N.Y. Acad. Sci. **764:**27-38.

25. **Kitamura, D., J. Roes, R. Kühn, and K. Rajewsky.** 1991. A B cell-deficient mouse by targeted disruption of the membrane exon of the immunoglobulin μ chain gene. Nature **350:**423-426.

26. **Kring, S. C., C. S. King, and K. R. Spindler.** 1995. Susceptibility and signs associated with mouse adenovirus type 1 infection of adult outbred Swiss mice. J. Virol. **69:**8084-8088.

27. **Lane, T. E., M. T. Liu, B. P. Chen, V. C. Asensio, R. M. Samawi, A. D. Paoleti, I. L. Campbell, S. L. Kunkell, H. S. Fox, and M. J. Buchmeier.** 2000. A central role for CD4+ T cells and RANTES in virus-induced central nervous system inflammation and demyelination. J. Virol. **74:**1415-1424.

28. **Makino, Y., D. N. Cook, O. Smithies, O. Y. Hwang, E. G. Neilson, L. A. Turka, H. Sato, A. D. Wells, and T. M. Danoff.** 2002. Impaired T cell function in RANTES-deficient mice. Clin. Immunol. **102:**302-309.

29. **McCarrick, J. W. r., J. R. Parnes, R. H. Seong, D. Solter, and B. B. Knowles.** 1993. Positive-negative selection gene targeting with the diphtheria toxin A-chain gene in mouse embryonic stem cells. Transgenic Res. **2:**183-190.

30. **Mombaerts, P., A. R. Clarke, M. A. Rudnicki, J. Iacomini, S. Itohara, J. J. Lafaille, L. Wang, Y. Ichikawa, R. Jaenisch, M. L. Hooper, and S. Tonegawa.** 1992. Mutations in T-cell antigen receptor genes α and β block thymocyte development at different stages. Nature **360:**225-231.

31. **Mombaerts, P., J. Iacomini, R. S. Johnson, K. Herrup, S. Tonegawa, and V. E. Papaionnou.** 1992. RAG-1-deficient mice have no mature B and T lymphocytes. Cell **68:**869-877.

32. **Mond, J. J., I. Scher, D. E. Mosier, M. Baese, and W. E. Paul.** 1978. T-independent responses in B cell-defective CBA/N mice to Brucella abortus and to trinitrophenyl (TNP) conjugates of Brucella abortus. Eur. J. Immunol. **8:**459-463.

33. **Moore, M. L., C. C. Brown, and K. R. Spindler.** 2003. T cells cause acute immunopathology and are required for long term survival in mouse adenovirus type 1-induced encephalomyelitis. J. Virol. **77:**10060-10070.

34. **Orinska, Z., A. Osiak, J. Lohler, E. Bulanova, V. Budagian, I. Horak, and S. Bulfone-Paus.** 2002. Novel B cell population producing functional IgG in the absence of membrane IgM expression. Eur. J. Immunol. **32:**3472-3480.

35. **Pirofski, L., M. S. Horwitz, M. D. Scharff, and S. M. Factor.** 1991. Murine adenovirus infection of SCID mice induces hepatic lesions that resemble human Reye syndrome. Proc. Natl. Acad. Sci. USA **88:**4358-4362.

36. **Reale, M. A., C. A. Bona, and J. L. Schulman.** 1985. Isotype profiles of anti-influenza antibodies in mice bearing the xid defect. J. Virol. **53:**425-429.

37. **Reed, L. J., and H. Muench.** 1938. A simple method of estimating fifty per cent endpoints. Am. J. Hyg. **27:**493-497.

38. **Sanna, P. P., and D. R. Burton.** 2000. Role of antibodies in controlling viral disease: Lessons from experiments of nature and gene knockouts. J. Virol. **74:**9813-9817.

39. **Schmitt, R. M., E. Bruyns, and H. R. Snodgrass.** 1991. Hematopoietic development of embryonic stem cells in vitro: cytokine and receptor gene expression. Genes Dev. **5:**728-740.

40. **Smith, K., C. C. Brown, and K. R. Spindler.** 1998. The role of mouse adenovirus type 1 early region 1A in acute and persistent infections in mice. J. Virol. **72:**5699-5706.

41. **Spindler, K. R., L. Fang, M. L. Moore, C. C. Brown, G. N. Hirsch, and A. K. Kajon.** 2001. SJL/J mice are highly susceptible to infection by mouse adenovirus type 1. J. Virol. **75:**12039-12046.

42. **Szomolanyi-Tsuda, E., J. D. Brien, J. E. Dorgan, R. L. Garcea, R. T. Woodland, and R. M. Welsh.** 2001. Antiviral T-cell-independent type 2 antibody responses induced *in vivo* in the absence of T and NK cells. Virology **280:**160-168.

43. **Szomolanyi-Tsuda, E., and R. M. Welsh.** 1996. T cell-independent antibody-mediated clearance of polyomavirus in T cell-deficient mice. J. Exp. Med. **280:**160-168.

44. **Walls, T., A. G. Shankar, and D. Shingadia.** 2003. Adenovirus: an increasingly important pathogen in paediatric bone marrow transplant patients. Lancet Infect. Dis. **3:**79-86.

45. **Wang, W. H., and H. L. Wang.** 2003. Fulminant adenovirus hepatitis following bone marrow transplantation. A case report and brief review of the literature. Arch. Pathol. Lab Med. **127:**e246-248.

46. **Watson, V. E., L. L. Hill, L. B. Owen-Schaub, D. W. Davis, D. J. McConkey, C. Jagannath, R. L. J. Hunter, and J. K. Actor.** 2000. Apoptosis in mycobacterium tuberculosis infection in mice exhibiting varied immunopathology. J. Pathol. **190:**211-220.

Table 3.1. Mice used in this study

Strain name	Abbreviation	Defect
C57BL/6J, C57BL/6NCr	B6	None
BALB/CAnNCr	BALB/c	None
B6.129S7-Rag1^{tm1Mom}	RAG-1$^{-/-}$	T and B cell-deficient
B6.129S2-Igh-6^{tm1Cgn}	μMT	B cell-deficient; B6 background
B6;129S-Btk^{tm1Wk}	Btk$^{-/-}$	Bruton's tyrosine kinase deficient
B6.129S-Tcra^{tm1Mom}	TCRα$^{-/-}$	α/β T cell-deficient
B6.129P-Tcrb^{tm1Mom}Tcrd^{tm1Mom}	TCRβxδ$^{-/-}$	α/β and γ/δ T cell-deficient
B6.129S6-Cd4^{tm1Knw}	CD4$^{-/-}$	CD4^{+} T cell deficient
B6.129-Abb^{tm1}N5	$A^{b}_{\beta}{}^{-/-}$	MHC class II-deficient
C.129(B6)-Jhd^{tm1}	Jh	B cell-deficient; BALB/c background

FIG. 3.1. Survival of (A) B6 (n=3) and RAG-$1^{-/-}$ (n=5), (B) B6 (n=6), μMT (n=6), and TCRβxδ$^{-/-}$ (n=6), (C) B6 (n=6), BALB/c (n=6), $Btk^{-/-}$ (n=9), and Jh (n=6), and (D) B6 (n=3) and $Btk^{-/-}$ (n=6) mice. Mice were injected i.p. with (A) 100 PFU, (B) 700 PFU, (C) 700 PFU, and (D) 1 PFU.

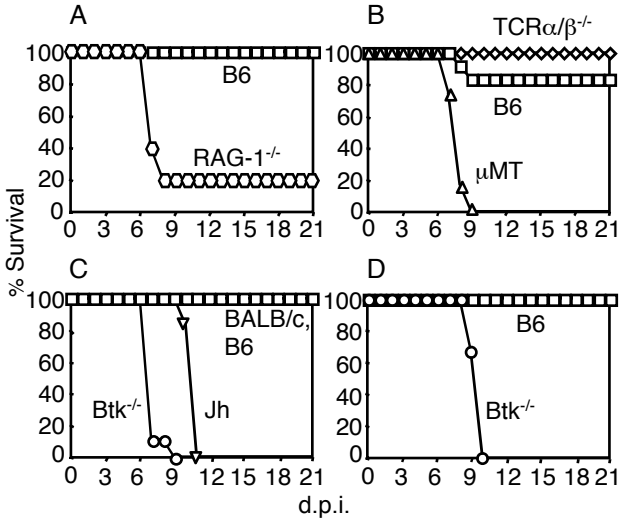
A
B
C
D
% Survival
d.p.i.
B6
RAG-1-/-
TCRα/β-/-
μMT
BALB/c,
Btk-/-
Jh
0 3 6 9 12 15 18 21
0 20 40 60 80 100

FIG. 3.2. Quantitation of virus from (A to C) B6 and μMT, (D) BALB/c and Jh, and (E to F) B6 and $Btk^{-/-}$ mice; (E) 3 mice each were infected i.p. or i.v. (left and right symbols in each group, respectively). Each symbol represents an individual mouse. B6, □; μMT, △; BALB/c, □; Jh, ▽; $Btk^{-/-}$, ○. Filled symbols, mice were moribund when euthanized. The short horizontal lines indicate means of three or more log-transformed titers; the dotted line at 2×10^3 PFU/g indicates the limit of detection. *, $P < 0.01$; in (E) the * relates to moribund $Btk^{-/-}$ mice compared to B6 mice and to $Btk^{-/-}$ mice not showing disease signs.

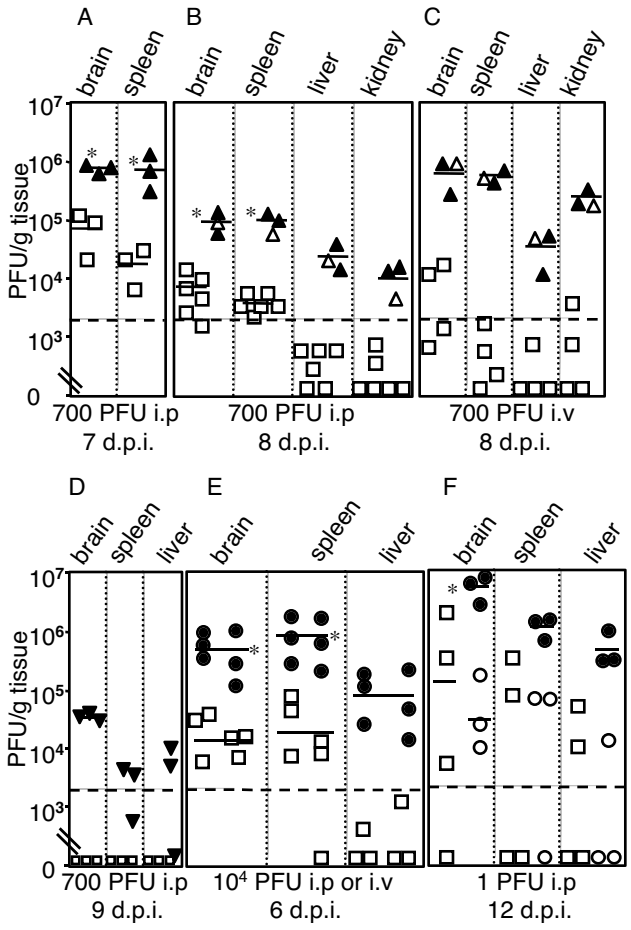
A
B
C
brain
spleen
liver
kidney
PFU/g tissue
700 PFU i.p
7 d.p.i.
700 PFU i.p
8 d.p.i.
700 PFU i.v
8 d.p.i.
D
E
F
700 PFU i.p
9 d.p.i.
10⁴ PFU i.p or i.v
6 d.p.i.
1 PFU i.p
12 d.p.i.

FIG. 3.3. (A-L) Organs 7 d.p.i. from B6, μMT, and $Btk^{-/-}$ mice infected with 700 PFU. Tissue sections were stained with H&E or processed for ISH. Insets (400x) show EC of the same organ stained positively with a viral ISH probe. (M-T) Organs 9 d.p.i. from BALB/c and Jh mice infected with 700 PFU. Tissue sections were stained with H&E. Arrowheads in N and P, boundary of germinal centers. Inset in T, 400x view of boxed area showing a viral inclusion body. e, perivascular edema; f, fibrin in the perivascular space; hn, hepatic necrosis; pp, Peyer's patch; v, blood vessel.

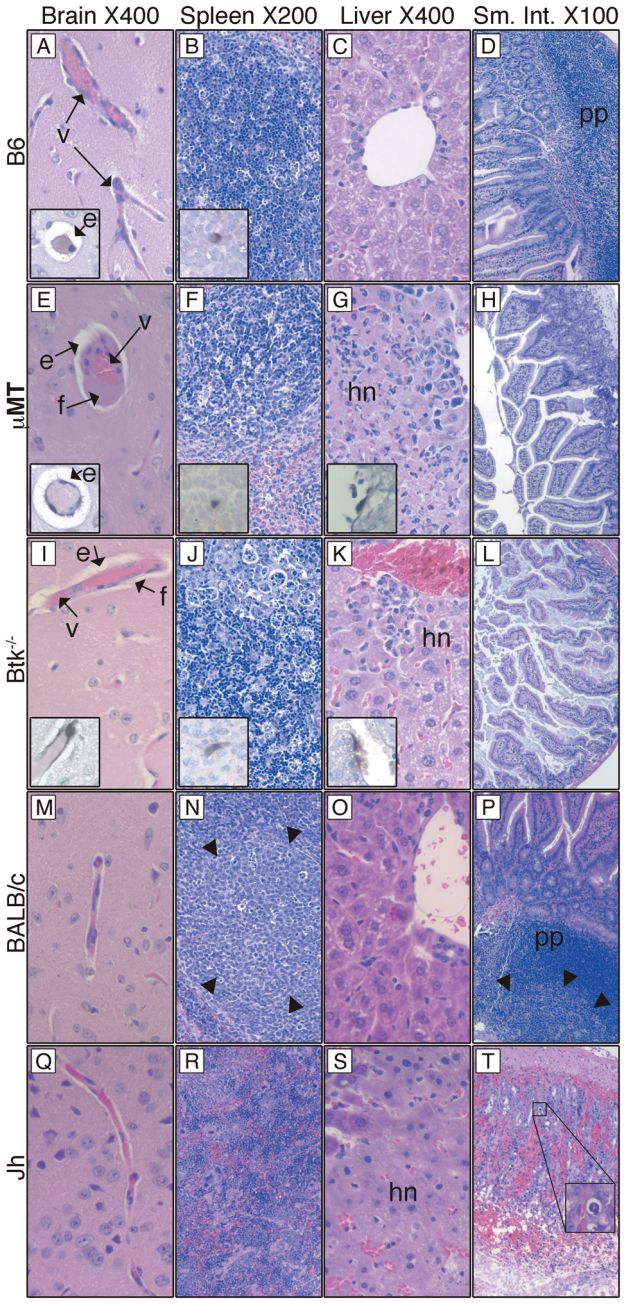
Brain X400
Spleen X200
Liver X400
Sm. Int. X100
B6
μMT
Btk-/-
BALB/c
Jh
A
B
C
D
E
F
G
H
I
J
K
L
M
N
O
P
Q
R
S
T
v
e
f
hn
pp

FIG. 3.4. Representative H&E-stained tissue sections from organs 12 d.p.i. from B6 and $Btk^{-/-}$ mice mock-infected or infected with 1 PFU. Arrowheads in E, germinal center boundary. *, lymphocytes adherent to EC. va, vasculitis; m, meningeal vascular necrosis; h, hepatitis.

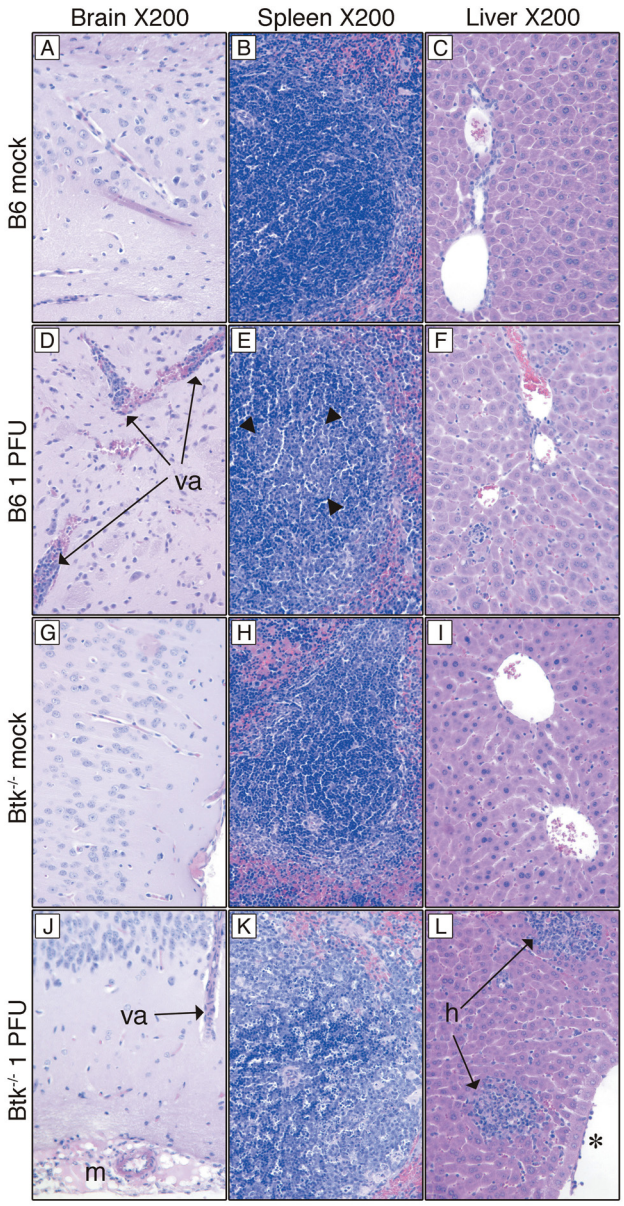
Brain X200
Spleen X200
Liver X200
B6 mock
B6 1 PFU
Btk-/- mock
Btk-/- 1 PFU
A
B
C
D
E
F
G
H
I
J
K
L
va
va
m
h
*

FIG. 3.5. Northern analysis of FasL and RANTES polyA+ RNA in BALB/c and Jh liver. RNA was isolated 9 d.p.i. from liver of BALB/c and Jh mice mock-infected (m) or infected (i) with 700 PFU. Each lane has RNA from an individual mouse. The level of FasL or RANTES was normalized to the actin level and then to the value for the mock-infected BALB/c mouse, as indicated under the lanes. FasL levels were higher in infected Jh than BALB/c livers ($P = 0.002$). RANTES levels were lower in infected Jh than BALB/c livers ($P = 0.006$).

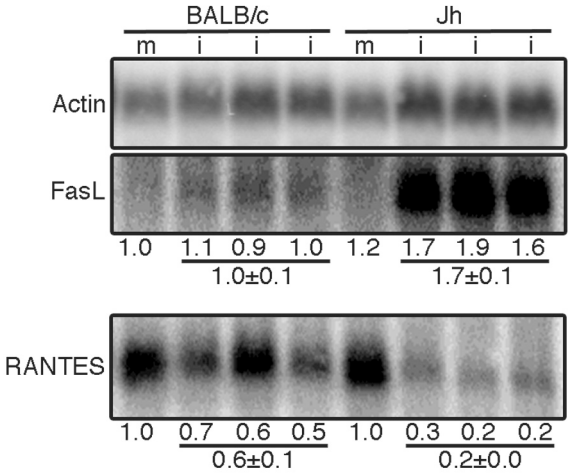
BALB/c
Jh
m i i i m i i i
Actin
FasL
1.0 1.1 0.9 1.0 1.2 1.7 1.9 1.6
1.0±0.1
1.7±0.1
RANTES
1.0 0.7 0.6 0.5 1.0 0.3 0.2 0.2
0.6±0.1
0.2±0.0

FIG. 3.6. Serum nAb titers. Sera (A) pre-infection (open symbols) and 6 d.p.i. (filled symbols) from B6, TCR$\alpha^{-/-}$, and Btk$^{-/-}$ mice infected with 1 x 10^4 PFU, (B) 7 d.p.i. from B6 and Btk$^{-/-}$ mice infected with 700 PFU, (C) 9 d.p.i. from B6 and $A^b_\beta{}^{-/-}$ mice mock-infected (open) or infected (filled) with 700 PFU, and (D) 12 d.p.i. from B6 and Btk$^{-/-}$ mice mock-infected (open) or infected (filled) with 1 PFU of MAV-1. The dotted line represents the limit of detection. Each symbol represents serum from an individual mouse.

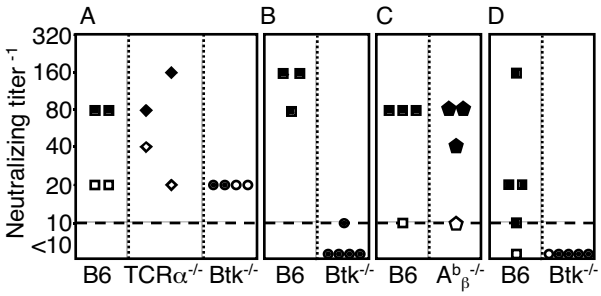
A
B
C
D
320
160
80
40
20
10
<10
Neutralizing titer -1
B6
TCRα-/-
Btk-/-
B6
Btk-/-
B6
Ab β -/-
B6
Btk-/-

FIG. 3.7. Anti-MAV-1 IgM and IgG. (A) Pooled sera pre-infection (open) and 6 d.p.i. (filled) from B6 (□, n=3), $TCRa^{-/-}$ (◇, n =5), and $Btk^{-/-}$ (○, n=2) mice infected with 1 x 10^4 PFU assayed for antiviral IgM. (B) Sera pre-infection (open) and 6 d.p.i. (filled) from 5 B6 and 5 $TCR\beta x\delta^{-/-}$ mice infected with 700 PFU assayed for antiviral IgM. Mean values ± standard deviation are shown. (C) Sera from mock-infected B6 (□, n=1) or $Btk^{-/-}$ (○, n=1) mice and pooled sera from B6 (■, n=4) or $Btk^{-/-}$ (●, n=6) mice infected with 1 PFU were assayed for antiviral IgM (solid lines) and antiviral IgG (dashed lines) 12 d.p.i. (D) Mean values for sera from 5 B6 (■) mice and 5 $CD4^{-/-}$ (★) mice, pooled sera from 5 A^b_β (⬟) mice, and pooled sera from 2 $TCR\beta x\delta^{-/-}$ (◆) mice assayed for antiviral IgG 12 weeks p.i. with 700 PFU. Mean values ± standard deviation are shown for B6 and $CD4^{-/-}$ samples.

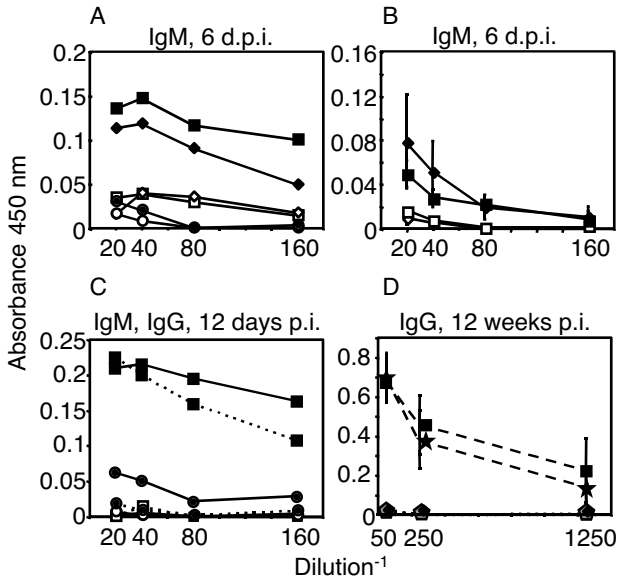
A
IgM, 6 d.p.i.
B
IgM, 6 d.p.i.
C
IgM, IgG, 12 days p.i.
D
IgG, 12 weeks p.i.
Absorbance 450 nm
Dilution-1
20 40 80 160
50 250 1250

Fig. 3.8. (A) RAG-1$^{-/-}$ mice infected with 100 PFU were treated i.v. daily 0-7 d.p.i. with 1, 0.25 ml of PBS, 2, pooled sera from naïve RAG-1$^{-/-}$ mice, 3, pooled sera from naïve B6 mice, or 4, pooled MAV-1-immune sera diluted 1:4 in PBS. MAV-1-immune sera were harvested 12 weeks p.i. from B6 mice infected with 700 PFU and had nAb titers >1:1000, high levels of antiviral IgG, and no detectable antiviral IgM (data not shown and Fig. 3.5Bd). Virus levels were determined 7 d.p.i. (B) Sera pooled 6 to 9 d.p.i. from MAV-1-infected Btk$^{+/+}$ (■) or Btk$^{-/-}$ (●) mice were assayed for antiviral IgM (solid line), IgG (dashed line), and nAb (box). (C) Btk$^{-/-}$ mice infected with 100 PFU were treated i.p. daily 4 to 9 d.p.i with 0.1 ml of the Btk$^{+/+}$ (●, n=4) or Btk$^{-/-}$ (○, n=3) 6 to 9 d.p.i. antiserum shown in Fig. 3.8B.

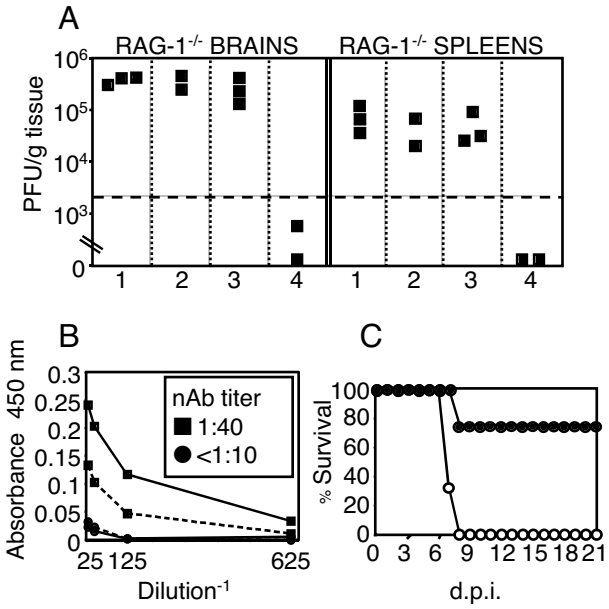
A
RAG-1-/- BRAINS
RAG-1-/- SPLEENS
PFU/g tissue
10^6
10^5
10^4
10^3
0
1 2 3 4 1 2 3 4
B
Absorbance 450 nm
0.3
0.25
0.2
0.15
0.1
0.05
0
nAb titer
1:40
<1:10
25 125 625
Dilution-1
C
% Survival
100
80
60
40
20
0
0 3 6 9 12 15 18 21
d.p.i.

CHAPTER 4

ALPHA/BETA INTERFERON SIGNALING IS A KEY DETERMINANT OF MOUSE ADENOVIRUS TYPE 1 ORGAN TROPISM[1]

[1] Moore, M.L., Brown, C.C., and K.R. Spindler. To be submitted to Journal of Virology.

ABSTRACT

Infection of most mouse strains with mouse adenovirus type 1 (MAV-1) results in dose-dependent encephalomyelitis. MAV-1 has a tropism for vascular endothelial cells and replicates to highest levels in the central nervous system (CNS) and the spleen. We analyzed the role of interferon-alpha/beta (IFN-α/β) in MAV-1-induced encephalomyelitis by comparing the pathogenesis of MAV-1 in 129 Sv/Ev and IFN-α/β receptor null (IFN-α/β$R^{-/-}$) mice. Surprisingly, disruption of IFN-α/β signaling had no effect on virus replication in the brain, and IFN-α/β$R^{-/-}$ mice were more susceptible than controls to MAV-1-induced disease only at a high dose. IFN-α/β$R^{-/-}$ mice exhibited a more disseminated MAV-1 infection than controls and had higher virus loads than control mice in all organs except the brain. We identified interferon-stimulated genes (ISGs) whose steady-state RNA levels were increased by MAV-1 infection in vitro and in vivo. Northern analyses of mRNAs in infected mice suggest that interferon regulatory factor 7 (IRF-7) and major histocompatibility complex (MHC) class I play a role in IFN-α/β signaling-dependent control of MAV-1 organ tropism. Thus, IFN-α/β signaling prevents systemic MAV-1 infection but does not play a critical role in protecting against MAV-1-induced encephalomyelitis or preventing MAV-1 replication in the CNS. We propose that brain vascular endothelial cells of 129 Sv/Ev mice are defective for IFN-α/β signaling in vivo.

INTRODUCTION

Since adenoviruses are species-specific, mouse adenovirus type 1 (MAV-1) provides a good model of adenovirus pathogenesis. The genome of MAV-1 is similar to that of human adenoviruses (hAds) in overall organization, but there are significant differences, e.g. MAV-1

lacks a VA RNA gene and the MAV-1 early 3 (E3) bears no sequence similarity to that of hAds (reviewed in reference 35). Infection of adult mice of outbred and most inbred strains results in dose-dependent encephalomyelitis (12, 14, 18, 36). MAV-1 infects cells of the monocyte/macrophage lineage and endothelial cells of the microvasculature, and highest levels of virus are found in the spleen and central nervous system (CNS) (6, 14). MAV-1 has not been observed in the brain parenchyma; rather it is restricted to the vascular endothelium (6, 12, 14). Sublethal irradiation of inbred mice that are resistant to MAV-1 infection renders them susceptible, suggesting that resistance to MAV-1 infection has an immunological basis (36). Elucidation of immune mechanisms elicited by MAV-1 may provide strategies for countering hAd-induced disease and facilitating adenovirus-mediated gene therapy.

We have used immunodeficient mouse strains to investigate the role of adaptive immunity in MAV-1 pathogenesis. α/β T cells and perforin contribute to MAV-1-induced acute encephalomyelitis (26 and Chapter 2). In contrast, mice lacking B cells or Bruton's tyrosine kinase (Btk) are highly susceptible to acute MAV-1 infection, and survival correlates with early T cell-independent antiviral IgM production (Chapter 3; M.L. Moore, E.L McKissic, J.E.Wilkinson, C.C. Brown, and K. R. Spindler, submitted). Btk-dependent control of virus infection in mice is unique to MAV-1.

Although Btk plays a critical role in early protection from MAV-1 infection, we hypothesized that the interferon-alpha/beta (IFN-α/β) system is also an important component of the antiviral response to acute MAV-1 infection. In single-cycle infectious yield reduction assays in L929 cells in vitro, MAV-1 is much more resistant than vesicular stomatitis virus (VSV) Indiana to pretreatment with mouse IFN-α/β, but MAV-1 replication is not completely resistant to IFN-α/β (15). Early region 1A (E1A) mutants of MAV-1 are more sensitive to

IFN-α/β than wt MAV-1. These data indicated that MAV-1 interferes with the IFN-α/β antiviral response and implicated a role for IFN-α/β in MAV-1 immunopathogenesis.

The IFN-α/β (type I IFN) system is a key component of innate immunity to viruses; α and β interferons are cytokines produced by most cells in culture in response to virus infection (39). IFN-α/β cytokines exert their function via interaction with the IFN-α/β receptor (IFN-α/βR) and subsequent activation of JAK-STAT signal transduction pathways, leading to a regulated cascade of transcription of interferon-stimulated genes (ISGs) and establishment of the antiviral state (reviewed in reference 31). The use of IFN-α/βR null (IFN-α/βR$^{-/-}$) mice has demonstrated the critical role of IFN-α/β in protecting against infection and acute disease induced by VSV (29), Semliki Forest virus (29), Theiler's virus (8), measles virus (28), Venezuelan equine encephalitis virus (11), and Sindbis virus (30). Furthermore, the use of these mice in models of viral pathogenesis has given insight into the functional role of IFN-α/β in regulating cytotoxic T lymphocyte (CTL) responses (38), macrophage function (13), and virus organ and cell tropism (9, 27, 37).

We report here an analysis of the role of IFN-α/β in MAV-1 infection. IFN-α/βR$^{-/-}$ mice were no more susceptible than 129 Sv/Ev controls to MAV-1-induced encephalomyelitis at moderate doses, but they were slightly more susceptible than controls at a high dose. However at moderate doses IFN-α/βR$^{-/-}$ mice had higher levels of infectious MAV-1 in spleens at 4 and 7 days post-infection (p.i) and exhibited a more disseminated MAV-1 infection at 7 days p.i. than control mice. We identified several ISGs whose steady-state RNA levels were increased by MAV-1 infection in vitro and in vivo. Our results suggest that IFN-α/β signaling limits MAV-1 replication in the spleen and prevents widespread infection of vascular endothelial cells but does not prevent MAV-1-induced encephalomyelitis or limit MAV-1 replication in the brain. We

propose that brain vascular endothelial cells of 129 Sv/Ev mice are defective for IFN-α/β signaling in vivo.

MATERIALS AND METHODS

Virus and mice. Wild-type MAV-1, originally obtained from S. Larsen (1), was grown and passaged in NIH 3T6 fibroblasts, and titers of viral stocks were determined by plaque assay on 3T6 cells as previously described (5). All animal work complied with all relevant federal and institutional policies. 129 Sv/Ev mice were purchased from Taconic. IFN-α/βR$^{-/-}$ mice were a kind gift from Kate Ryman. Mice were infected with the indicated doses by the intraperitoneal (i.p.) route in a volume of 0.1 ml of phosphate-buffered saline. Mice were housed in microisolator cages and infected between 4-6 weeks of age. Infected mice were scored twice daily for the presence or absence of any disease signs, i.e., hunched posture, ataxia, ruffled fur, and in moribund mice, abdominal breathing, hindlimb paralysis, seizure, and tremor. Moribund mice were euthanized by CO_2 asphyxiation.

Quantitation of virus from organs. Organs were harvested aseptically from euthanized mice, and homogenates were prepared as described previously (36). Virus was titrated by plaque assay on 3T6 cells as previously described (5). Briefly, 20 to 200 mg of tissue was homogenized in phosphate-buffered saline in a microcentrifuge tube by using a plastic pestle and sterile sand. Organ homogenates (5 to 10% wt/vol) were serially diluted and assayed. The means of the log titers were compared by a two-tailed *t* test, assuming equal variance. Counts of fewer than 20 plaques per 60 mm diameter plate were considered unreliable. Therefore, 2 x 10^3 PFU/g of tissue was calculated as the detection limit. Values below the detection limit were excluded from statistical analyses (calculations of means and t test statistics).

ISH and histology. The following organs were harvested and fixed in 10% formalin: spleen, kidney, liver, small and large intestines, Peyer's patches, mandibular lymph nodes, thymus, lung, heart, and brain. The lungs were not inflated prior to fixation. Sections were stained with hematoxylin and eosin (H-E) or processed for in situ hybridization (ISH) and viewed by light microscopy. ISH was performed as previously described (14). Briefly, sections were deparaffinized, rehydrated, digested with proteinase K, and probed with an antisense digoxigenin riboprobe transcribed from a segment of the E3 region inserted into pBluescript SK(-) (Stratagene) vector. Following hybridization, slides were incubated with antidigoxigenin-alkaline phosphatase (Boehringer Mannheim), and the substrate nitroblue tetrazolium and 5-bromo-4-chloro-3-indolylphosphate (Boehringer Mannheim) was added. Slides were lightly counterstained with hematoxylin and coverslipped with Permount.

RPA. Mouse brain microvascular endothelial cells (MBMEC) were maintained as previously described (4). Subconfluent MBMEC were infected with MAV-1 at a MOI of 5, and total cellular RNA was harvested by Nonidet P-40 (NP-40) phenol/chloroform extraction (3). The RNA (1 mg/ml) was then treated with DNAse I (0.1 unit/μg RNA) at 37° C for 30 min, phenol/chloroform extracted twice, ethanol-precipitated, and resuspended in RNAse-free water. The plasmids pHEX (36), pZU14 (2), and rk+7 (containing a *Sal*I-*Bgl*II fragment corresponding to MAV-1 nt 828 to 1179 inserted into a pBS+ [Stratagene] vector) were linearized with the appropriate enzyme and used as templates for transcription of MAV-1 hexon, MAV-1 early gene region 3 (E3), and MAV-1 early gene region 1A (E1A) antisense riboprobes, respectively, using T3 or T7 RNA polymerase in the presence of [α-^{32}P]-UTP. A mouse actin ^{32}P-labeled probe was prepared by T7 polymerase transcription of pTRI-actin-mouse (Ambion). Ribonuclease protection assays were performed using the Ambion RPA II^{TM} system according to the

manufacturer's protocol. Briefly, probes were electrophoresed on 5% acrylamide/8M urea gels and eluted after excision. Probes were mixed with 10 to 25 μg of sample RNA, ethanol-precipitated, resuspended in hybridization buffer, incubated at 95° C for 3 min and overnight at 42° C. The samples were then treated with an RNAse A/T_1 mixture for 30 min at 37° C, precipitated, and RNA duplexes were loaded on 5% acrylamide/8M urea gels. Molecular size markers were end-labeled *Rsa*I fragments of ΦX174 replicative form DNA.

cDNA array analysis. Subconfluent MBMEC were infected with MAV-1 at a MOI of 5. Total cellular RNA was harvested at 20 h post-infection (p.i.) by the NP-40 method and treated with DNAse I as described above. PolyA+ RNA was isolated from total RNA using the PolyATract system (Promega). Clontech Atlas™ Mouse 1.2 nylon membrane arrays were used according to the provided protocol. Briefly, polyA+ RNA samples were reverse-transcribed with Moloney murine leukemia virus reverse transcriptase using the Clontech CDS primer mixture to produce [α-^{32}P]-dATP-labelled cDNA probes. The membranes were hybridized overnight and washed according to the protocol, scanned with a phosphorimager, and the data were analyzed with Clontech AtlasImage™ 1.01 software. Briefly, "adjusted intensity" values for spots were calculated by adjusting for the background intensity immediately surrounding the spot then multiplying by a normalization coefficient defined as the average of the ratios of the intensities of actin and glyceraldehyde-3-phosphate dehydrogenase (G3PDH) on two arrays. The ratio of signals for a particular gene was defined as the ratio of the adjusted intensities. Thus, a signal at background level in one array results in an undefined ratio.

Northern analysis. J774A.1 macrophage cells were grown in Dulbecco's modified Eagle's medium (DMEM) supplemented with 10% fetal bovine serum and 1.0 mM sodium pyruvate and passaged by scraping. Subconfluent MBMEC and J774A.1 cells were infected with MAV-1 at a

MOI of 5, and total cellular RNA was harvested at 20 h post-infection (p.i.) by NP-40 method described above. Spleens were homogenized in 900 μL TRI Reagent (Molecular Research Center, Inc.), and total RNA was isolated by the manufacturer's protocol. PolyA+ RNA was isolated as described above. 1 μg of each polyA+ RNA was electrophoresed on a 1% agarose/3% formaldehyde/40 mM MOPS pH 7.0/10 mM NaOAc/1 mM EDTA gel and then transferred to a nylon membrane (Boehringer Mannheim). For probes, oligonucleotides (β-actin 3' primer (34); regulated upon activation, normal T cell expressed and secreted (RANTES) 3' primer (19); interferon regulatory factor 1 (IRF-1) Clontech Atlas™ cDNA Array primer sequence M174-238; interferon regulatory factor 7 (IRF-7) Clontech Atlas™ cDNA Array primer sequence MA328_A; signal transducer and activator of transcription 1 (STAT-1) Clontech Atlas™ cDNA Array primer sequence M423-600; β_2-microglobulin (β_2m) 3' primer (17); interferon-beta (IFN-β) probe sequence (23); and MHC class I heavy chain 3' primer (17)) were end-labeled with γ-^{32}P using polynucleotide kinase. Membranes were hybridized, stripped, and re-probed as described (15). mRNA levels were quantitated with a phosphorimager using ImageQuant software (Molecular Dynamics).

RESULTS

Virulence of MAV-1 in IFN-α/βR$^{-/-}$ mice. wt MAV-1 replication is significantly more resistant to IFN-α/β pretreatment in vitro than VSV Indiana (15). To investigate the role of IFN-α/β in MAV-1-induced disease, we compared the virulence of MAV-1 in IFN-α/βR$^{-/-}$ and control 129 Sv/Ev mice. There were no differences in clinical disease signs or survival between IFN-α/βR$^{-/-}$ and 129 Sv/Ev mice infected i.p. with 10^2 to 10^4 PFU of MAV-1 and monitored for 3 months in independent experiments (data not shown). However, IFN-α/βR$^{-/-}$ mice inoculated

with 10^5 PFU were slightly more susceptible than controls to acute MAV-1 infection (Fig. 4.1). These data indicate that IFN-α/β plays a minor role in protection from MAV-1-induced disease and are consistent with the findings that wt MAV-1 counteracts the IFN-α/β response (15).

Disseminated MAV-1 infection in IFN-α/βR$^{-/-}$ mice. In mice, IFN-α/β restricts the cell and organ tropism of viruses (9, 28, 30). We tested whether levels and distribution of infectious MAV-1 were altered in IFN-α/βR$^{-/-}$ mice relative to 129 Sv/Ev controls. MAV-1 replicates to highest levels in the central nervous system and the spleen (14, 18). We harvested brains, spleens, livers, and kidneys of infected mice and titrated infectious MAV-1 by plaque assay. There were significantly higher viral loads at 4 days p.i. in spleens of IFN-α/βR$^{-/-}$ mice infected with 10^4 PFU than controls (Fig. 4.2A). Figure 4.2B shows that at 7 days p.i. with 700 PFU, levels of infectious virus were higher in spleens, livers, and kidneys, but not brains, of IFN-α/βR$^{-/-}$ mice than controls. Mice lacking α/β T cells have high levels of infectious MAV-1 in spleens and brains at 3 weeks p.i., whereas control mice clear the virus; and mice lacking α/β T cells succumb to MAV-1 infection 9 to 16 weeks p.i. with high virus loads (26 and Chapter 2). No infectious MAV-1 was recovered from IFN-α/βR$^{-/-}$ or control mice at 14 weeks p.i. (data not shown), suggesting that α/β T cell-dependent control of MAV-1 replication does not depend on IFN-α/β signaling.

We analyzed the histological consequences and distribution of MAV-1 infection in the mice shown in Figure 4.2B. H-E-stained sections revealed no histopathological difference between infected IFN-α/βR$^{-/-}$ and control mice (data not shown). Perivascular edema was observed in the brains of infected IFN-α/βR$^{-/-}$ and control mice that is typical of MAV-1-induced encephalomyelitis in C57BL/6 (B6) mice (12, 26 and Chapter 2), and there were no other significant lesions (data not shown). However, consistent with the virus load data (Fig. 4.2B),

ISH analysis showed a disseminated MAV-1 infection in endothelial cells of IFN-α/βR$^{-/-}$ mice (Fig. 4.3). In contrast, in control mice, positive staining for MAV-1 nucleic acid was not observed in endothelial cells of the kidneys or lungs, and positive staining was rare in endothelial cells of the liver (data not shown). Together the data indicate that IFN-α/β signaling is a key determinant of MAV-1 organ tropism.

ISG expression in MBMEC and J774A.1 cells. Since MAV-1 infects vascular endothelial cells and replicates to high titers in the brain (6, 14), we identified cellular genes that are transcriptionally activated early in MAV-1 infection in mouse brain microvascular endothelial cells (MBMEC) vitro. Growth curve analyses have shown that MAV-1 replicates in 3T6 cells and MBMEC with similar kinetics (4). We analyzed the time course of early and late MAV-1 gene transcription in MBMEC infected at a MOI of 5. In RPA analyses MAV-1 hexon (late) gene transcription was detected at 24 hours p.i., MAV-1 early 1A (E1A) gene transcription was detected at 16 hours p.i., and MAV-1 early 3 (E3) gene trancription was detected at 12 hours p.i. (Fig 4.4). In RT-PCR and Western analyses, both E1A and E3 expression were detected 12 hours p.i. in MBMEC infected at an MOI of 5 (data not shown). We chose to assay cellular mRNA levels in MBMEC at 20 hours p.i. using commercially available mouse gene cDNA arrays. Figure 4.5 shows selected areas of two arrays probed with cDNAs derived from infected or mock-infected MBMEC (top and bottom panels, respectively). STAT-1 steady-state mRNA levels were increased 6.7 fold. MAV-1 infection also increased steady-state IRF-7 mRNA levels by an undefined ratio (see Materials and Methods).

Northern analyses confirmed and extended the results obtained with the cDNA arrays. Since MAV-1 infects cells of the macrophage/monocyte lineage as well as vascular endothelial cells, we infected J774A.1 macrophage cells and MBMEC. STAT-1 and IRF-7 polyA+ RNA

steady-state levels were higher in MBMEC and J774A.1 cells upon MAV-1 infection, supporting the cDNA array results (Fig. 4.6). STAT-1 and IRF-7 are ISGs (7). We tested whether steady-state levels of other ISG mRNAs were increased by MAV-1 infection. PolyA+ steady-state RNA levels of the transcription factor IRF-1 and the MHC class I antigen presenting molecules β_2m and MHC class I heavy chain were also higher in infected MBMEC and J774A.1 cells than mock-infected cells (Fig. 4.6). PolyA+ RNA steady-state levels of the chemokine RANTES were greatly increased in MBMEC but not J774A.1 cells by MAV-1 infection (Fig. 4.6). Human RANTES is an ISG (10). IFN-β steady-state polyA+ RNA levels were not detected in MBMEC and were unchanged by MAV-1 infection in J774A.1 cells (Fig. 4.6). The results obtained for each gene shown in Fig 4.6 were reproducibly observed in three Northern blots from three independent infections of MBMEC and J774A.1 cells (data not shown). Thus we identified several ISGs whose mRNA steady-state levels were increased during the early phase of MAV-1 infection in vitro.

ISG expression in vivo. We analyzed the expression of ISGs whose levels were increased in vitro by MAV-1 infection in mock-infected and MAV-1-infected 129 Sv/Ev and IFN-$\alpha/\beta R^{-/-}$ mice. STAT-1, IRF-7, IRF-1, and β_2m polyA+ RNA steady-state levels were higher in MAV-1-infected 129 Sv/Ev spleens than a mock-infected 129 Sv/Ev spleen 4 days p.i., whereas only STAT-1 and IRF-1 levels were higher in MAV-1-infected IFN-$\alpha/\beta R^{-/-}$ spleens than a mock-infected IFN-$\alpha/\beta R^{-/-}$ spleen (Fig. 4.7, same mice as Fig. 4.2A). Thus higher viral loads in IFN-$\alpha/\beta R^{-/-}$ spleens than controls (Fig. 4.2A) correlated with the lack of increased steady-state levels of IRF-7 and β_2m polyA+ RNAs in these organs (Fig. 4.7). We also found that β_2m and MHC class I heavy chain levels were higher in the infected lungs of 129 Sv/Ev mice 6 day p.i. relative to mock and slightly higher relative to infected IFN-$\alpha/\beta R^{-/-}$ lungs (Fig. 4.8). IRF-7

expression was detected in the lungs of MAV-1-infected 129 Sv/Ev but not IFN-α/βR$^{-/-}$ mice 6 days p.i. (Fig. 4.8). Together, the data suggest that MHC class I and IRF-7 may play a role in IFN-α/βR-dependent control of MAV-1 replication in lymphoid tissue and in restricting MAV-1 organ tropism.

DISCUSSION

MAV-1 infects monocyte/macrophage cells and endothelial cells, replicates to highest levels in lymphoid tissue and the CNS, and induces dose-dependent encephalomyelitis (6, 14). We show here that IFN-α/β signaling reduces MAV-1 dissemination but does not prevent MAV-1-induced encephalomyelitis or MAV-1 replication in the brain. MAV-1 infection increases ISG steady-state mRNA levels in vitro and in vivo. Increased steady-state levels of IRF-7 and MHC class I molecule mRNAs in infected tissues correlated with control of MAV-1.

Disruption of IFN-α/β signaling resulted in a more widespread MAV-1 infection without inflammatory consequences. Infection of type I IFN-deficient mice has repeatedly demonstrated the importance of this system for protection against virus replication and dissemination (8, 9, 11, 22, 28-30, 37). Relative to control mice, infection of IFN-α/βR$^{-/-}$ mice with moderate doses of MAV-1 resulted in higher levels of infectious virus in spleen, liver and kidney (Fig. 4.2B) and significant infection in lung (Fig. 4.3). However, this disseminated MAV-1 infection in IFN-α/βR$^{-/-}$ mice did not show clinical or histopathological differences from control mice (data not shown). These results are similar to those found in LCMV infection, where IFN-α/βR$^{-/-}$ mice are more resistant than 129 Sv/Ev controls to CTL-mediated immunopathology (29). We believe that IFN-α/β signaling contributes to cytotoxic T cell (CTL)-mediated immunopathology in MAV-1-infected mice for the following reason. β_2m mRNA steady-state levels were lower in

the spleens of IFN-α/βR$^{-/-}$ mice than control mice at 4 days p.i. (Fig. 4.7), and α/β T cell-deficient, perforin-deficient, and β_2m-deficient mice exhibit less acute MAV-1 disease than controls (26 and Chapter 2). An implication of widespread MAV-1 infection without significant cellular inflammation is that modulation of the type I IFN system may improve the efficacy of adenovirus-mediated gene therapy by decreasing inflammation and/or increasing vector dissemination.

MAV-1 is useful for investigating type I IFN signaling in vitro and in vivo. STATs and IRFs are important transcriptional regulators of other ISGs and coordinate the antiviral state (reviewed in reference 31). Experiments with Newcastle disease virus in vitro led to a multiphasic model of IFN-α/β transcriptional regulation in which early IFN-β is produced and secreted in response to virus infection, IFN-β stimulates the IFN-α/βR in an autocrine fashion, IRF-7 expression is induced by an IFN-α/βR-dependent mechanism, and then IRF-7 activates a later phase of robust ISG and IFN-β transcription. (25, 32, 33). We showed that the STAT-1, IRF-1, and IRF-7 are transcriptionally induced by MAV-1 infection in vitro and in vivo and that induction of IRF-7 by MAV-1 depends on the IFN-α/βR in vivo (Figs. 4.5 through 4.8). These results are consistent with and provide in vivo support for the multiphasic model. In contrast to NDV-infected fibroblasts, increased IFN-β levels did not coincide with increased IRF-7 levels in MAV-1-infected MBMEC or J774A.1 cells (33; Fig. 4.6). Interestingly, IFN-β mRNA was not detected in MBMEC (Fig. 4.6). More experiments are needed to determine if type I IFN signaling responses to MAV-1 and Newcastle disease virus differ. It is likely that differences in cell lines and/or in the IFN response to different viruses affects type I IFN signaling pathways.

IFN-α/β signaling is a key regulator of effector T cell function (reviewed in reference 20). We also identified MAV-1-induced ISGs that are involved in T cell function. Steady-state

levels of the MHC class I antigen presenting molecules β_2m and MHC class I heavy chain were increased by MAV-1 infection in MBMEC and J774A.1 cells and mouse tissues (Fig. 4.6 through 4.8). Like IRF-7, induction of β_2m levels in spleens of MAV-1-infected mice depended on the IFN-α/βR (Fig. 4.7). However, IFN-$\alpha/\beta R^{-/-}$ mice had higher levels of infectious virus in spleens than control mice at 4 days p.i. and 8 days p.i. (Fig. 4.2) whereas MAV-1-infected β_2m-deficient mice had spleen virus loads equivalent to B6 controls at 8 days p.i. (26 and Chapter 2). One interpretation of these results is that higher levels of infectious MAV-1 in spleens of IFN-$\alpha/\beta R^{-/-}$ mice than controls may be a direct consequence of innate antiviral IFN-α/β deficiency in IFN-$\alpha/\beta R^{-/-}$ mice rather than a downstream effect on β_2m transcription and T cell-mediated viral clearance.

Steady-state mRNA levels of the ISG RANTES were increased by MAV-1 infection in MBMEC but not J774A.1 cells (Fig. 4.6). RANTES is a chemokine that attracts monocytes and T cells and is required for T cell function in mice (24). Consistent with this increase in RANTES in a brain endothelial cell line, we have detected induced steady-state levels of RANTES mRNA in the brains of MAV-1 infected B6 mice at 9 days p.i. (Moore and Spindler, unpublished data). Interestingly, we did not detect RANTES mRNA in the brains of MAV-1-infected BALB/c mice at 9 days p.i. It is possible that RANTES contributes to MAV-1-induced encephalomyelitis, because MAV-1 induces encephalomyelitis in B6 mice (where RANTES is detected) but not BALB/c mice (where it is not) (12).

A key issue concerning type I IFN in MAV-1 pathogenesis is the role of the viral E1A protein. E1A mutants of MAV-1 are less resistant to IFN-α/β treatment in vitro than wt MAV-1, and expression of MAV-1 E1A in mouse fibroblasts rescues VSV from the antiviral effect of IFN-α/β (15). hAd5 E1A directly binds STAT-1 and blocks ISG transcription in primary human

cells (21). We have preliminary evidence that MAV-1 E1A binds STAT-1 (L. Fang and K. Spindler, unpublished data). We hypothesized that *pm*E109 (MAV-1 E1A null mutant) virus replication would be partially restored in IFN-α/βR$^{-/-}$ mice because *pm*E109 is sensitive to IFN-α/β in vitro (15). Preliminary viral load data supports this hypothesis, and immunohistochemistry and Northern analyses suggest that MAV-1 E1A null mutants induce STAT-1 and IRF-7 to higher levels than wt virus in 129 Sv/Ev mice (M. Moore and K. Spindler, unpublished data). We are exploring the role of E1A in modulating IFN signaling in vivo.

A key finding of this report is that IFN-α/β signaling did not protect against MAV-1 replication in the brain or play an important role in protecting against MAV-1-induced encephalomyelitis (Fig. 4.1, 4.2, and data not shown). MAV-1 may effectively counteract the antiviral effects of IFN-α/β signaling in endothelial cells of the brain. Alternatively, IFN-α/β signaling may be defective in endothelial cells of the brain in 129 Sv/Ev mice. These hypotheses are not mutually exclusive. 129 Sv/Ev mice are known to have a defect in inflammatory cell recruitment (40). This may reflect an underlying defect in the type I IFN system. IFN-β mRNA was not detected in MBMEC in contrast to J774A.1 cells (Fig. 4.6) and 3T6 fibroblasts (data not shown), indicating that MBMEC have unconventional IFN-α/β signaling. Human brain microvascular endothelial cells differ from aorta large vessel endothelial cells in MHC class II expression (16). It is possible that defective IFN-α/β signaling in endothelial cells of the CNS relative to other organs contributes to the neurotropism of MAV-1 in 129 Sv/Ev and other strains of mice.

ACKNOWLEDGMENTS

We thank Gwen Hirsch, Adriana Kajon, Carla Sturkie, James Stanton, Katie Kempke, Brian Waters, and Amanda Welton for technical assistance. This work was supported by NIH grant R01 AI023762 to K.R.S. and by an NIH predoctoral traineeship (GM 07103) and an ARCS Foundation Scholarship to M.L.M.

REFERENCES

1. **Ball, A. O., C. W. Beard, P. Villegas, and K. R. Spindler.** 1991. Early region 4 sequence and biological comparison of two isolates of mouse adenovirus type 1. Virology **180:**257-265.

2. **Beard, C. W., A. O. Ball, E. H. Wooley, and K. R. Spindler.** 1990. Transcription mapping of mouse adenovirus type 1 early region 3. Virology **175:**81-90.

3. **Berk, A. J., F. Lee, T. Harrison, J. Williams, and P. A. Sharp.** 1979. Pre-early adenovirus 5 gene product regulates synthesis of early viral messenger RNAs. Cell **17:**935-944.

4. **Cauthen, A. N., C. C. Brown, and K. R. Spindler.** 1999. In vitro and in vivo characterization of a mouse adenovirus type 1 early region 3 mutant. J. Virol. **73:**8640-8646.

5. **Cauthen, A. N., and K. R. Spindler.** 1999. Construction of mouse adenovirus type 1 mutants, p. 85-103. *In* W. S. M. Wold (ed.), Adenovirus methods and protocols. Humana Press, Totowa, NJ.

6. **Charles, P. C., J. D. Guida, C. F. Brosnan, and M. S. Horwitz.** 1998. Mouse adenovirus type-1 replication is restricted to vascular endothelium in the CNS of susceptible strains of mice. Virology **245:**216-228.

7. **de Veer, M. J., M. Holko, M. Frevel, E. Walker, S. Der, J. M. Paranjape, R. H. Silverman, and B. R. Williams.** 2001. Functional classification of interferon-stimulated genes identified using microarrays. J. Leukoc. Biol. **69:**912-20.

8. **Fiette, L., C. Aubert, U. Muller, S. Huang, M. Aguet, M. Brahic, and J. F. Bureau.** 1995. Theiler's virus infection of 129Sv mice that lack the interferon alpha/beta or interferon gamma receptors. J. Exp. Med. **181:**2069-76.

9. **Garcia-Sastre, A., R. K. Durbin, H. Zheng, P. Palese, R. Gertner, D. E. Levy, and J. E. Durbin.** 1998. The role of interferon in influenza virus tissue tropism. J. Virol. **72:**8550-8558.

10. **Genin, P., M. Algarte, P. Roof, R. Lin, and J. Hiscott.** 2000. Regulation of RANTES chemokine gene expression requires cooperativity between NF-kappa B and IFN-regulatory factor transcription factors. J. Immunol. **164:**5352-61.

11. **Grieder, F. B., and S. N. Vogel.** 1999. Role of interferon and interferon regulatory factors in early protection against Venezuelan equine encephalitis virus infection. Virol. **257:**106-118.

12. **Guida, J. D., G. Fejer, L.-A. Pirofski, C. F. Brosnan, and M. S. Horwitz.** 1995. Mouse adenovirus type 1 causes a fatal hemorrhagic encephalomyelitis in adult C57BL/6 but not BALB/c mice. J. Virol. **69:**7674-7681.

13. **Hwang, S. Y., P. J. Hertzog, K. A. Holland, S. H. Sumarsono, M. J. Tymms, J. A. Hamilton, G. Whitty, I. Bertoncello, and I. Kola.** 1995. A null mutation in the gene encoding a type I interferon receptor component eliminates antiproliferative and antiviral responses to interferons alpha and beta and alters macrophage responses. Proc. Natl. Acad. Sci. U S A **92:**11284-8.

14. **Kajon, A. E., C. C. Brown, and K. R. Spindler.** 1998. Distribution of mouse adenovirus type 1 in intraperitoneally and intranasally infected adult outbred mice. J. Virol. **72:**1219-1223.

15. **Kajon, A. E., and K. R. Spindler.** 2000. Mouse adenovirus type 1 replication *in vitro* is resistant to interferon. Virology **274:**213-219.

16. **Karasin, A., S. Macvilay, M. N. Hart, and Z. Fabry.** 1998. Murine endothelia do not express MHC class II I-Ealpha subunit and differentially regulate I-Aalpha expression along the vascular tree. Endothelium **6:**83-93.

17. **Kimura, T., and D. E. Griffin.** 2000. The role of CD8+ T cells and major histocompatibility complex class I expression in the central nervous system of mice infected with neuroadapted Sindbis virus. J. Virol. **74:**6117-6125.

18. **Kring, S. C., C. S. King, and K. R. Spindler.** 1995. Susceptibility and signs associated with mouse adenovirus type 1 infection of adult outbred Swiss mice. J. Virol. **69:**8084-8088.

19. **Lane, T. E., M. T. Liu, B. P. Chen, V. C. Asensio, R. M. Samawi, A. D. Paoleti, I. L. Campbell, S. L. Kunkell, H. S. Fox, and M. J. Buchmeier.** 2000. A central role for

CD4+ T cells and RANTES in virus-induced central nervous system inflammation and demyelination. J. Virol. **74:**1415-1424.

20. **Levy, D. E., I. Marie, and A. Prakash.** 2003. Ringing the interferon alarm: differential regulation of gene expression at the interface between innate and adaptive immunity. Curr. Opin. Immunol. **15:**52-8.

21. **Look, D. C., W. T. Roswit, A. G. Frick, Y. Gris-Alevy, D. M. Dickhaus, M. J. Walter, and M. J. Holtzman.** 1998. Direct suppression of Stat1 function during adenoviral infection. Immunity **9:**871-880.

22. **Luker, G. D., J. L. Prior, J. Song, C. M. Pica, and D. A. Leib.** 2003. Bioluminescence imaging reveals systemic dissemination of herpes simplex virus type 1 in the absence of interferon receptors. J. Virol. **77:**11082-10093.

23. **Mahalingam, S., J. M. Farber, and G. Karupiah.** 1999. The interferon-inducible chemokines MuMig and Crg-2 exhibit antiviral activity in vivo. J. Virol. **73:**1479-1491.

24. **Makino, Y., D. N. Cook, O. Smithies, O. Y. Hwang, E. G. Neilson, L. A. Turka, H. Sato, A. D. Wells, and T. M. Danoff.** 2002. Impaired T cell function in RANTES-deficient mice. Clin. Immunol. **102:**302-309.

25. **Marie, I., J. E. Durbin, and D. E. Levy.** 1998. Differential viral induction of distinct interferon-alpha genes by positive feedback trhough interferon regulatory factor-7. EMBO J. **17:**6660-6669.

26. **Moore, M. L., C. C. Brown, and K. R. Spindler.** 2003. T cells cause acute immunopathology and are required for long term survival in mouse adenovirus type 1-induced encephalomyelitis. J. Virol. **77:**10060-10070.

27. **Mrkic, B., B. Odermatt, M. A. Klein, M. A. Billeter, J. Pavlovic, and R. Cattaneo.** 2000. Lymphatic dissemination and comparative pathology of recombinant measles viruses in genetically modified mice. J. Virol. **74:**1364-72.

28. **Mrkic, B., J. Pavlovic, T. Rülicke, P. Volpe, C. J. Buchholz, D. Hourcade, J. P. Atkinson, A. Aguzzi, and R. Cattaneo.** 1998. Measles virus spread and pathogenesis in genetically modified mice. J. Virol. **72:**7420-7427.

29. **Muller, U., U. Steinhoff, L. F. L. Reis, S. Hemmi, J. Pavlovic, R. M. Zinkernagel, and M. Aguet.** 1994. Functional role of type I and type II interferons in antiviral defense. Science **264:**1918-1921.

30. **Ryman, K. D., W. B. Klimstra, K. B. Nguyen, C. A. Biron, and R. E. Johnston.** 2000. Alpha/beta interferon protects adult mice from fatal Sindbis virus infection and is an important determinant of cell and tissue tropism. J. Virol. **74:**3366-3378.

31. **Samuel, C. E.** 2001. Antiviral actions of interferons. Clin. Microbiol. Rev. **14:**778-809.

32. **Sato, M., N. Hata, M. Asagiri, T. Nakaya, T. Taniguchi, and N. Tanaka.** 1998. Positive feedback regulation of type I IFN genes by the IFN-inducible transcription factor IRF-7. FEBS Lett **441:**106-10.

33. **Sato, M., H. Suemori, N. Hata, M. Asagiri, K. Ogasawara, K. Nakao, T. Nakaya, M. Katsuki, S. Noguchi, N. Tanaka, and T. Taniguchi.** 2000. Distinct and essential roles of transcription factors IRF-3 and IRF-7 in response to viruses for IFN-alpha/beta gene induction. Immunity **13:**539-48.

34. **Schmitt, R. M., E. Bruyns, and H. R. Snodgrass.** 1991. Hematopoietic development of embryonic stem cells in vitro: cytokine and receptor gene expression. Genes Dev. **5:**728-740.

35. **Smith, K., and K. R. Spindler.** 1999. Murine adenovirus, p. 477-484. *In* R. Ahmed and I. Chen (ed.), Persistent viral infections. John Wiley & Sons, New York.

36. **Spindler, K. R., L. Fang, M. L. Moore, C. C. Brown, G. N. Hirsch, and A. K. Kajon.** 2001. SJL/J mice are highly susceptible to infection by mouse adenovirus type 1. J. Virol. **75:**12039-12046.

37. **Steinhoff, U., U. Muller, A. Schertler, H. Hengartner, M. Aguet, and R. M. Zinkernagel.** 1995. Antiviral protection by vesicular stomatitis virus-specific antibodies in alpha/beta interferon receptor-deficient mice. J. Virol. **69:**2153-2158.

38. **van den Broek, M. F., U. Muller, S. Huang, M. Aguet, and R. M. Zinkernagel.** 1995. Antiviral defense in mice lacking both alpha/beta and gamma interferon receptors. J. Virol. **69:**4792-6.

39. **Vilcek, J., and G. C. Sen.** 1996. Interferons and other cytokines, p. 375-399. *In* B. N. Fields, D. M. Knipe, and P. M. Howley (ed.), Fields Virology, Third ed. Lippincott-Raven, Philadelphia.

40. **White, P., S. A. Liebhaber, and N. E. Cooke.** 2002. 129X1/SvJ mouse strain has a novel defect in inflammatory cell recruitment. J. Immunol. **168:**869-874.

FIG. 4.1. 129 (■) and IFN-α/βR$^{-/-}$ (□) mice were infected i.p. with 10^5 PFU of MAV-1 and monitored for survival. Two experiments are shown and indicated. For each strain, n = 5 (Expt. 1) or n = 6 (Expt. 2).

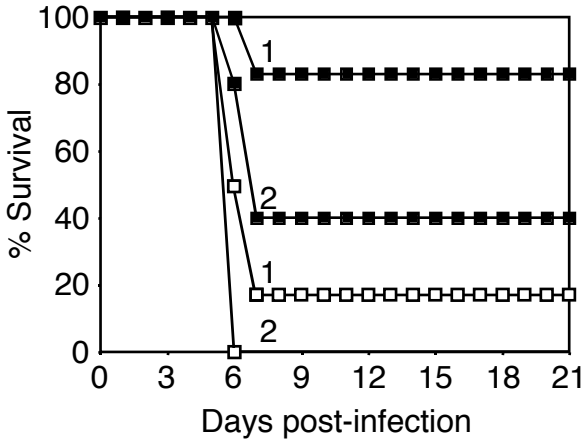
100
80
60
40
20
0
% Survival
0
3
6
9
12
15
18
21
Days post-infection
1
2
1
2

FIG. 4.2. Quantitation of virus from 129 (■) and IFN-α/βR$^{-/-}$ (□) mice. Virus was titrated from homogenized organs by plaque assay. Each symbol represents an individual mouse. The short horizontal lines represent the means of the log-transformed titers. The dotted line at 2 x 10^3 represents the lower limit of detection of the assay. (A) Brains, spleens, livers, and kidneys obtained 4 days p.i from mice infected with 10^4 PFU of MAV-1. (B) spleens and brains obtained 7 days p.i. from mice infected with 700 PFU of MAV-1. Data points below the limit of detection were excluded when calculating mean titers and t statistics. *, $P < 0.02$.

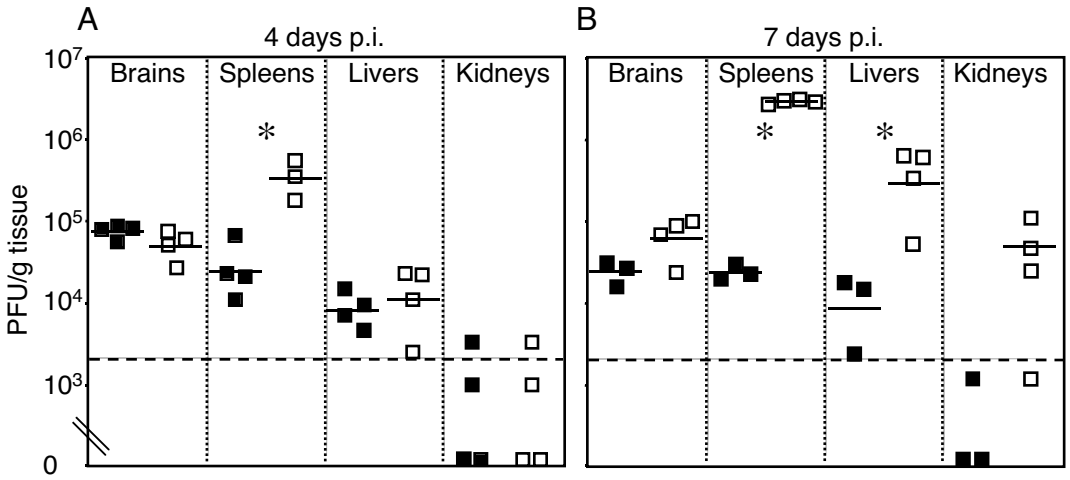
A
4 days p.i.
B
7 days p.i.
Brains
Spleens
Livers
Kidneys
PFU/g tissue
10^7
10^6
10^5
10^4
10^3
0
*

FIG. 4.3. Disseminated MAV-1 infection in MAV-1-infected IFN-α/βR$^{-/-}$ mice. Tissues were harvested 7 days p.i. from mice infected with 700 PFU of MAV-1. Sections from paraffin-embedded tissues were processed for ISH. Positive brown staining of MAV-1 nucleic acid in vascular endothelial cells in the indicated organs is evident. Magnification, 400x.

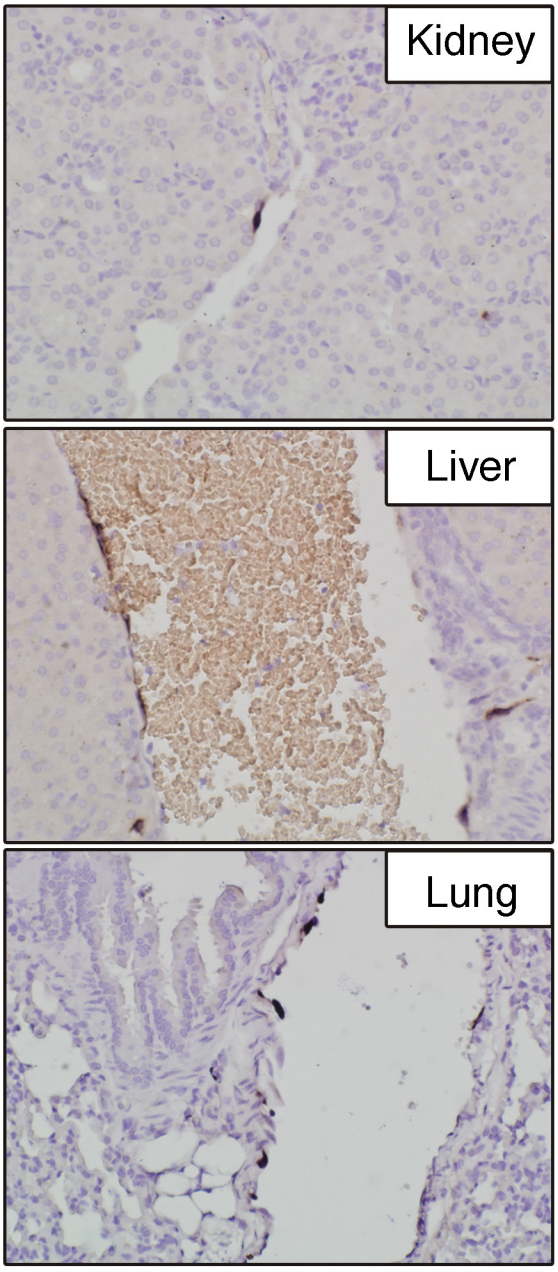
Kidney
Liver
Lung

FIG. 4.4. Time course of MAV-1 gene transcription in MBMECs. Twenty-five μg of total RNA isolated from mock-infected (m) and MAV-1-infected cells at the indicated hours post-infected were subjected to RPA as outlined in the Material and Methods. (A) MAV-1 hexon and actin. (B) MAV-1 E1A and actin. (C) MAV-1 E3 and actin. The full-length probe sizes are indicated on the right (-RNAse, tRNA plus probe) and the protected probe sizes are indicated on the left (+, positive control RNA isolated 48 h p.i. from 3T6 cells infected with MAV-1 at a MOI of 5). +RNAse, tRNA plus probe treated with RNAse A/T_1. Marker was labeled ΦX174 replicative form DNA digested with *Rsa*I. Using Acrobat Photshop 7.0 software, lanes 1 to 10 were adjusted to be 5X as intense as lanes 11 to 13 for all three panels.

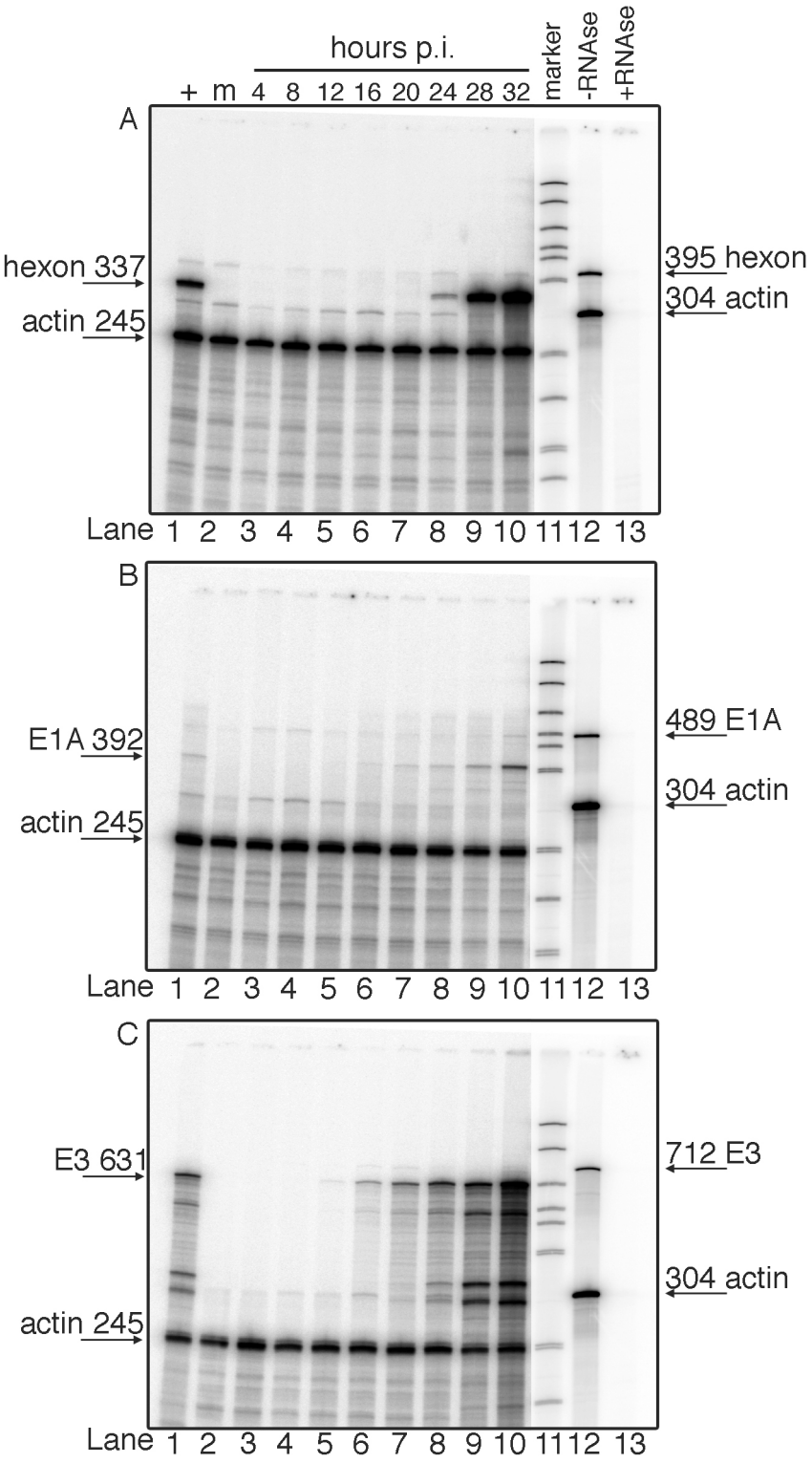
hours p.i.
+ m 4 8 12 16 20 24 28 32
marker
-RNAse
+RNAse
A
hexon 337
actin 245
395 hexon
304 actin
Lane 1 2 3 4 5 6 7 8 9 10 11 12 13
B
E1A 392
actin 245
489 E1A
304 actin
Lane 1 2 3 4 5 6 7 8 9 10 11 12 13
C
E3 631
actin 245
712 E3
304 actin
Lane 1 2 3 4 5 6 7 8 9 10 11 12 13

FIG. 4.5. Selected areas of an autoradiogram of cDNA array membranes hybridized to labeled complex cDNA probes derived from MAV-1-infected MBMECs (top row) and mock-infected MBMECs (bottom row) 20 hours p.i. All panels are shown at the same scale. The membranes were exposed for 72 hours.

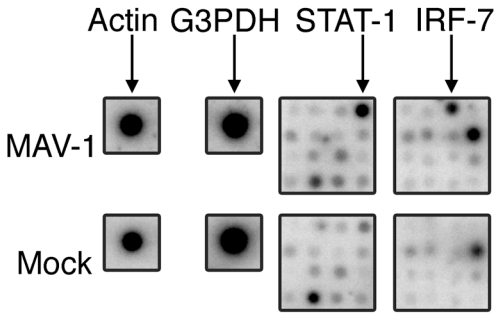
Actin
G3PDH
STAT-1
IRF-7
MAV-1
Mock

FIG. 4.6. Northern blot analysis of mock (m)- and MAV-1 (wt)-infected MBMEC and J774A.1 cells. Data from two blots are shown. PolyA+ RNAs analyzed on the first blot were actin, STAT-1, IRF-7, IRF-1, β_2m, and MHC class I heavy chain (MHC I HC). PolyA+ RNAs analyzed on the second blot were actin, IRF-1, and RANTES. Each lane was loaded with 1 μg of polyA+ RNA harvested 20 hours p.i. The levels were normalized to the actin level and then to the value of actin in mock-infected cells, as indicated under the lanes.

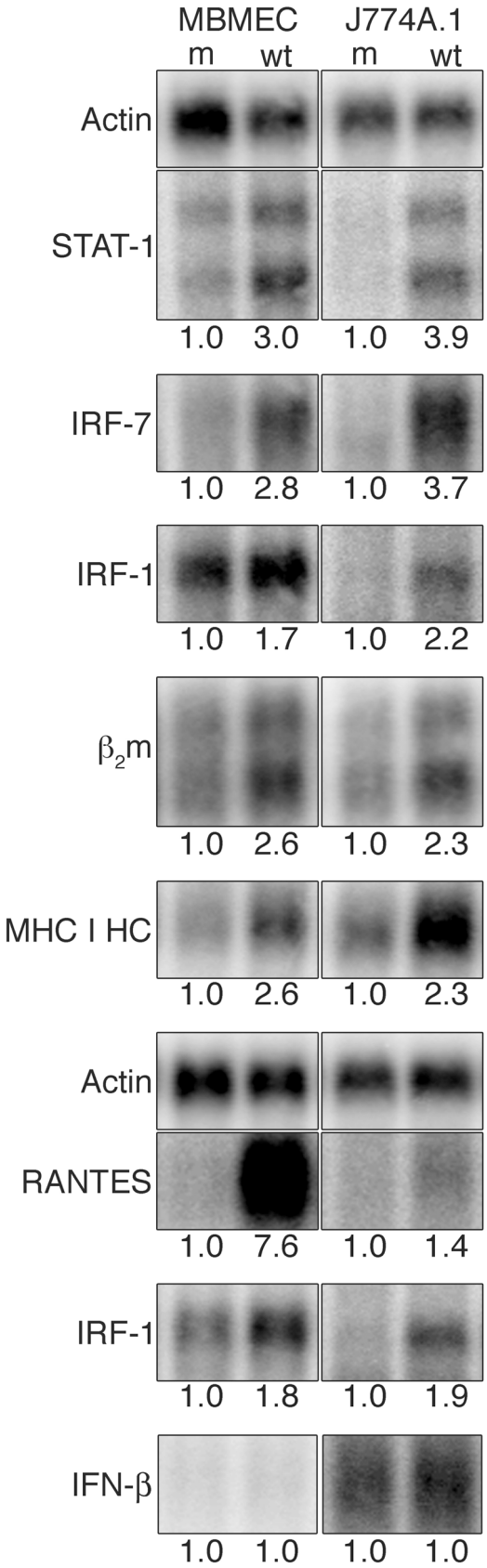
MBMEC
J774A.1
m
wt
m
wt
Actin
STAT-1
1.0 3.0 1.0 3.9
IRF-7
1.0 2.8 1.0 3.7
IRF-1
1.0 1.7 1.0 2.2
β2m
1.0 2.6 1.0 2.3
MHC I HC
1.0 2.6 1.0 2.3
Actin
RANTES
1.0 7.6 1.0 1.4
IRF-1
1.0 1.8 1.0 1.9
IFN-β
1.0 1.0 1.0 1.0

FIG 4.7. Northern analysis of STAT-1, IRF-7, IRF-1, and β_2m polyA+ RNA in 129 and IFN-$\alpha/\beta R^{-/-}$ spleens. RNA was isolated 4 day p.i. from 129 and IFN-$\alpha/\beta R^{-/-}$ mice mock-infected (m) and infected (wt) with 10^4 PFU of wt MAV-1. Each lane has RNA from one half of the spleen of one animal. The level of STAT-1, IRF-7, IRF-1, and β_2m was normalized to the actin level and then to the value for the mock-infected 129 mouse, as indicated under the lanes.

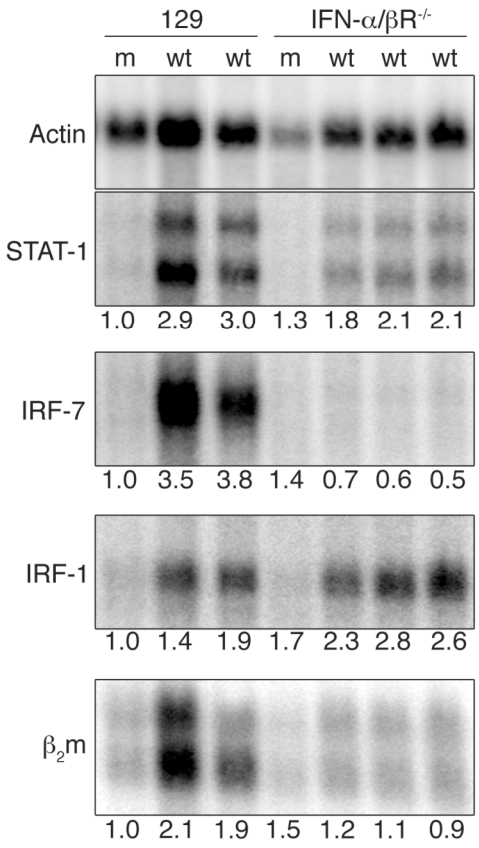
129
IFN-α/βR-/-
m wt wt m wt wt wt
Actin
STAT-1
1.0 2.9 3.0 1.3 1.8 2.1 2.1
IRF-7
1.0 3.5 3.8 1.4 0.7 0.6 0.5
IRF-1
1.0 1.4 1.9 1.7 2.3 2.8 2.6
β2m
1.0 2.1 1.9 1.5 1.2 1.1 0.9

FIG 4.8. Northern analysis of β_2m, MHC class I heavy chain (MHC I HC), and IRF-7 polyA+ RNA in 129 and IFN-$\alpha/\beta R^{-/-}$ lung. RNA was isolated 6 days p.i. from 129 and IFN-$\alpha/\beta R^{-/-}$ mice mock-infected (m) or infected (wt) with 10^4 PFU of wt MAV-1. Each lane has RNA from one animal. The level of β_2m, MHC class I heavy chain, and IRF-7 was normalized to the actin level and then to the value for the mock-infected 129 mouse, as indicated under the lanes.

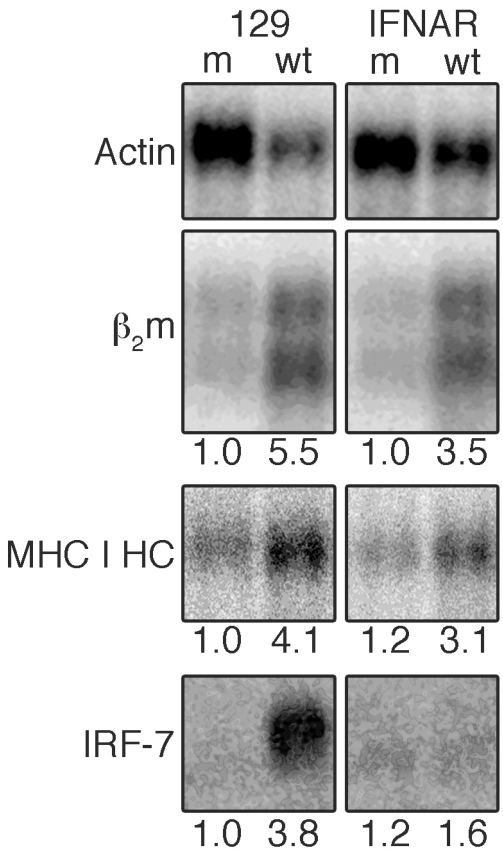
129
IFNAR
m
wt
m
wt
Actin
β2m
1.0
5.5
1.0
3.5
MHC I HC
1.0
4.1
1.2
3.1
IRF-7
1.0
3.8
1.2
1.6

CHAPTER 5

DISCUSSION

Mouse adenovirus type 1 (MAV-1) induces dose dependent encephalomyelitis in C57BL/6 (B6) and 129 Sv/Ev mice, infecting cells of the mononuclear/macrophage lineage and endothelial cells and replicating to highest levels in the central nervous system (CNS) and spleen (Chapters 2 and 4). In the preceding chapters, the functions of T cells, B cells, and type I IFN in MAV-1 pathogenesis were investigated using immunodeficient mouse strains. Previous studies indicated that T cells (17, 37, 47), B cells (9, 37, 45), and type I IFN (20) are involved in the host immune response to MAV-1, but the role these systems play in MAV-1 pathogenesis was largely unexplored.

This work began with MAV-1 infection of RAG-$1^{-/-}$ mice, which lack T cells and B cells. RAG-$1^{-/-}$ mice were more susceptible to MAV-1 infection than B6 controls (Chapter 3). These data agree with increased susceptibility of SCID mice (which are also T cell- and B cell-deficient) to MAV-1 infection relative to BALB/c controls (7). To determine the relative contribution of T cells and B cells to protection against MAV-1-induced acute encephalomyelitis in B6 mice, I infected mice lacking T cells and mice lacking B cells.

Infection of mice deficient for T cells, T cell subsets, and T cell-related functions suggested that cytotoxic T cells (CTL) may mediate acute immunopathology, contributing to MAV-1-induced encephalomyelitis (29 and Chapter 2). Mice lacking α/β T cells, mice lacking major histocompatibility complex (MHC) class I ($\beta_2m^{-/-}$), and mice lacking perforin had fewer disease signs at 8 days post-infection (p.i.) than control mice, whereas mice lacking MHC class II had acute disease signs equivalent to B6 controls. Brains harvested from MAV-1-infected mice lacking α/β T cells and MAV-1-infected mice lacking perforin had less histological evidence of MAV-1 encephalomyelitis and less cellular inflammation than brains harvested from control mice. T cell-mediated acute immunopathology is characteristic of experimental infection

of mice with a number of viruses (8, 14, 18, 24, 34, 38). Similar to virus-induced disease in these virus infections, MAV-1-induced disease in B6 mice depended on virus dose and cell-mediated immunity (Chapter 2), supporting the view that antigen quantity controls T cell-mediated immunity (48).

α/β T cells limited acute MAV-1 replication, but levels of infectious MAV-1 did not differ between perforin-deficient mice and controls. The immunopathologic role of perforin in MAV-1 infection is similar to the role of perforin in coxsackievirus B3 (CVB3)-induced myocarditis. Perforin-deficient mice are resistant to acute CVB3 disease and exhibit less myocarditis and inflammatory cell infiltration than controls, but perforin plays no role in clearance of CVB3 (14). These observations suggest that perforin can mediate inflammatory cell recruitment, possibly by the release of pro-inflammatory molecules by cells targeted with perforin. Interestingly, CVB3 and human adenoviruses bind the same cellular receptor, the coxsackievirus-adenovirus receptor (CAR); the receptor for MAV-1 is not known (41). Our results are also interesting because both MAV-1 and CVB3 infect endothelial cells in vivo, and MAV-1 induces myocarditis in suckling mice (4). Infection of suckling perforin-deficient mice with MAV-1 may reveal a general role for perforin in virus-induced myocarditis. Perforin-deficient suckling mice would likely exhibit less MAV-1-induced myocardidits than control mice.

Mice lacking α/β T cells succumbed to MAV-1 infection 9 to 16 weeks p.i. These mice had detectable viral loads in spleens and brains at 3 weeks p.i. and high viral loads in spleen and brains when moribund (Chapter 2). In contrast, B6 mice cleared MAV-1 to a level below the detection limit of our plaque assay by approximately 12 days p.i., and no infectious virus was recovered 12 weeks p.i. from B6 mice (Chapter 2 and M. Moore and K. Spindler, unpublished

data). Somewhat surprisingly, neither MHC class I-deficient, MHC class II-deficient, $CD8^{-/-}$, $CD4^{-/-}$, perforin-deficient, nor interferon-γ-deficient mice had any detectable infectious virus in spleens or brains at 12 weeks p.i. Since almost all α/β T cells are either $CD8^+$ or $CD4^+$ (28), we believe that having either $CD8^+$ or $CD4^+$ effector α/β T cells is sufficient for α/β T cell-mediated clearance of MAV-1. An alternative though less likely hypothesis is that $CD8^-CD4^-$ α/β T cells are required for control of MAV-1 infection. Since endothelial cells are antigen presenting cells that express both MHC class I and II molecules (1) and $CD4^+$ α/β T cells can be cytotoxic for MHC class II-expressing cells ex vivo (2), it is possible that $CD4^+$ CTL play a role in α/β T cell-dependent long-term survival of MAV-1 infection. The effector mechanism(s) involved in α/β T cell-mediated control of MAV-1 are not known. The Fas/Fas ligand system is a candidate. The human adenovirus receptor internalization and degradation (RID) protein complex removes Fas from the surface of cells in vitro, suggesting that Fas may play a role in human adenovirus pathogenesis (44). Antibody depletion of T cell subsets in long-term MAV-1-infected B6 mice and infection of mice deficient in the Fas-mediated pathway of cytotoxicity may clarify the cell type(s) and mechanism(s) of α/β T cell-mediated control of long-term MAV-1 infection.

As mentioned above, mice lacking T cells and mice lacking B cells were infected to determine the relative contributions of T cells and B cells to protection from acute MAV-1-induced encephalomyelitis. In contrast to mice lacking T cells, mice lacking B cells (μMT mice) were more susceptible to acute MAV-1-induced disease than B6 controls (Chapter 3). μMT mice were highly susceptible to MAV-1-induced disease. Since B cell-deficient mice died early (7 to 10 days p.i.) in independent experiments and T cells were not required for survival of acute infection (Chapter 2), we postulated that early T cell-independent (TI) B cell responses are critical for protection against MAV-1-indcued encephalomyelitis. Bruton's tyrosine kinese

(Btk)-deficient mice have the X-linked immunodeficient (Xid) phenotype and are unable to produce TI antibodies (Abs) in response to some viruses (43). Btk was required for survival of acute MAV-1 infection (Chapter 3). Survival correlated with the production of early TI antiviral IgM and TI neutralizing Ab. This is the first demonstration that Btk plays a role in protection from virus-induced disease in mice. Mice lacking B cells are highly susceptible to acute West Nile virus and herpes simplex type 1 virus infection (10, 11). The pathogenesis of these viruses in Xid mice has not been reported.

Our data raise questions about B cell function in response to virus infection. Btk deficiency in humans results in the complete absence of B cells and is called X-linked agammaglobulinemia (XLA) (5). Thus it is not surprising that XLA patients are more susceptible to virus infections (including human adenovirus infections) than immunocompetent patients (40). The Xid phenotype is milder than the XLA phenotype; Btk-deficient mice have an ~50% reduction in conventional B cells, and they lack peritoneal B-1 cells (22). However, the Xid phenotype is not completely characterized, and "conventional" B cells in Xid mice, though capable of mounting T cell-dependent Ab responses, differ in cell surface markers from conventional B cells of control mice (W. Khan, personal communication). Since Btk-deficient mice were unable to control any dose of MAV-1, it is unlikely that the cause of susceptibility relative to controls is the 50% reduction in their peripheral B cells. It is more likely that B-1 cells and/or some other function of Btk are required for protection against MAV-1. The antiviral effect of TI IgM in MAV-1 infection may extend beyond straightforward neutralization. IgM interacts with the complement system, and early TI IgM production in response to vesicular stomatitis virus (VSV) was reduced in $C3^{-/-}C4^{-/-}$ mice (35). Early TI IgM may be an important

regulator of T cell-dependent B cell functions (3). MAV-1 provides a unique opportunity to study the functional relevance of B cell populations and TI Ab.

Early TI IgM may be a good therapeutic treatment for acute infection by some viruses. Intraperitoneal injection of MAV-1-infected Btk-deficient mice with early anti-MAV-1 antiserum from four to nine days p.i. was protective (Chapter 3). This early antiviral antiserum contained both MAV-1-specific IgM and MAV-1-specific IgG. It would be interesting to test the hypothesis that treatment with early TI antiviral IgM is protective. One approach would be to isolate B cells from MAV-1-infected mice, generate B cell hybridomas, screen these clones for anti-MAV-1 IgM production, purify the IgM, and test whether it has an antiviral effect in infected mice in vivo. These B cell hybridomas would be useful reagents for future analyses of the role of B cells in MAV-1 pathogenesis. It would also be interesting to determine whether early antiviral antiserum is neutralizing and/or immunoregulatory in vivo. One experiment would be to compare the survival of MAV-1-infected Btk-deficient mice treated four to nine days p.i. with early antiviral antiserum (high antiviral IgM level, low antiviral IgG level, low neutralizing titer) or late antiviral antiserum (undetectable antiviral IgM level, high antiviral IgG level, high neutralizing titer [Chapter 3]). My prediction is that late (IgG) antiviral antiserum will not protect Btk-deficient mice as well as early (IgM) antiviral antiserum and that antiviral TI IgM has an immunoregulatory as well as protective function. Alternatively, late (IgG) antiviral antiserum may be a better therapeutic for acute MAV-1 infection than early (IgM) antiviral antiserum because late antiserum has a higher neutralizing titer than early antiserum . Despite the unquestionable importance of Ab in preventing virus infection and reinfection, there is little evidence for a role of Ab in resolution of virus disease (40). However Gerhard's group has demonstrated a role for B cells in resolution of influenza virus infection in mice and

characterized the therapeutic and prophylactic activities of monoclonal IgG Abs to influenza virus (30, 31, 36).

Btk-deficient and μMT mice succumbed to acute MAV-1 infection with systemically high viral loads and histological evidence of hepatitis in addition to the histological evidence of MAV-1-induced encephalomyelitis (Chapter 3). B cell-deficient mice on a BALB/c background (Jh mice) were more susceptible to acute MAV-1-induced disease, and these mice also succumbed with systemically high viral loads and evidence of significant hepatitis. However moribund Jh mice did not exhibit encephalomyelitis; MAV-1-infected Jh mice likely died of hemorrhagic enteritis (Chapter 3). Interestingly, SCID (T cell- and B cell-deficient) mice on a BALB/c background succumb to acute MAV-1 infection with evidence of liver infection but no histological evidence of hepatitis (7). One explanation for this strain-specific pathology is as follows. In the absence of B cells, MAV-1 replicates to high titers throughout the mouse (Chapter 3). In the presence of T cells, acute MAV-1 infection elicits dose-dependent immunopathology (Chapter 2). T cell-mediated immunopathology may be directed to various organs in different mouse strains by strain-specific innate immune responses, e.g. differential chemokine expression in the brains of MAV-1-infected B6 and BALB/c brains (6). Data showing that MAV-1 replicates to high levels in the brains of Jh mice without inducing encephalomyelitis (Chapter 3) supports this model rather than the model that receptor differences account for differential pathology in MAV-1-infected B6 and BALB/c mice (7).

Although B cells and Btk are critical for protection against acute MAV-1-induced disease, we speculated that the IFN-α/β (type I IFN) system also plays a protective role in the disease process. In single-cycle infectious yield reduction assays in vitro, MAV-1 is more resistant than vesicular stomatitis virus (VSV) to pretreatment with mouse IFN-α/β, but MAV-1

replication is not completely resistant to IFN-α/β (20). E1A mutants of MAV-1 are more sensitive to IFN-α/β than wt MAV-1. These data indicated that MAV-1 counteracts the IFN-α/β antiviral response and suggested that IFN-α/β plays a role in MAV-1 immunopathogenesis. Also, as mentioned above, we speculate that innate immunity may be a key mediator of mouse strain-specific pathology.

We analyzed the role of IFN-α/β in MAV-1-induced encephalomyelitis by comparing the pathogenesis of MAV-1 in 129 Sv/Ev and IFN-α/β receptor null (IFN-α/β$R^{-/-}$) mice. Disruption of IFN-α/β signaling resulted in a more widespread MAV-1 infection without an increase in inflammation or disease (Chapter 4). Infection of IFN-α/β$R^{-/-}$ mice has demonstrated the importance of this system for protection against many viruses, including Theiler's virus, influenza, Venezuelan equine encephalitis virus, herpes simplex type 1, measles, lymphocyte choriomeningitis virus (LCMV), VSV, Semliki Forest virus, Sindbis virus, and vaccinia virus, particularly with respect to virus dissemination (12, 13, 15, 26, 32, 33, 39, 42). Relative to control mice, infection of IFN-α/β$R^{-/-}$ mice with 700 PFU of MAV-1 resulted in higher levels of infectious virus in spleen, liver and kidney and significant infection in lung. However, this disseminated MAV-1 infection in IFN-α/β$R^{-/-}$ mice did not show clinical or histopathological differences from infection of control mice. These results are similar to those found in LCMV infection, where IFN-α/β$R^{-/-}$ mice are more resistant than 129 Sv/Ev controls to CTL-mediated immunopathology (33).

IFN-α/β signaling is a key regulator of effector T cell function (reviewed in reference 23). As discussed above, we believe that innate immunity regulates CTL-mediated immunopathology in MAV-1-infected mice. We believe that that IFN-α/β signaling contributes this process for the following reason. β_2m mRNA steady-state levels were lower in the spleens

of IFN-α/βR$^{-/-}$ mice than control mice at 4 days p.i. (Chapter 4), and α/β T cell-deficient, perforin-deficient, and β_2m-deficient mice exhibited less acute MAV-1 disease than controls (29 and Chapter 2). An implication of widespread MAV-1 infection without significant cellular inflammation is that dampening the type I IFN system may improve the safety and/or efficacy of adenovirus-mediated gene therapy by decreasing inflammation and/or increasing vector dissemination.

MAV-1 is useful for investigating type I IFN signaling. We identified interferon-stimulated genes (ISGs, see Chapter 1) whose steady-state RNA levels were increased by MAV-1 infection in vitro and in vivo. We showed that steady-state levels of the transcription factors interferon regulatory factor 7 (IRF-7), interferon regulatory factor 1 (IRF-1), and signal transducer and activator of transcription 1 (STAT-1) are increased by MAV-1 infection in vitro and in vivo. Northern analyses of mRNAs in infected 129 Sv/Ev and IFN-α/βR$^{-/-}$ mice showed that induction of IRF-7 and β_2m by MAV-1 depended on the IFN-α/βR in the spleen and that induction of IRF-7 by MAV-1 depended on the IFN-α/βR in the lung. We thus propose that IRF-7 and major histocompatibility complex (MHC) class I play a role in IFN-α/β signaling-dependent control of MAV-1 replication in the spleen and MAV-1 organ tropism.

Steady-state mRNA levels of the ISG regulated upon activation, normal T cell expressed and secreted (RANTES) were increased by MAV-1 infection in vitro (Chapter 4). RANTES is a chemokine that attracts monocytes and T cells and that is required for T cell function in mice (27). Consistent with this increase in RANTES in a brain endothelial cell line, we have detected induced steady-state levels of RANTES mRNA in the brains of MAV-1 infected B6 mice at 9 days p.i. (Moore and Spindler, unpublished data). Interestingly, we did not detect RANTES mRNA in the brains of MAV-1-infected BALB/c mice at 9 days p.i. It is possible that RANTES

contributes to MAV-1-induced encephalomyelitis, because MAV-1 induces encephalomyelitis in B6 mice (where RANTES is detected) but not BALB/c mice (where it is not) (16).

A line of investigation worth pursuing is the role of the viral E1A protein in counteracting the effects of IFN-α/β on MAV-1 in vivo. E1A mutants of MAV-1 are less resistant to IFN-α/β treatment in vitro than wt MAV-1, and expression of MAV-1 E1A in mouse fibroblasts rescues VSV from the antiviral effect of IFN-α/β (20). Human adenovirus type 5 E1A directly binds STAT-1 and blocks ISG transcription in primary human cells (25). There is preliminary evidence that MAV-1 E1A binds STAT-1 (L. Fang and K. Spindler, unpublished data). We hypothesized that *pm*E109 (MAV-1 E1A null mutant) virus replication would be partially restored in IFN-α/βR$^{-/-}$ mice because *pm*E109 is sensitive to IFN-α/β in vitro (20). Preliminary viral load data supports this hypothesis, and immunohistochemistry and Northern analyses suggest that MAV-1 E1A null mutants induce STAT-1 and IRF-7 to higher levels than wt virus in 129 Sv/Ev mice (M. Moore and K. Spindler, unpublished data).

There are two working hypotheses as to why IFN-α/β signaling did not protect against MAV-1 replication in the brain or MAV-1-induced encephalomyelitis. MAV-1 may effectively counteract the antiviral effects of IFN-α/β signaling in endothelial cells of the brain. Alternatively, IFN-α/β signaling may be defective in endothelial cells of the brain in 129 Sv/Ev mice. These hypotheses are not mutually exclusive. 129 Sv/Ev mice are known to have a defect in inflammatory cell recruitment (46). This may reflect an underlying defect in the type I IFN system. IFN-β mRNA was not detected in mouse brain microvascular endothelial cells (MBMEC) in contrast to J774A.1 macrophage cells and 3T6 fibroblasts (Chapter 4), suggesting that MBMEC have unconventional IFN-α/β signaling. Unlike human aorta large vessel endothelial cells, human brain microvascular endothelial cells do not express the I-E subunit of

MHC class II molecules (21). It is possible that defective IFN-α/β signaling in endothelial cells of the CNS relative to other organs contributes to the neurotropism of MAV-1 in 129 Sv/Ev and other strains of mice.

Investigation of the roles of T cells, B cells, and type I IFN in this work has clearly shown that each of these aspects of the host immune response to MAV-1 has a distinct, protective role in MAV-1 pathogenesis and that T cells contribute to acute immunopathology. Also, the data suggest that the functions of T cells, B cells, and type I IFN in MAV-1 pathogenesis are interrelated. B cell-deficient mice succumbed to disseminated infection with high virus loads throughout the mouse (Chapter 3). T cell-mediated immunopathology was implicated in exacerbating disease in B cell-deficient mice (Chapter 3). Similar to B cell-deficient mice, type I IFN-deficient mice also had a more disseminated infection with higher virus loads than control mice (Chapter 4). However, unlike B cell-deficient mice, type I IFN-deficient did not exhibit more clinical disease than control mice, and type I IFN-deficient mice did not exhibit more histopathological evidence of disease than control mice, even in organs with high virus loads, e.g. the liver (Chapter 4). The most likely explanation for these observations is that type I IFN controls MAV-1 replication but also contributes to T cell-mediated immunopathology. Investigation of the role of macrophages and/or dendritic cells may shed light on the relationship between innate, cellular, and humoral immunity in MAV-1pathogenesis. MAV-1 infects cells of the monocyte/macrophage lineage, and these could include dendritic cell precursors (19). These cell types play important roles in regulating T cell and B cells responses and are major producers of type I IFN.

REFERENCES

1. **Abbas, A. K., A. H. Lichtman, and J. S. Pober.** 2000. Cellular and molecular immunology, 4th ed. W.B. Saunders Co., Philadelphia.

2. **Appay, V., J. J. Zaunders, L. Papagno, J. Sutton, A. Jaramillo, A. Waters, P. Easterbrook, P. Grey, D. Smith, A. J. McMichael, D. A. Cooper, S. L. Rowland-Jones, and A. D. Kelleher.** 2002. Characterization of CD4(+) CTLs ex vivo. J. Immunol. **168:**5954-5958.

3. **Baumgarth, N.** 2000. A two-phase model of B-cell activation. Immunol. Rev. **176:**171-180.

4. **Blailock, Z. R., E. R. Rabin, and J. L. Melnick.** 1967. Adenovirus endocarditis in mice. Science **157:**69-70.

5. **Bruton, O. C., L. Apt, D. Gitlin, and C. A. Janeway.** 1952. Absence of serum gamma globulins. AMA Am. J. Dis. Child. **84:**632-6.

6. **Charles, P. C., X. Chen, M. S. Horwitz, and C. F. Brosnan.** 1999. Differential chemokine induction by the mouse adenovirus type-1 in the central nervous system of susceptible and resistant strains of mice. J. Neurovirol. **5:**55-64.

7. **Charles, P. C., J. D. Guida, C. F. Brosnan, and M. S. Horwitz.** 1998. Mouse adenovirus type-1 replication is restricted to vascular endothelium in the CNS of susceptible strains of mice. Virology **245:**216-228.

8. **Cole, G. A., N. Nathanson, and R. A. Prendergast.** 1972. Requirement for theta-bearing cells in lymphocytic choriomeningitis virus-induced central nervous system disease. Nature **238:**335-337.

9. **Coutelier, J.-P., P. G. Coulie, P. Wauters, H. Heremans, and J. T. M. van der Logt.** 1990. In vivo polyclonal B-lymphocyte activation elicited by murine viruses. J. Virol. **64:**5383-8388.

10. **Deshpande, S. P., M. Zheng, M. Daheshia, and B. T. Rouse.** 2000. Pathogenesis of herpes simplex virus-induced ocular immunoinflammatory lesions in B-cell deficient mice. J. Virol. **74:**3517-3524.

11. **Diamond, M. S., B. Shrestha, A. Marri, D. Mahan, and M. Engle.** 2003. B cells and antibody play critical roles in the immediate defense of disseminated infection by West Nile encephalitis virus. J. Virol. **77:**2578-86.

12. **Fiette, L., C. Aubert, U. Muller, S. Huang, M. Aguet, M. Brahic, and J. F. Bureau.** 1995. Theiler's virus infection of 129Sv mice that lack the interferon alpha/beta or interferon gamma receptors. J. Exp. Med. **181:**2069-76.

13. **Garcia-Sastre, A., R. K. Durbin, H. Zheng, P. Palese, R. Gertner, D. E. Levy, and J. E. Durbin.** 1998. The role of interferon in influenza virus tissue tropism. J. Virol. **72:**8550-8558.

14. **Gebhard, J. R., C. M. Perry, S. Harkins, T. Lane, I. Mena, V. C. Asensio, I. L. Campbell, and J. L. Whitton.** 1998. Coxsackievirus B3-induced myocarditis: Perforin

exacerbates disease, but plays no detectable role in virus clearance. Am. J. Pathol. **153:**417-428.

15. **Grieder, F. B., and S. N. Vogel.** 1999. Role of interferon and interferon regulatory factors in early protection against Venezuelan equine encephalitis virus infection. Virol. **257:**106-118.

16. **Guida, J. D., G. Fejer, L.-A. Pirofski, C. F. Brosnan, and M. S. Horwitz.** 1995. Mouse adenovirus type 1 causes a fatal hemorrhagic encephalomyelitis in adult C57BL/6 but not BALB/c mice. J. Virol. **69:**7674-7681.

17. **Inada, T., and H. Uetake.** 1980. Cell-mediated immunity to mouse adenovirus infection: Blocking of macrophage migration inhibition and T cell-mediated cytolysis of infected cells by anti-S antigen or anti-alloantigen serum. Microbiol. Immunol. **24:**525-535.

18. **Kagi, D., B. Ledermann, K. Burki, R. M. Zinkernagel, and H. Hengartner.** 1996. Molecular mechanisms of lymphocyte-mediated cytotoxicity and their role in immunological protection and pathogenesis in vivo. Annu. Rev. Immunol. **14:**207-232.

19. **Kajon, A. E., C. C. Brown, and K. R. Spindler.** 1998. Distribution of mouse adenovirus type 1 in intraperitoneally and intranasally infected adult outbred mice. J. Virol. **72:**1219-1223.

20. **Kajon, A. E., and K. R. Spindler.** 2000. Mouse adenovirus type 1 replication *in vitro* is resistant to interferon. Virology **274:**213-219.

21. **Karasin, A., S. Macvilay, M. N. Hart, and Z. Fabry.** 1998. Murine endothelia do not express MHC class II I-Ealpha subunit and differentially regulate I-Aalpha expression along the vascular tree. Endothelium **6:**83-93.

22. **Khan, W. N., F. W. Alt, R. M. Gerstein, B. A. Malynn, I. Larsson, G. Rathbun, L. Davidson, S. Muller, A. B. Kantor, L. A. Herzenberg, F. S. Rosen, and P. Sideras.** 1995. Defective B cell development and function in Btk-deficient mice. Immunity **3:**283-299.

23. **Levy, D. E., I. Marie, and A. Prakash.** 2003. Ringing the interferon alarm: Differential regulation of gene expression at the interface between innate and adaptive immunity. Curr. Opin. Immunol. **15:**52-8.

24. **Licon Luna, R. M., E. Lee, A. Mullbacher, R. V. Blanden, R. Langman, and M. Lobigs.** 2002. Lack of both Fas ligand and perforin protects from flavivirus-mediated encephalitis in mice. J. Virol. **76:**3202-3211.

25. **Look, D. C., W. T. Roswit, A. G. Frick, Y. Gris-Alevy, D. M. Dickhaus, M. J. Walter, and M. J. Holtzman.** 1998. Direct suppression of Stat1 function during adenoviral infection. Immunity **9:**871-880.

26. **Luker, G. D., J. L. Prior, J. Song, C. M. Pica, and D. A. Leib.** 2003. Bioluminescence imaging reveals systemic dissemination of herpes simplex virus type 1 in the absence of interferon receptors. J. Virol. **77:**11082-10093.

27. **Makino, Y., D. N. Cook, O. Smithies, O. Y. Hwang, E. G. Neilson, L. A. Turka, H. Sato, A. D. Wells, and T. M. Danoff.** 2002. Impaired T cell function in RANTES-deficient mice. Clin. Immunol. **102:**302-309.

28. **Mombaerts, P., A. R. Clarke, M. A. Rudnicki, J. Iacomini, S. Itohara, J. J. Lafaille, L. Wang, Y. Ichikawa, R. Jaenisch, M. L. Hooper, and S. Tonegawa.** 1992. Mutations in T-cell antigen receptor genes α and β block thymocyte development at different stages. Nature **360:**225-231.

29. **Moore, M. L., C. C. Brown, and K. R. Spindler.** 2003. T cells cause acute immunopathology and are required for long term survival in mouse adenovirus type 1-induced encephalomyelitis. J. Virol. **77:**10060-10070.

30. **Mozdzanowska, K., M. Furchner, G. Washko, J. Mozdzanowski, and W. Gerhard.** 1997. A pulmonary influenza virus infection in SCID mice can be cured by treatment with hemagglutinin-specific antibodies that display very low virus-neutralizing activity in vitro. J. Virol. **71:**4347-55.

31. **Mozdzanowska, K., K. Maiese, and W. Gerhard.** 2000. Th cell-deficient mice control influenza virus infection more effectively than Th- and B cell-deficient mice: Evidence for a Th-independent contribution by B cells to virus clearance. J. Immunol. **164:**2635-43.

32. **Mrkic, B., J. Pavlovic, T. Rülicke, P. Volpe, C. J. Buchholz, D. Hourcade, J. P. Atkinson, A. Aguzzi, and R. Cattaneo.** 1998. Measles virus spread and pathogenesis in genetically modified mice. J. Virol. **72:**7420-7427.

33. **Muller, U., U. Steinhoff, L. F. L. Reis, S. Hemmi, J. Pavlovic, R. M. Zinkernagel, and M. Aguet.** 1994. Functional role of type I and type II interferons in antiviral defense. Science **264:**1918-1921.

34. **Murray, P. D., K. D. Pavelko, J. Leibowitz, X. Lin, and M. Rodriguez.** 1998. CD4+ and CD8+ T cells make discrete contributions to demyelination and neurologic disease in a viral model of multiple sclerosis. J. Virol. **72:**7320-7329.

35. **Ochsenbein, A. F., D. D. Pinschewer, B. Odermatt, M. C. Carroll, H. Hengartner, and R. M. Zinkernagel.** 1999. Protective T cell-independent antiviral antibody responses are dependent on complement. J. Exp. Med. **190:**1165-1174.

36. **Palladino, G., K. Mozdzanowska, G. Washko, and W. Gerhard.** 1995. Virus-neutralizing antibodies of immunoglobulin G (IgG) but not of IgM or IgA isotypes can cure influenza virus pneumonia in SCID mice. J. Virol. **69:**2075-81.

37. **Pirofski, L., M. S. Horwitz, M. D. Scharff, and S. M. Factor.** 1991. Murine adenovirus infection of SCID mice induces hepatic lesions that resemble human Reye syndrome. Proc. Natl. Acad. Sci. USA **88:**4358-4362.

38. **Rowell, J. F., and D. E. Griffin.** 2002. Contribution of T cells to mortality in neurovirulent Sindbis virus encephalomyelitis. J. Neuroimmmunol. **127:**106-114.

39. **Ryman, K. D., W. B. Klimstra, K. B. Nguyen, C. A. Biron, and R. E. Johnston.** 2000. Alpha/beta interferon protects adult mice from fatal Sindbis virus infection and is an important determinant of cell and tissue tropism. J. Virol. **74:**3366-3378.

40. **Sanna, P. P., and D. R. Burton.** 2000. Role of antibodies in controlling viral disease: Lessons from experiments of nature and gene knockouts. J. Virol. **74:**9813-9817.

41. **Shenk, T. E.** 2001. Adenoviridae: The viruses and their replication, p. 2265-2300. *In* D. M. Knipe and P. M. Howley (ed.), Fields Virology, 4th ed, vol. 2. Lippincott Williams & Wilkins, Philadelphia.

42. **Steinhoff, U., U. Muller, A. Schertler, H. Hengartner, M. Aguet, and R. M. Zinkernagel.** 1995. Antiviral protection by vesicular stomatitis virus-specific antibodies in alpha/beta interferon receptor-deficient mice. J. Virol. **69:**2153-2158.

43. **Szomolanyi-Tsuda, E., and R. M. Welsh.** 1998. T-cell-independent antiviral antibody responses. Curr. Op. Immunol. **10:**431-435.

44. **Tollefson, A. E., T. E. Hermiston, D. L. Lichtenstein, C. F. Colle, R. A. Tripp, T. Dimitrov, K. Toth, C. E. Wells, P. C. Doherty, and W. S. M. Wold.** 1998. Forced degradation of Fas inhibits apoptosis in adenovirus-infected cells. Nature **392:**726-730.

45. **van der Veen, J., and A. Mes.** 1973. Experimental infection with mouse adenovirus in adult mice. Arch. Gesamte Virusforsch. **42:**235-241.

46. **White, P., S. A. Liebhaber, and N. E. Cooke.** 2002. 129X1/SvJ mouse strain has a novel defect in inflammatory cell recruitment. J. Immunol. **168:**869-874.

47. **Winters, A. L., and H. K. Brown.** 1980. Duodenal lesions associated with adenovirus infection in athymic "nude" mice. Proc. Soc. Exp. Bio. Med. **164:**280-286.

48. **Zinkernagel, R. M., and H. Hengartner.** 2001. Regulation of the immune response by antigen. Science **293:**251-253.